technische universität
dortmund

2015

SCIENTIFIC HIGHLIGHTS

Annual Report

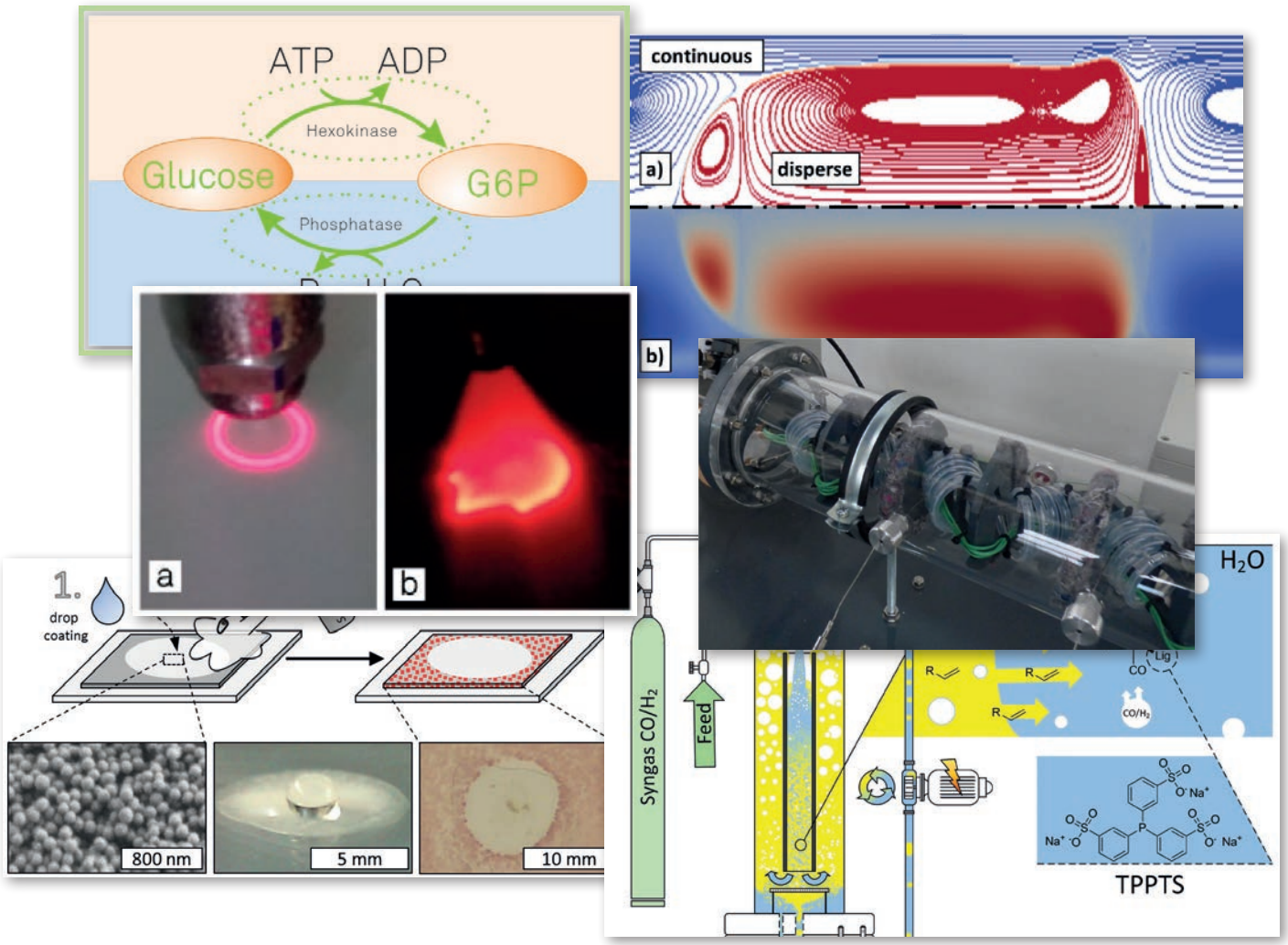

Fakultät Bio- und
Chemieingenieurwesen

Content

Content

Department of BCI

Preface

Dear Readers,

Another year of scientific productivity at the Faculty of Bio- and Chemical Engineering has passed and I am proud to present the 6th volume of our Scientific Highlights of the year 2015. These Highlights is the best of research of our professors or better of their research groups. The scientific outcome is the product of the joined work of undergraduate and graduate students, who perform their research as Bachelor, Master, and PhD thesis. This learning of scientific research taught by internationally acknowledged researchers is the unique education offered by universities. As you can easily see from the presented scientific outcome, our students are educated on cutting etch science and will carry this knowledge to industry, academia, and society.

Besides the students, not only chemical and biochemical engineers, but also physicists, chemists, biologists, pharmacists and mathematicians are involved in our research work, which would not be possible without the strong support we receive from our technicians and administrative staff. Thank you!

As every year, I hope that this brochure attracts the interest of students to join our research groups and academic as well as industrial researchers to find collaboration partners here.

Enjoy the reading,

Joerg Tiller

Equipment Design (AD)

Design of a Temperature Control for Microstructured Reactor Systems Based on Peltier Elements

Development of an Individual and Flexible Temperature Control System within Microstructured Reactor Systems Containing Standardized Elements for High Adaptability in Process Control

Felix Reichmann, Norbert Kockmann

Peltier elements have been used for the temperature control for microstructured reactor systems showing short response times. Switching from cooling to heating mode and the other way round was done by reversing polarity, resulting in a wide operating range. The easy handling and high ability of control contribute to a good applicability.

Developmental periods and scale-up times from laboratory to production can be reduced with continuous processes in microstructured devices. Standardization of these devices within channel elements enables faster application of chosen equipment combined with a better prediction regarding the scalability. Temperature control is of high interest for nearly each unit operation especially for complex or exothermic reactions influencing the reactor performance and safety issues. Here isothermal process conditions secure constant product quality.

A stainless steel microfluidic reactor system was extended by temperature measurement and control for each single channel element using Peltier elements. The system consists of a reactor plate frame, in which different standardized modules are inserted to create a reaction volume for single- or multiphase applications (Figure 1). All modules can be easily exchanged guaranteeing a high flexibility on demand and optical characterization due to a sealing glass plate from the top.

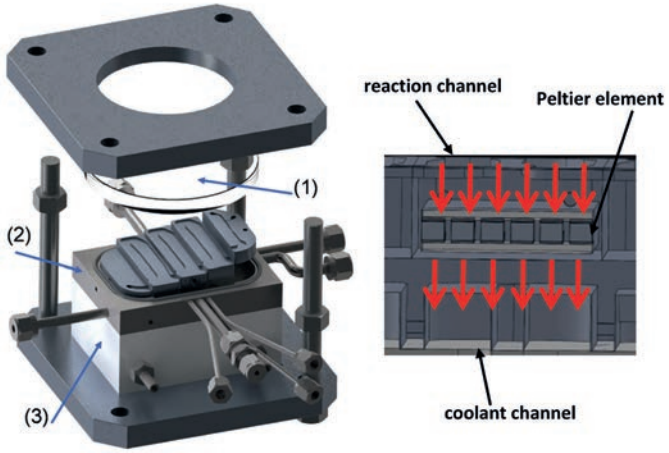

Figure 1: Left: Reactor system made of stainless steel. Up to 5 standardized channel elements can be inserted and tempered individually. Right: Section view of inserted Peltier element within a channel element and direction of heat flow.

The temperature control via Peltier elements showed short response times in the range of one second and a rapid change from cooling to heating mode was realized by reversing polarity (Figure 2).

Contact:
felix.reichmann@udo.edu
norbert.kockmann@udo.edu

A cooling capacity of up to 13 W was attained per single Peltier element.

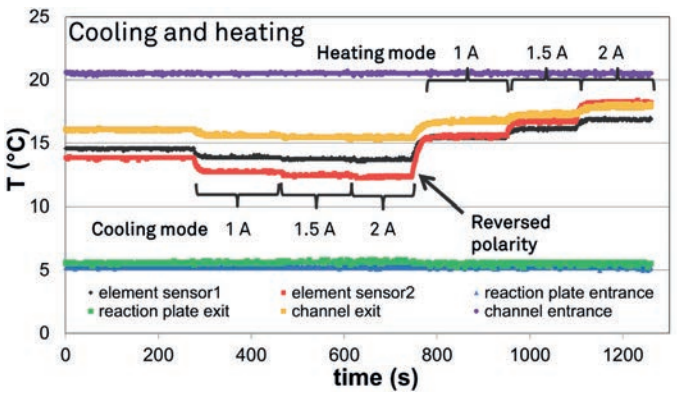

Figure 2: Displaying the switch between cooling and heating mode for temperature control of a microreactor system. Electrical currents for the supply of the Peltier elements are shown.

A similar set up was also used for the tempering of a second microstructured reactor system made of hot embossed polymer foils. The Peltier elements were situated beneath the reaction channel on a fluidic tempered ground plate to ensure sufficient heat removal from the Peltier's hot side. Applying an electric current of maximal 2 A, temperatures as deep as -35°C were obtained on the cold side, hence, cooling the reactor and the reaction fluid.

Publications:
F. Reichmann, A. Tollkötter, N. Kockmann, Jahrestreffen ProcessNet-Mikroverfahrenstechnik, Poster "Design of a Temperature Control for Microstructured Reactor Systems Based on Peltier Elements", Frankfurt a.M. (DE), 2015.
F. Reichmann, A. Tollkötter, N. Kockmann, European Congress on Chemical Engineering, Poster "Individual Temperature Control of Modules within a Microstructured Reaction System", Nice (FR), 2015.

Safety Aspects in Planning and Construction of Modularly Built Chemical Production Plants

General Safety Requirements for the Reduction of the Lead Time by Reusing of Already Developed Modules for Modularly Built Production Plants

Christoph Fleischer, Norbert Kockmann

The development and application of modularly built production plants is a strategy to respond to ever increasing demands on the global chemical market. Similar to conventionally planned production plants the new developed plant type must be checked for safe use. Therefore risk analysis methods must be identified and applied effectively which ensure a safe operation. Based on intra- and inter-modular safety assessments, a module database and by assigning modules to operating windows the effort for achieving a safe production plant can be reduced.

Due to the fact that the application of conventional risk assessment methods regarding the detailed safety review can only be applied in the advanced concept phase, the potential of modularization is not exploited. There are following disadvantages:

- Potential of modularization particularly the reuse of already available P&IDs of modules remains unused for a long time
- The flexibility of modularly built plants conflicts with the overall detailed safety review as any process modification has to be assessed again
- There is a no systematic safety review from process design phase to the application for approval that uses available knowledge to identify potential hazards

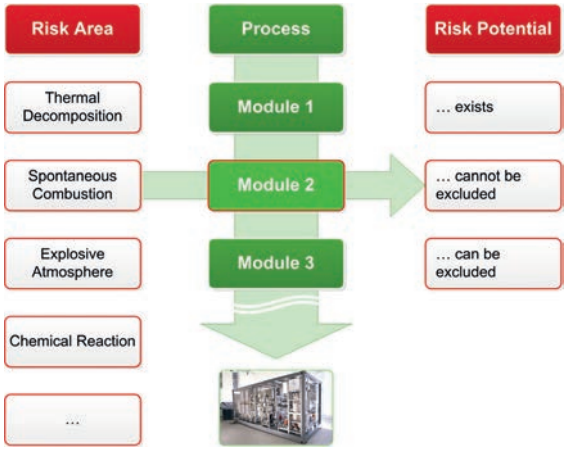

Figure 1: Workflow of the intra-modular safety assessment in an early phase of the process design.

For that reasons the development of a two-step safety assessment approach is necessary. Based on intra-modular safety assessments (Figure 1) and the support of a module database an early evaluation proves the operational fitness of modules already in the planning phase. The intra-modular approach focuses on safety relevant aspects and intra modular interactions. The area under consideration of the intra-modular assessment refers to the equipment, which is built in a module and the direct surroundings.

With the restriction to a manageable modular subsystem and the relevant module information from the module database, module relevant risk fields can be identified or excluded in an early stage of a project.

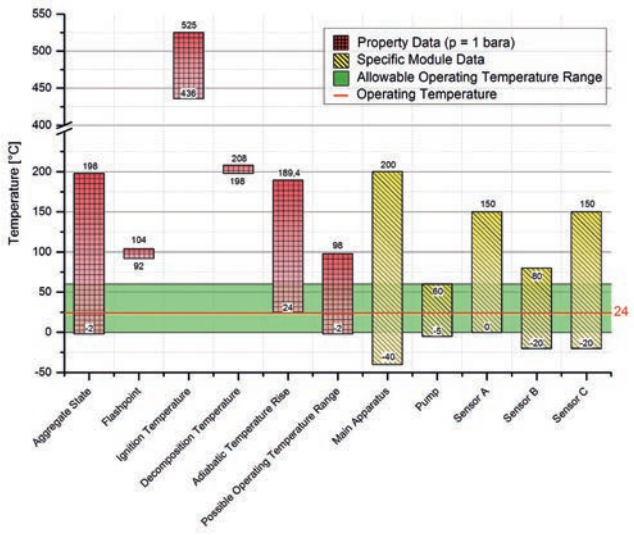

Figure 2: Applicable modular operating window (Temperature).

An essential advantage of the early safety analysis method is that after hazard identification the time for the modification or in worst case the time for a complete new development of a module up to the next project phase extends. To ensure a safety status of a production plant, a safety reassessment has to be executed after every variation of process parameters or structural modifications. On this account strategies are developed that allow first effort estimations. One strategy is the categorizing of modules in operating windows (Figure 2) regarding to substance classes, reaction classes, pressure and temperature ranges etc. After the intra-modular pre-assessment, an inter-modular safety assessment that assesses the interaction of the modules takes place.

Publications:
C. Fleischer, J. Wittmann, N. Kockmann, T. Bieringer, C. Bramsiepe, CIT 87 (9),1258-1269 (2015).
C. Fleischer, T. Bieringer, N. Kockmann: Poster Presentation „Safety Aspects in Planning and Construction of Modularly Built Production Plants", ECCE-EPIC5.

Contact:
christoph.fleischer@udo.edu
norbert.kockmann@udo.edu

Design of a Lab-scale Continuous Tubular Cooling Crystallizer

Development of Innovative Continuous Production Processes in Flexible Devices

Lukas Hohmann, Norbert Kockmann

A tubular device has been designed to develop continuous solution crystallization processes on lab-scale. Experimental characterization of residence time distribution, axial temperature profile and heat transfer was carried out. The amino acid system L-alanine (water) was used for unseeded and seeded case studies.

Continuous production processes offer various advantages, e.g. according to product quality, resource and energy efficiency, or process safety. Therefore, large-scale products in the chemical industry are manufactured in continuous operation. Even though the advantages of continuous production can be generally considered as well for small-scale products, such as fine chemicals and pharmaceuticals, these products are conventionally produced in batch operation. This can be attributed to a lack of suitable continuously operated devices for early stage process development on lab-scale. Thus, process development is still often carried out in the batch mode, which hinters a later shift to continuous operation.

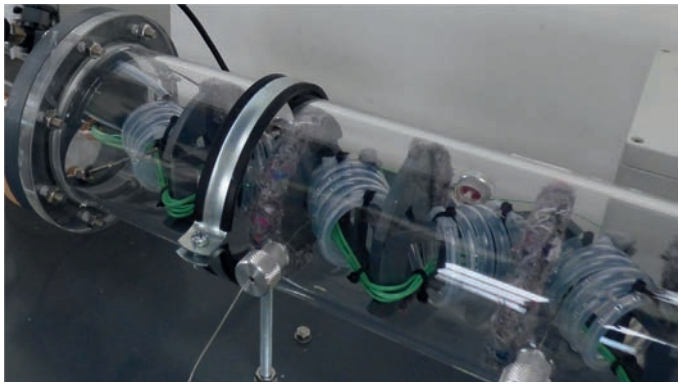

Figure 1: Tubular crystallizer with jacket pipe on lab bench.

For most fine chemical and pharmaceutical products, crystallization is an important downstream operation. The tubular crystallizer, which was designed in this project, consists of fluorinated ethylene propylene (FEP) tubing with an inner diameter of d_i = 4 mm. The nominal mass flow rate was set to 10 g min^{-1} of aqueous amino acid solution. The tubes are coiled on a supporting structure with multiple 90° bends (see Figure 1), creating the coiled flow inverter (CFI) design. Due to the flow on a circular pathway, Dean vortices are induced by centrifugal forces, leading to intensified radial mixing, particle fluidization and a narrow residence time distribution (RTD) close to ideal plug flow (see Table 1), even though the crystallizer is operated in the laminar flow regime.

The hot saturated solution is fed to the tubular section, whereas pre-cooled air is flushed through the jacket pipe in counter-current mode.

Contact:
lukas.hohmann@udo.edu
norbert.kockmann@udo.edu

Table 1: Results of experimental RTD characterization, step-response experiments, tracer: $Na_2S_2O_3$, detection: UV/VIS flow cell (λ = 219 nm).

$\dot{m}$ [g min^{-1}]	τ [min]	Re [-]	Dn [-]	Bo [-]
3.01 ± 0.02	26.1 ± 0.2	17.9 ± 0.1	5.60 ± 0.04	165.6 ± 2.2
4.92 ± 0.03	16.0 ± 0.1	29.3 ± 0.2	9.15 ± 0.06	147.5 ± 4.3
9.94 ± 0.08	7.9 ± 0.0	55.0 ± 0.5	17.18 ± 0.14	113.1 ± 2.6

By adjusting the flow rate and inlet temperature of the cooling gas, similar heat capacity flows $\dot{m} \cdot c_p$ can be achieved on the tube and the shell side. Therefore, an approximately linear axial temperature profile can be adjusted (see Figure 2).

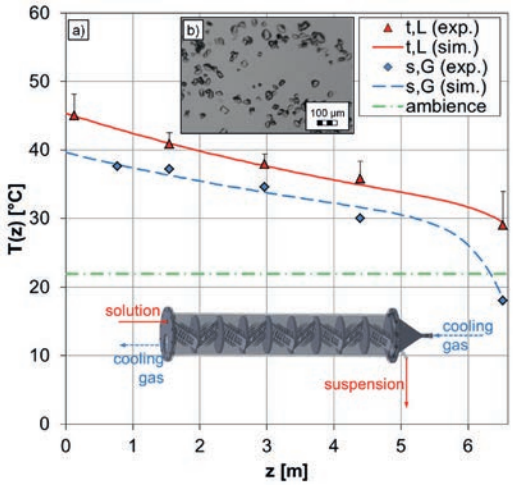

Figure 2: a) Axial temperature profiles in the tubular crystallizer at $\dot{m}_L$ = 10 g min^{-1} and $\dot{m}_G$ = 11.5 g min^{-1}, measured data and simulation results. b) Microscopic image of L-alanine product crystals in the product suspension.

The L-alanine (water) system was used as test system for continuous cooling crystallization. Primary nucleation led to unstable operation and to clogging. Continuous seeding enabled a stabile operation.

Publications:
L. Hohmann, K. Kössl, M. Ostermann, S. Petrusch, T. Westhuis, G. Schembecker, C. Bramsiepe, N. Kockmann, ProcessNet PAAT, "Process Development on Lab-Scale for a Continuous Crystallization Process with a Modular Miniplant", Bruchsal (DE), 2015.

L. Hohmann, N. Kockmann, "Continuous Cooling Crystallization of Amino Acids in a Flexible Milli-Structured Tubular Device", BIWIC, Daejeon (KR), 2015.

L. Hohmann, R. Gorny, N. Kockmann, ProcessNet Kristallisation, „Continuous Cooling Crystallization in a Coiled Flow Inverter (CFI)", ProcessNet Kristallisation, Magdeburg (DE), 2015.

3D-Printed Ceramic Internals for Small Scale Extraction Columns

Iterative Design of 3D-Printed Ceramic Internals which Offer High Chemical and Mechanical Resistance

Sebastian Soboll, Norbert Kockmann

Continuous processes attain increasing interest in production of specialty chemicals and pharmaceutics, in which the amounts of produced goods are rather small. To improve chemical and mechanical resistance and widen the operational windows, Lapp Insulators Alumina GmbH and the Laboratory of Equipment Design have developed new concepts for small-scale plants with integrated key-components made of ceramics. The development of a small scale extraction column is presented with ceramic internals made of Al_2O_3 that are produced by 3D-printing.

Whenever aggressive substances have to be handled, the applied apparatuses must provide high chemical resistance. In case of laboratory scale extraction columns, the column shell is usually made of glass, which is not affected by most chemicals. However, the typical material used for the column internals is ordinary stainless steel, which is vulnerable to highly aggressive compounds. In addition to highly corrosion-resistant steels, such as Hastelloy or Inconel, ceramics are also a promising raw material for the manufacture of these internals.

This work presents the whole workflow from the 3D-construction of the internals to their fabrication and to their experimental evaluation. The experiences gained in the fabrication and characterization steps are used to refine the design of the internals, resulting in an iterative process. In the 3D-construction step, stirrers, plates and bearings are designed using the CAD program SolidWorks. The internals have to fit into the existing DN15 extraction column of the Laboratory. The fabrication is done by LAPP Insulators Alumina GmbH. The applied material is aluminum oxide which is printed as a mixture with a solvent and a binder. After the printing, a drying step, the removal of the binder and the sintering step follow. Finally, a slight mechanical machining of the parts is done. Figure 1 shows some of the prototypes that were manufactured.

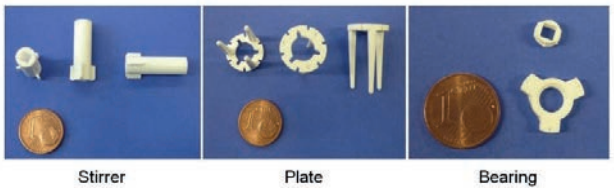

Figure 1: Prototypes of the ceramic internals.

For the experimental characterization, the internals are integrated into the DN15 stirred-pulsed extraction column. While the plates can easily be stacked one above the other within the column, the stirrers are mounted on a central stirrer shaft, which is connected to the stirrer drive and supported by the bearing. In case of the first plate prototype, difficulties occurred during the fabrication, leading to inaccurate dimensions of the plates. Since these plates were not applicable within the column, only the stirrers were characterized at first. Figure 2 presents photos of the dispersion generated by the stirrers at different rotational speeds.

Figure 2: Photos of the dispersion at different stirrer speeds.

At 900 rpm, the dispersion is spatially uniformly distributed and small droplets are generated with a mean Sauter diameter of 0.6 mm.

By modifying the design of the plates, the difficulties with their fabrication were eliminated. After the integration of both stirrers and plates into the column, the maximum capacity and extraction efficiency were determined. At a stirrer speed of 400 rpm and a load of 7.5 $m^3/(m^2h)$, 12 theoretical stages per meter are achieved, which is in the same range as for metal internals at the same operating conditions. However, the capacity is much lower in case of the ceramic internals. Consequently, further design iterations have to be performed in order to optimize the structure of the internals.

Publications:
S. Soboll, I.C. Stark, C. Schulze, N. Kockmann, K. Sauerzapfe, H. Wampers: Jahrestreffen ProcessNet Fluiddynamik und Trenntechnik 2015, lecture „Miniaturized Extraction Column with Ceramic Internals“, Bamberg (2015).

S. Soboll, I.C. Stark, C. Schulze, N. Kockmann, K. Sauerzapfe, H. Wampers: 2015 AIChE Annual Meeting, lecture “Additive Manufactured Ceramic Internals for Small Scale Extraction Columns”, Salt Lake City (2015).

Contact:
sebastian.soboll@udo.edu
norbert.kockmann@udo.edu

Coiled Flow Inverter for Single Stage Extraction Applications

The Effects of Secondary Flow Profiles along with their Alternating Inversions on the Liquid-Liquid Mass Transfer within Helically Coiled Tubular Devices

Safa Kutup Kurt, Norbert Kockmann

Process intensification via miniaturization has become an attractive research field for industry and academia especially for the production of fine chemicals and pharmaceuticals. Additionally, small-scale equipment enables rapid process development in the lab with consistent scale-up capability. Tubular devices with dedicated arrangement are cost-efficient, reliable, and can serve for different purposes. In this work, the design and the characterization of tubular devices are introduced for the liquid-liquid mass transfer processes.

Coiled flow inverter (CFI) is a type of helically coiled tubular device (HCTD), which includes 90°-bends in its specific structure with a certain design configuration. The direction of the centrifugal forces that induce the formation of the secondary flow profile in HCTDs is changed by introducing 90°-bends (Figure 1). As a result, the complete inversion of the flow can be achieved and thus the radial mixing can be further enhanced in CFI in comparison to helically coiled tube (HCT). Hence, a narrow residence time distribution can be achieved even in a flow reactor at laminar flow regimes [1].

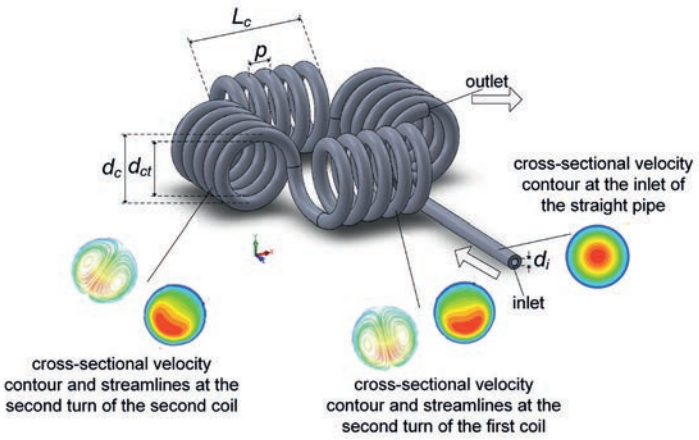

Figure 1: Design parameters of a frame-wise CFI configuration and the cross-sectional velocity contours at the inlet, before, and after (with streamlines) 90° bend.

This work presents the experimental characterization of the liquid-liquid (L-L) mass transfer in microstructured helically coiled tubular devices, i.e. coiled flow inverter (MCFI), and helically coiled tube (MHCT). A comparison between these devices and straight capillaries (SC) is introduced in terms of the extraction efficiency by utilizing n-butyl acetate / acetone / water test systems for L-L extraction.

The complete experimental setup (Figure 2) incorporates three main steps, i.e. the generation of L-L slug flow patterns, residence time (RT) for L-L mass transfer, and continuously working, in-line L-L phase splitter.

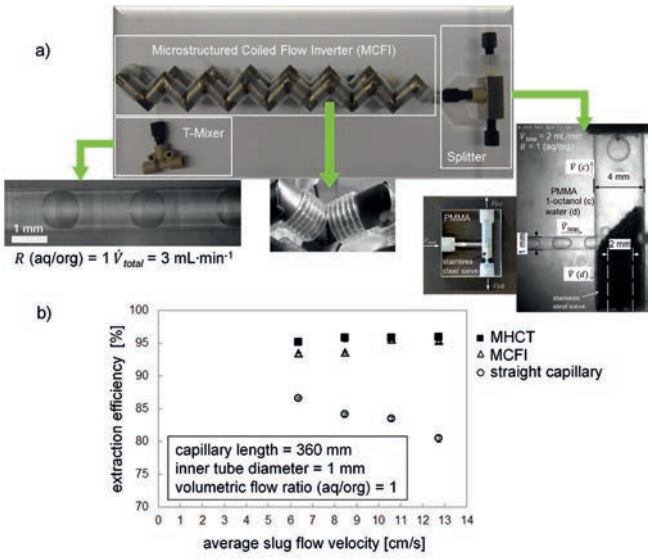

Figure 2: a) Complete experimental setup with MCFI as RT unit; b) Extraction efficiency as a function of mean slug flow velocity [2].

Extraction efficiency results revealed that the MHCT and MCFI provide better extraction efficiencies up to 20% in comparison to SC (Figure 2). Volumetric L-L mass transfer coefficient values in MHCT and MCFI were 1.5 to 2 fold greater compared to SC. Therefore, HCTDs can be applied in L-L extraction processes requiring longer residence times due to the slow mass transfer rates, e.g. a single stage continuous extraction unit or a back extraction step in a complete extraction process [2].

Contact:
kutup.kurt@udo.edu
norbert.kockmann@udo.edu

Publications:
[1] S.K. Kurt, M.G. Gelhausen, N. Kockmann, Chem. Eng. Technol., 38(7), 2015.
[2] S.K. Kurt, I. Vural Gürsel, V. Hessel, K.D.P. Nigam, N. Kockmann, Chem. Eng. J., 284, 764-777, 2016.

Plant and Process Design (APT)

Identification of Agglomeration Processes within the Crystallization Process Chain

Stefan Heisel, Lisa-Marie Terdenge, Kerstin Wohlgemuth

The quality of crystalline products is primarily dominated by crystallization conditions but influenced by further downstream processes like solid-liquid separation and drying as well. Through uncontrolled agglomeration during all steps within the crystallization process chain, the purity or crystal size distribution (CSD) can be affected negatively. Using the width of the CSD (d_{90}-d_{10}), the overall agglomeration degree (Ag) as well as the agglomeration degree distribution (AgD), the crystalline product batches of L-alanine/water and adipic acid/water are quantified and compared to each other before and after downstream processing to identify the most critical process step.

Solid-Liquid separation and drying of the crystalline product batch may have a huge effect on the crystal form and therewith purity (Figure 1). Therefore, localization of the process steps where agglomeration takes place is a first step in optimizing the whole process chain with respect to a higher product quality.

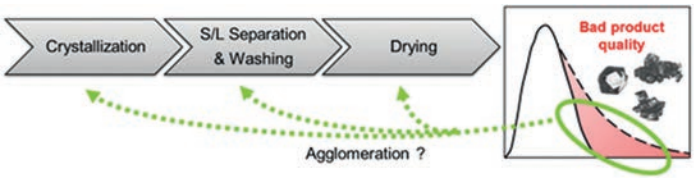

Figure 1: Sequences in a crystallization process chain (left) and product crystal size distribution (right).

To determine whether a crystalline particle is agglomerated or not, image analysis is performed. The tool calculates the values for specific image descriptors like the diameter of a coextensive circle or the number of concave points for every single crystalline particle. With this information obtained, discriminant factorial analysis is applied to the data set, classifying the crystals automatically. The results are used to calculate the overall agglomeration degree (Ag), defined as the number of agglomerates to the overall number of crystalline particles. Moreover, the Ag for every single size fraction of the CSD is calculated, resulting in the AgD curve. These characteristic variables are used to characterize the crystalline product batch not qualitatively but quantitatively as well.

Both L-alanine/water and adipic acid/water (Figure 2) crystalline product batches were analyzed directly after the crystallization step (dashed lines) as well as after the drying step (solid lines). As can be seen, L-alanine crystals show a relatively low Ag right after the crystallization step with the AgD showing a low amount of agglomerates for most of the size fractions. Nevertheless, after solid-liquid separation and drying the L-alanine crystals strongly agglomerate, indicating that the agglomeration mainly takes place in or between these steps of the downstream process.

On the other hand, the AgD of the adipic acid crystals shows no significant difference before or after the downstream process steps, suggesting that the agglomeration of the crystals mainly occurs during the crystallization process itself.

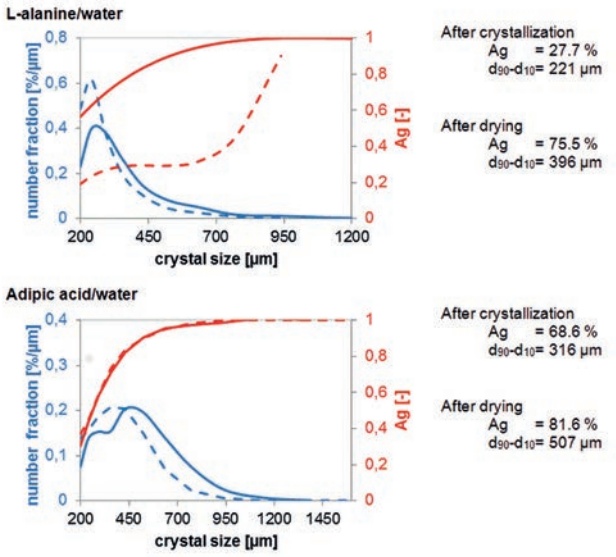

Figure 2: CSD (blue) and AgD (red) of L-alanine/water (top) and adipic acid/water (bottom) crystalline product batches directly after crystallization (dashed lines) and after drying (solid lines).

The differences in agglomeration behavior of L-alanine/water and adipic acid/water crystalline product batches show the need for understanding the agglomeration processes in certain process steps. Therefore, future research should investigate the influence of specific process parameters like drying temperature on crystal agglomeration and the used chemical system in detail.

Contact:
kerstin.wohlgemuth@bci.tu-dortmund.de
stefan.heisel@bci.tu-dortmund.de

Publications:
L.-M. Terdenge, S. Heisel, K. Wohlgemuth, G. Schembecker, Chemical Engineering Science 133, 157-169 (2015).

Lipase Catalyzed Hydrolysis of Hardly Soluble Substrates using Centrifugal Partition Chromatography as Novel Multiphase Reaction System

New Innovative Reactor Concept for Solid Free Immobilization of Enzymes, *in-situ* Product Removal, Processing of Non-Polar Substrates

Jonas Krause, Thomas Oeldorf, Gerhard Schembecker, Juliane Merz

Multi-phase reaction systems, mostly aqueous organic systems, are used in enzyme catalysis to convert hydrophobic substrates which are hardly soluble in aqueous media. In this study, a Centrifugal Partition Chromatograph (CPC) is evaluated as a compact device for enzymatic multi-phase reaction. A process design procedure to systematically select the aqueous and organic phase to achieve stable and efficient reaction rates and the operation conditions of the CPC for efficient mixing and separation of the phases is proposed. The procedure is applied to the hydrolysis of 4-nitrophenyl palmitate with a lipase derived from Candida rugosa*. It was shown that the hydrolysis rate of 4-nitrophenyl palmitate was two times higher in Centrifugal Partition Chromatography than in comparable stirred tank reactor experiments.*

Different approaches to enhance the use of multi-phase systems for enzymatic reactions are available. Strategies like genetic engineering to stabilize the enzymes towards organic solvents and harsh process conditions or different reactor concepts, ranging from classical mixer-settler devices to membrane contactors, to increase mixing or interfacial area for mass transfer, respectively and/or to enhance phase separation to get a product rich phase. In this content the CPC as a liquid-liquid chromatography device is investigated as an alternative reactor concept. In CPC one phase of any two-phase system is immobilized and used as stationary phase. The immobilization is achieved in a chamber system that is arranged around a rotary axis. By rotating the system a centrifugal field is generated which keeps the stationary phase in the chamber cascade. The second phase is pumped through the stationary one and therefore referred to as mobile phase. The benefit of this technique is that a large interfacial area for an efficient distribution of components between the two phases is created while separation of the phases is allowed in one device.

CPC is commonly used for the purification of natural exracts. In this study the Centrifugal Partition Chromatography is investigated as a new reactor concept for aqueous-organic enzyme catalysis. The stationary liquid phase is used to immobilize the catalytic active enzyme in an aqueous solution without handling solid materials or functionalizing surfaces as proposed for other multi-phase reactor concepts. The mobile organic phase supplied the substrate and removed the product simultaneously. The concept is presented in Figure 1.

A methodology for designing biocatalytic processes in CPC was developed and tested by the hydrolysis of 4-nitrophenyl palmitate using a lipase from *Candida rugosa*. As enzymes were used the preservation of their activity was of main importance during the selection of the biphasic system.

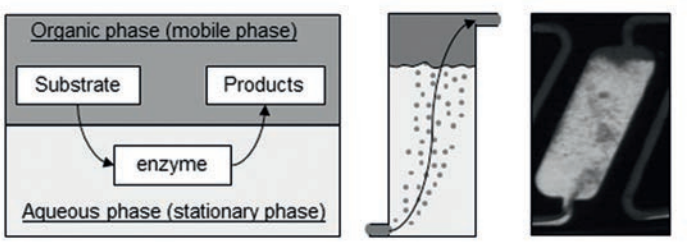

Figure 1: From left to right: Basic scheme of enzymatic multi-phase biocatalysis; CPC chamber in ascending mode (aqueous catalytically stationary phase (light)) and organic mobile phase (dark); Image of hydrodynamic in a single CPC chamber.

After screening several buffers (pH-value, buffer type) and solvents, a phase system consisting of MTBE and 50 mM MOPS buffered aqueous solution at pH 7.2 is chosen and a stable conversion of 4-nitrophenyl palmitate in the biphasic system could be achieved. To evaluate the reaction performance in CPC, stirred tank reactor experiments are run in parallel.

The conversion in CPC was two times higher than in stirred tank reactor experiments, although the phases in CPC were not completely emulsified shown by videos taken during the experiments. It is assumed, that the dispersion and simultaneously settling of the mobile phase in each chamber of the multi-chamber cascade and the mixing of the stationary phase by the mobile phase increased the overall performance as diffusion of substrate and/or enzyme to the interface was not limiting. In addition, the lipases are not trapped at interfaces as interface is continuously generated and destroyed.

Publications:
J. Krause, T. Oeldorf, G. Schembecker, J. Merz; Enzymatic Hydrolysis in an Aqueous Organic Two-Phase System Using Centrifugal Partition Chromatography; J. Chromatogr. A; 1391 (2015) 72-79.

Contact:
juliane.merz@bci.tu-dortmund.de

Biomaterials and Polymer Science (BMP)

Non-Cytotoxic Antimicrobial Polymers: Hydrophilic Polyionenes

A new Class of Antimicrobial Polymers

Arne Strassburg, Frauke Kracke, Julia Wenners, Anna Jemeljanova, Jannis Kuepper, Hanne Petersen, Jörg C. Tiller

Antimicrobial polymers are an alternative to low molecular weight biocides and potentially even to antibiotics. According to the literature antimicrobial polymers are supposed to be amphiphilic cations, which makes them inevitably toxic to mammalian cells, because they act at the cell membrane. Here, we could show that hydrophilic polycations are not only very quick killing biocides but also show no toxicity towards blood cells, which suggests that they act differently compared to amphiphilic polycations.

Antimicrobial, amphiphilic polycations follow the general motiv of the antimicrobial membrane-active peptide Magainin. Due to their relatively high toxicity, they are rarely FDA-approved. Interestingly, hydrophilic polycations are also known to be antimicrobially active, but do not structurally mimic Magainin. We proposed that they may act differently and are therefore not cytotoxic towards mammals.

In order to investigate this poly(4en,4en-ionene), poly(6,6-ionene) and poly(3,4en-ionene) (PBI_n) were synthesized by polyaddition of *N,N,N´,N´*-tetramethyldiamines and the respective α,ω-dibromoalkanes. All polyionenes showed similar very good antimicrobial activities against *E. coli*, *S. aureus* and *S. mutans* in terms of minimal inhibitory concentration (MIC), the concentration where 99% of all bacterial cells are inhibited in growth. The microbial cells were even killed by more than 99.99% after only one min contact at the respective MIC. That is very efficient and ultrafast. Additional, no lysis (less than 1 %) of porcine red blood cells (RBC) was measured even at concentrations of 40000 µg/mL. Typically, hemotoxicity is given as concentration, where 50 % of the cells are lysed (HC_{50}). This result shows that the variation of the alkyl groups in the main chain from propyl to hexyl makes no significant difference in biological activity. Measurements of the novel polymer PBI_n against various Gram-positive and Gram-negative bacteria strains revealed that it kills microbial cells with very high HC_{50}/MIC selectivities of more than 20000 for *S. epidermidis*, which is the highest ever recorded value for antimicrobial polymers.

To obtain insights in the structure-activity-relation of the PBI, we prepared defined macromolecules with narrowly distributed molecular weights and controlled end groups (bromine, amine, alkyl) up to 5000 g/mol by sequential synthesis and tested their antimicrobial potential and cytotoxicity for RBCs. The investigations of the compounds showed that the antimicrobial activity increases with growing molecular weight and the nature of the end groups influences the activity particularly for smaller molecular weights (Figure 1).

Further, the antimicrobial activity of the PBI_n is specific for the investigated bacteria strains. The identified influences can be used to create various non-hemotoxic biocides with broad spectrum or microorganism-specific activity. Moreover, PBI can be used to detoxify antimicrobial monomers such as DTAC (dodecyltrimethylammonium chloride) without losing the antimicrobial activity.

The found structure-activity-relations of PBI as representative of hydrophilic, antimicrobial polymers, is profoundly different from amphiphilic, antimicrobial polymers. Particularly, the high selectivity for mammalian cells calls the commonly proposed working mechanism of membrane disruption in question. Thus, hydrophilic polycations were identified as a unique class of antimicrobial polymers.

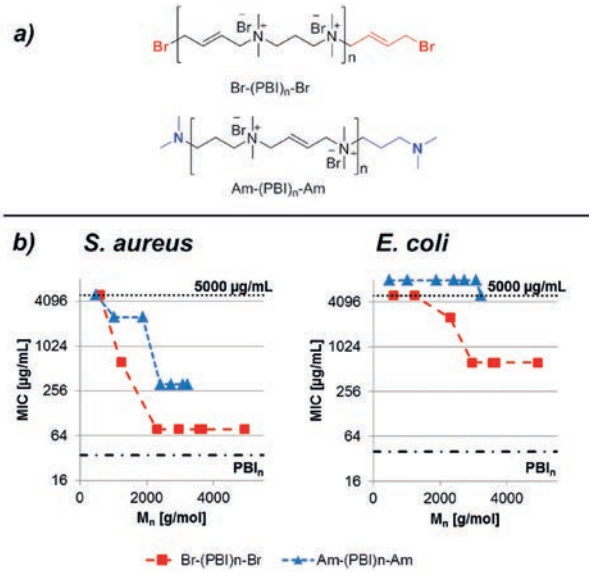

Figure 1: Chemical structures (1a) of PBI_n with specific end groups (bromine and amine) and their dependency of the antimicrobial activity (1b) against *E. coli* and *S. aureus* (below) of the sequential synthesized PBI_n. Additionally, the MIC of PBI_n (– ·) and the maximal concentration of MIC (····5000 µg/mL) are shown as dotted lines.

Contact:
arne.strassburg@tu-dortmund.de
joerg.tiller@tu-dortmund.de

Publications:
A. Strassburg, F. Kracke, J. Wenners, A. Jemeljanova, J. Kuepper, H. Petersen, J.C. Tiller, Macromolecular Bioscience 15 (12), 1710-1723 (2015).

Combining Lotus-Effect with Antimicrobial Contact-Activity

Protecting Surface Infection of Silicone by Fungi and Bacteria

Nicolas Rauner, Christoph Mueller, Sabine Ring, Sara Boehle, Arne Strassburg, Jörg C. Tiller

Silicones are an important factor for technical progress and irreplaceable in many applications, so the market for silicone products is still growing with sales totaling 15 billion US$ in 2013. Silicone elastomers exhibit excellent material properties, but they are either susceptible for fungi growth or filled with biocides causing allergies. Non-allergen, contact-active antimicrobials are not used, because they lead to a loss of the water-repelling properties of silicone that counteracts the antimicrobial effect. Here we show the first example for equipping silicon with the contact-active antimicrobial DOW5700 simultaneously improving the hydrophobic surface properties by a Lotus-Effect.

DOW5700 is known from hydrophobic, contact-active antimicrobial glass coatings. The hydrophobicity is caused by its long C_{18}-group shielding the polar ammonium group (Figure 1). Unfortunately, applying DOW5700 onto silicone results in rather hydrophilic surfaces without antimicrobial activity. The reason might be the favored interaction of the hydrophobic C_{18}-group with the silicone resulting in an inversed attachment of DOW5700 compared to glass, pointing the hydrophilic anchor group away from the hydrophobic surface (Figure 1). In order to solve this problem we developed a concept to equip silicone surfaces with DOW5700 by applying modified SiO_2-nanoparticles instead of modifying the surface directly. Besides the antimicrobial effect this should also grant ultrahydrophobic properties to the surface caused by the formed microstructure. Having established the synthesis, the modified nanoparticles form a transparent, stable colloidal solution in $CHCl_3$, while unmodified particles sediment directly. Applying the modified particles on a silicone elastomer results in a strong adhesion of the particles to the surface, contrary to glass where the particles are easily removable.

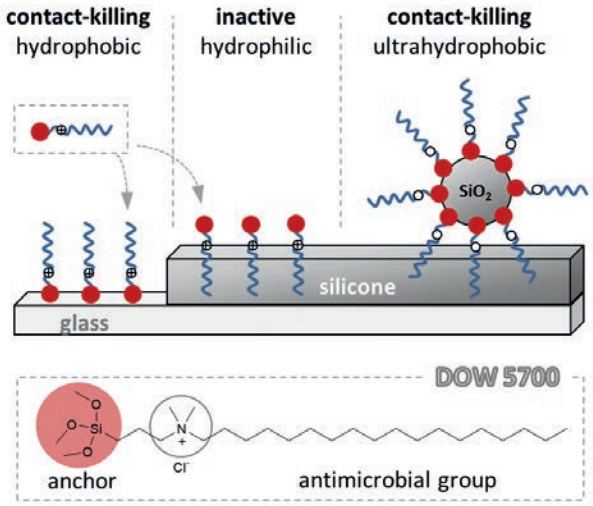

Figure 1: Bonding of DOW5700 and modified SiO_2-nanoparticles on glass/silicone with the resulting surface properties.

Placing a drop of water onto such a silicone particle coating, leads to no wetting of the surface and a contact angle of 155° (Figure 2). The drop easily rolls off when tilting the surface by just 5°, confirming a Lotus-Effect. The contact-active, antimicrobial effect was investigated by spraying *Staphylococcus aureus* on a particle coated silicone surface. After incubation and dyeing no bacteria growth was visible in the coated region unlike to the surrounding area.

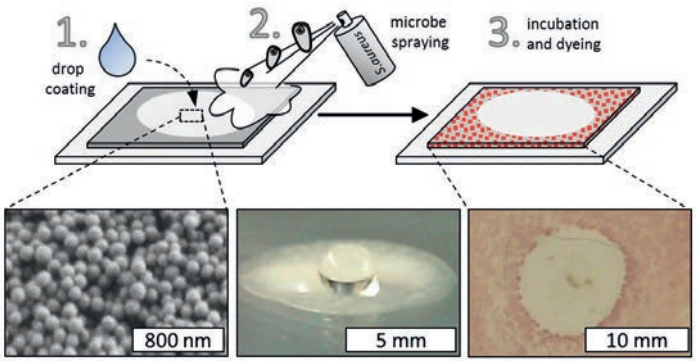

Figure 2: DOW5700 modified particles are drop coated on a silicone surface (1.) forming a dense surface layer. Additionally an image of water drop placed on the coated surface is pictured. In order to measure the antimicrobial properties *Staphylococcus aureus* is sprayed (2.) onto the surface. (3.) shows the sprayed sample after incubation and dyeing.

The modified nanoparticles are easily applicable and besides silicone also suited to coat other hydrophobic polymers, like polyethylene e.g. for an antimicrobial design of air filters.

Publications:
N. Rauner, C. Müller, J. C. Tiller; TU Dortmund. Derivatized Silicone Dioxide Nanoparticles. European patent WO 02015189405; patent registered 12.06.2014, publicized 17.12.2015.

Contact:
nicolas.rauner@tu-dortmund.de
joerg.tiller@tu-dortmund.de

Programming of Shape Memory Natural Rubber (SMNR) for Near-Discrete Shape Transitions

The First Shape Memory Material with a Real Trigger Point (instead of a Trigger Region)

Dominik Quitmann, Frank Katzenberg, Jörg C. Tiller

Typical shape memory polymers and even metal alloys show a shape transition over a broad temperature-range of 10 K and more. Cold-programmed shape memory natural rubber (SMNR) exhibits one of the most narrow temperature-induced shape transitions and recovers more than 80% of its original shape within 1 K. Unfortunately, the highest achievable trigger temperature upon cold-programming was found to be 26 °C, which is too low for most applications. Here we report on a suited method that shifts the trigger temperature of a cold-programmed SMNR to significantly higher trigger temperatures while retaining the narrow shape transition.

SMNR samples of different degrees of cross-linking X_c were cold-programmed, which results in relative low trigger temperatures T_{trig} but extremely narrow trigger ranges beneath 1 K. The strain of the programmed SMNR was kept constant while exposing it to different affine solvent vapors with different concentrations for 12 h, followed by air-drying for further 12 h.

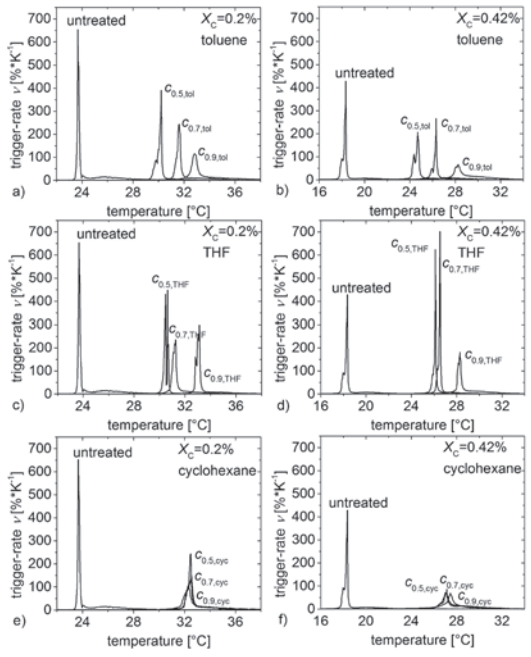

Figure 1: Trigger-processes of two differently cross-linked cold-programmed SMNRs with X_C=0.2% and X_C=0.42%, before and after treatment with different affine solvent vapors. The diagrams show the first derivative of the retraction vs. temperature curve.

The exposure to affine solvents results in all cases in higher T_{trigs} with narrow trigger ranges (see Figure 1). Applying such solvent treatment enables programming even of natural rubber vulcanizates with degrees of cross-linking above 0.4%, which cannot be programmed conventionally to trigger temperatures above room temperature.

Besides affine solvents also the influence of a treatment with non-affine solvent vapors was explored on the trigger temperature and trigger range. To this end, the two differently cross-linked, cold-programmed SMNRs were exposed to ethanol and acetone at equilibrium vapor pressure (EVP), while the strain was kept constant.

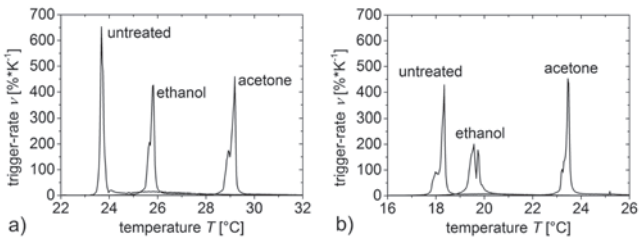

Figure 2: Trigger-processes of two differently cross-linked cold-programmed SMNRs with a) X_C=0.2% and b) X_C=0.42%, before and after treatment with ethanol, and acetone, respectively, under constraint conditions.

It was found that even non-affine solvents are capable of shifting T_{trig} while retaining the narrow trigger range of the originally cold-programmed SMNR (see Figure 2).

Further, it was found that consecutive treatment of cold-programmed, constraint SMNR with different solvent vapors can be efficiently used for systematic altering of its trigger-behavior. This offers a completely new way to specifically adjust the properties of an SMP after programming and to customize it according to its respective application.

Contact:
dominik.quitmann@tu-dortmund.de
frank.katzenberg@tu-dortmund.de
joerg.tiller@tu-dortmund.de

Publications:
D. Quitmann, F. M. Reinders, B. Heuwers, F. Katzenberg, J. C. Tiller, ACS Applied Materials and Interfaces 7 (3), 1486-1490 (2015).
D. Quitmann, M. Dibolik, F. Katzenberg, J.C. Tiller, Macromolecular Materials and Engineering 300 (1), 25-30 (2015).

Shape Memory PVDF Exhibiting Switchable Piezoelectricity

A Multifunctional Material that can be Changed by Temperature and Voltage

Robin Höher, Thomas Raidt, Frank Katzenberg, Jörg C. Tiller

Responsive materials will play a major role in future, since they are able to recognize environmental signals and react to them by self-healing, changing their physical properties or adapting their shape. Important classes of such responsive materials are electroactive polymers (EAPs) exhibiting for instance piezoelectric properties, and shape memory polymers (SMPs) that distinguish themselves by their ability to be deformed to a temporary shape, that is fixed until a suited trigger is added to initiate the recovery process back to their original, permanent shape. Current research is striving for designs of new shape-memory polymers that change more than just their shape upon triggering. Here we present a novel material that combines the properties of shape-memory and electroactive polymers.

Polyvinylidene fluoride (PVDF) was lightly cross-linked by usage of 2,2,4(2,4,4)-trimethyl-1,6-hexanediamine (THDA) as cross-linking agent. PVDF is the most important piezoelectric polymer. Usually it crystallizes in the helical, non-polar *α*-phase, which can be converted by cold-drawing to the *trans*-planar *β*-phase that exhibits a ten times stronger piezoelectricity than quartz. The netchain molecular weight M_c of the resulting PVDF network (x-PVDF) was determined to 29,900 g mol^{-1} according to the Mooney-Rivlin theory.

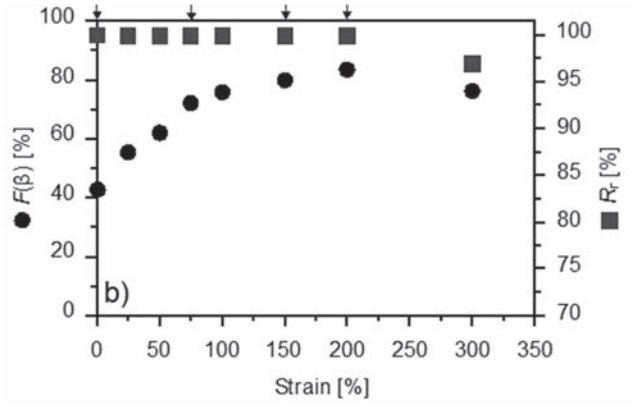

Figure 1: *β*-phase content $F(\beta)$ and recovery ratio R_r in dependence on applied programming strain.

x-PVDF samples were mechanically rolled for programming the temporary shape using a heatable double-roller at 90 °C. We found that programming upon rolling induces the transformation from the non-electro-active *α*-phase to the piezoelectric β-phase. The highest *β*-phase content was found to be 83% for a programming strain of 200% affording a d_{33} value of -30 pm/V. This is in good accordance with literature known values for piezoelectric properties.

Furthermore, x-PVDF shows excellent shape memory properties with fixity and recovery-ratios of 100% up to programming strains of 200% with a trigger temperature of T_{trig} = 167 °C.

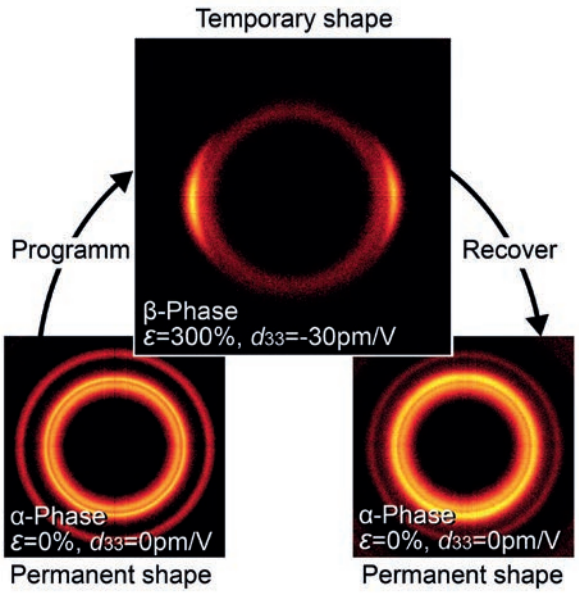

Figure 2: WAXS patterns of the permanent, temporary and recovered permanent shape after heat-triggering, showing the *α*- and *β*-phase and corresponding piezoelectric coefficient d_{33}.

Since thermal triggering this material does not only result in a shape change, but also renders the material non-electroactive, x-PVDF can be cyclically switched upon programming and triggering between the electrically non-active *α*- and the piezoelectric *β*-phase. Thus, we realized a shape-memory polymer with switchable piezoelectricity.

Publications:
R. Hoeher, T. Raidt, N. Nowak, F. Katzenberg, J. C. Tiller,
Molecular Rapid Communications 36 (8), 744-749 (2015).

Contact:
robin.hoeher@tu-dortmund.de
thomas.raidt@tu-dortmund.de
frank.katzenberg@tu-dortmund.de
joerg.tiller@tu-dortmund.de

Ciprofloxacin with a Tail

Polymer Antibiotic Conjugates with High Activity

Martin Schmidt, Christian Krumm, Jörg C. Tiller

Infections caused by multi-resistant bacteria are the reason why the demand for new antibiotics is bigger than ever. Nevertheless, only one new antibiotic per year reaches the market because of exploding costs for drug development. A promising alternative to the development of new antibiotics is the formulation and derivatization of existing antibiotics. Especially, the combination of antibiotics and macromolecules moved in the focus of research because macromolecules as carriers for therapeutics afford lower toxicity, increase solubility, and prolonged activity. Moreover, few polymers possess stealth properties, which can mask the antibiotic. These properties can impede the forming of resistant germs. The here developed polymer antibiotic conjugates (PAC) are promising candidates for a new, less resistant-building antibiotics.

The antibiotic ciprofloxacin (CIP) was covalently attached to poly(2-methyloxazoline) (PMOx), poly(2-ethyloxazoline) (PEtOx) and poly(ethylene glycol) (PEG) via end group modification. A polymer analog implementation was developed, in order to introduce a spacer between polymer and CIP (Figure 1). The structures of the different PACs were proven by ^{1}H NMR and electron spray ionization mass spectrometry.

The antimicrobial activity of these conjugates was tested against different bacteria, three Gram negative strains (*Escherichia coli*, *Pseudomonas aeruginosa* and *Kleisella pneumoniae*) and two Gram positive strains (*Staphylococcus aureus* and *Streptococcus mutans*).

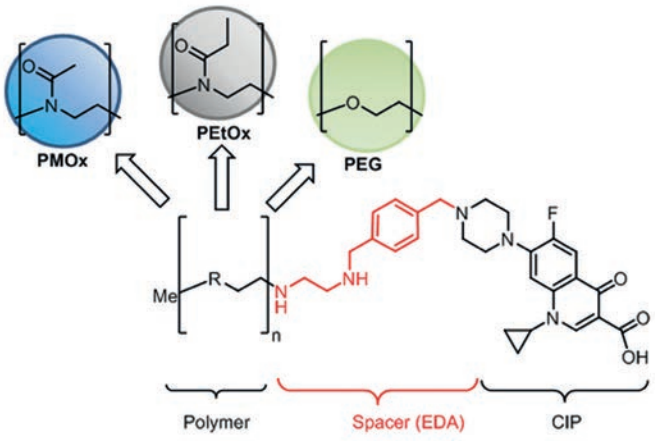

Figure 1: Chemical structure of polymer antibiotic conjugates.

The Me-PMOx$_{30}$-EDA-CIP conjugate shows the same activity against Gram positive strains as CIP. In case of the three Gram negative strains, the conjugate exhibits a drastically lower activity than CIP (Figure 2).

The MIC values of the poly(2-ethyloxazoline) and poly(ethylene glycol conjugates are generally lower than those of the respective Me-PMOx$_{30}$-EDA-CIP, but show a similar trend for the different bacteria.

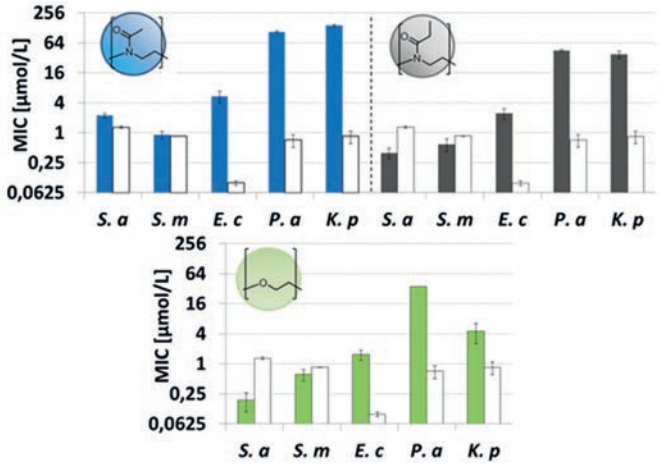

Figure 2: Molar MIC values of the different PACs against *S. aureus* (S.a.), *S. mutans* (S.m.), *E. coli* (E.c.), *P. aeruginosa* (P.a.) and *K. pneumoniae* (K.p.) in comparison to the molar MIC value of CIP against each strain (white columns).

The conjugates demonstrate excellent activity against *E. coli* and the two Gram positive strains.

The data show further that the nature on the polymer backbone has a strong influence on the antimicrobial activity. The activity of the conjugates increases in the order of PMOx<PEtOx<PEG. The greatest effect was found for *K. pneumoniae.*

Future work will explore the properties of the conjugates with respect to biodegradability, blood plasma halve life, and building up of bacterial resistances.

Contact:
martin2.schmidt@udo.edu
joerg.tiller@tu-dortmund.de

Publications:
M. Schmidt, S. Harmuth, E. R. Barth, E. Wurm, R. Fobbe, A. Sickmann, C. Krumm, J.C. Tiller, Bioconjugate Chem. 26, 1950-1962 (2015).

Chemical Biotechnology (BT)

Metabolic Network Response of *Escherichia coli* upon *Trans*-4-Hydroxy-L-Proline Synthesis

Identifying Factors Limiting Whole-Cell Biocatalyst Performance and Understanding Cellular Responses upon Environmental and Genetic Manipulations towards the Development of an Effective Bioprocess for *Trans*-4-Hydroxy-L-Proline Production

Eleni Theodosiou, Oliver Frick, Bruno Bühler, Andreas Schmid

Whole-cells are often used for synthetic reactions that require co-factors/-substrates that must be regenerated. Although regeneration in vitro is possible, in metabolically active cells it is not only easier but also cost-effective. The synthesis of trans*-4-hydroxy-L-proline using Escherichia coli cells is such a case, given that the employed proline hydroxylase (P4H) is α-ketoglutarate (α-KG) dependent, withdrawing α-KG from the host tricarboxylic acid (TCA) cycle. As this reaction depends on α-KG, P4H catalysis strongly interacts with host physiology (Figure 1).*

Understanding the metabolism of the microbial host is essential for the development and optimization of whole-cell based biocatalytic processes, as it dictates production efficiency. For the synthesis of *trans*-4-hydroxy-L-proline from proline, a commercially used whole-cell process has already been reported. However, the interdependency of process conditions, host metabolism, and catalyst performance has not been unraveled yet. By applying both experimental and computational biology tools, such as metabolic engineering and ^{13}C-metabolic flux analysis (^{13}C-MFA), we investigated and quantitatively described the physiological, metabolic, and bioenergetic response of the whole-cell biocatalyst to the targeted bioconversion and identified possible metabolic bottlenecks for further rational pathway engineering.

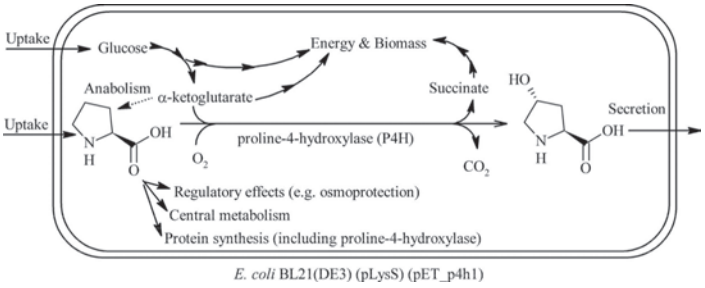

Figure 1: Scheme of proline hydroxylation catalyzed by recombinant *E. coli* containing proline-4-hydroxylase.

A proline degradation-deficient *E. coli* strain was constructed by deleting the *putA* gene encoding proline dehydrogenase. Whole-cell biotransformations with this mutant strain led not only to quantitative proline hydroxylation but also to a doubling of the specific *trans*-4-hydroxy-L-proline formation rate, compared to the wild type. Analysis of carbon flux through central metabolism of the mutant strain revealed that the increased *α*-KG demand for P4H activity did not enhance the *α*-KG generating flux, indicating a tightly regulated TCA cycle operation under the conditions studied. In the wild type strain, P4H synthesis and catalysis caused a reduction in biomass yield. Interestingly, the *ΔputA* strain additionally compensated the associated ATP and NADH loss by reducing maintenance energy demands at comparably low glucose uptake rates, instead of increasing the TCA activity.

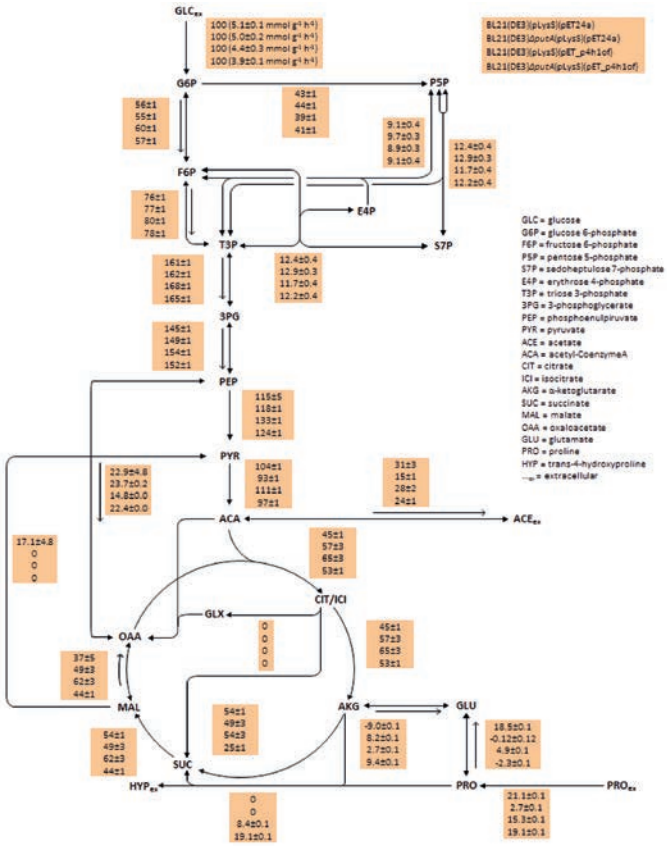

Figure 2: Metabolic fluxes in *E. coli* BL21(DE3)(pLysS) and *E. coli* BL21ΔputA(DE3)(pLysS) strains containing pET-24a or pET_p4h1of during exponential aerobic growth at 30°C in M9 medium containing 5 g L^{-1} glucose (4:1 mixture of 1-^{13}C-labeled and U-^{13}C-labeled glucose) in the presence of 5 mM proline.

Contact:
eleni.theodosiou@ufz.de
andreas.schmid@ufz.de

Publications:
Falcioni F, Blank LM, Frick O, Karau A, Bühler B, Schmid A, Appl Environ Microbiol 79(9):3091 (2013).
Theodosiou E, Frick O, Bühler B, Schmid A, Microb Cell Fact 14:108 (2015).

An Inert Continuous Microreactor for the Isolation and Analysis of a Single Microbial Cell

Katrin Rosenthal, Floris Falke, Oliver Frick, Christian Dusny, Andreas Schmid

Last year we introduced a versatile, chemically inert microfluidic lab-on-a-chip (LOC) device for biological and chemical analyses of isolated microorganisms. It is based on the Envirostat concept and guarantees constant environmental conditions. A new manufacturing process for direct fusion bonding chips with functional microelectrodes for selective and gentle cell manipulation via negative dielectrophoresis (nDEP) was generated.

Microfluidic lab-on-a-chip (LOC) systems, especially as miniaturized cultivation and analysis devices for microbes, open up new possibilities in biological research. Only the application of LOC technologies enables analyses of single microbes with spatiotemporal resolution, ultimately granting insights into the single cell as the basic functional unit beyond the bulk of a microbial population.

The developed LOC system (Envirostat) was kept as simple as possible, while enabling cell separation, cultivation and analysis, as well as medium change and supernatant sampling within one single microfluidic chip (Figure 1). The microfluidic network consisted solely of glass, which led to enhanced chip reusability and minimized interaction of the material with chemical and biological compounds. It offered a defined surface chemistry and exceptional operational stability, maintaining its structural integrity even after harsh chemical treatment. The microelectrode structures remained fully functional after thermal bonding during manufacturing and were proven to be efficient for contactless single-cell trapping via negative dielectrophoresis (nDEP).

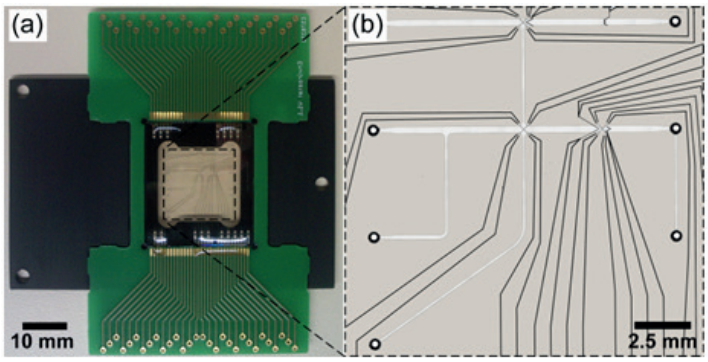

Figure 1: The Envirostat system: (a) The microfluidic chip is directly bonded and mounted on an aluminum plate and wire-bonded to a PCB-board. (b) Microscopic magnification of the chip with microfluidic channels, microelectrodes and in-/outlets.

The new Envirostat system was applied for cultivating the well-described bacterial strain *Corynebacterium glutamicum* (Figure 2). A single cell was trapped with an initial cell volume of 4.6 µm³. The cell volume was constantly increasing over time and resulted in a total cell volume of 8.1 µm³ after 1 h. The volume increase resulted in a specific growth rate of 0.52 h^{-1}. The trapped cell divided after 20 min and the daughter cells had specific growth rates of 0.48 and 0.55 h^{-1}. These rates were significantly higher compared to batch experiments in shake flaks, where cells were growing with a specific growth rate of 0.37 h^{-1} ± 0.03. Faster microbial growth in single-cell perfusion systems is most likely a result of the homogeneous extracellular environment with optimal nutrient supply and permanent removal of secreted metabolic products.

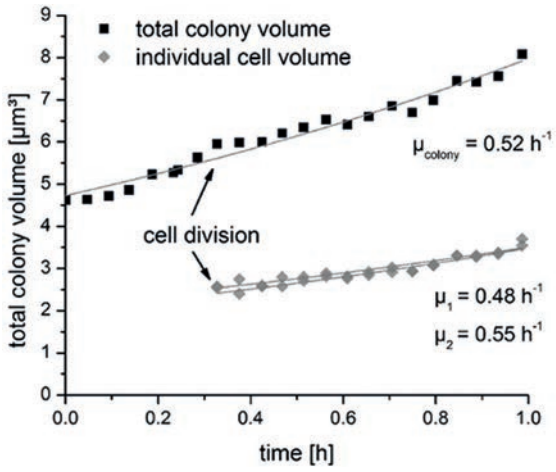

Figure 2: Volume growth of an initially single *C. glutamicum* cell, trapped with nDEP in the inert LOC device. Total colony volume and individual cell volumes were measured over time and exponentially fitted.

We validated the Envirostat system for single-cell production studies with the amino acid secreting bacterium *C. glutamicum.* Intracellular L-lysine production dynamics of individual bacteria were monitored based on a genetically encoded fluorescent nanosensor. In general, it was possible to quantify the dynamic L-lysine-dependent fluorescence-production of single cells.
The results demonstrated the applicability of the presented Envirostat system for pioneering chemical and biological studies, where robustness and chemically inert surfaces are essential parameters for approaching fundamental biological questions at a single-cell level.

Contact:
katrin.rosenthal@bci.tu-dortmund.de
andreas.schmid@ufz.de

Publications:
K. Rosenthal, F. Falke, O. Frick, C. Dusny, A. Schmid, Micromachines 6(12), 1836-1855 (2015).

Biochemical Engineering (BVT)

In-situ Product Removal for the Fermentative Production of Fusicoccadiene

Lisa Halka, Sven Kockelke, Rolf Wichmann

Fusicocca-2,10(14)-diene (FCdiene) has a potential in the pharmaceutical industry as a precursor of several anti-cancer drugs, like fusicoccin A for example. The industrial and commercial production of FCdiene is challenging regarding the producing organism (a genetically modified Saccharomyces cerevisiae *in this case) which cannot be applied for an economical production of FCdiene so far. After improving the product titer in fermentations, an economic separation and purification strategy has to be developed.*

FCdiene molecule's (Figure 1) strong hydrophobicity can be exploited by an *in-situ* product removal strategy due to the limited solubility of hydrophobic compounds in an aqueous fermentation medium. In addition possible negative influences of FCdiene on its own production by *Saccharomyces cerevisae* thus can be avoided. Due to an observable decreasing product concentration in batch experiments after a certain time, two different strategies for the removal of FCdiene from fermentation broth are considered: *in-situ* liquid-liquid extraction and *in-situ* adsorption.

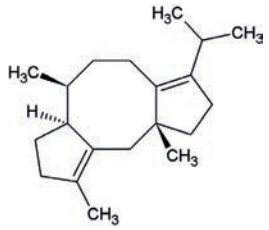

Figure 1: Chemical structure of FCdiene.

For the adsorption of FCdiene from aqueous fermentation broth, several adsorbent materials have been tested *in-situ* in batch experiments and *ex-situ* in cartridges. Depending on these prior observed results and the geometric dimensions one adsorbent was tested in a fixed bed during a fed-batch fermentation process with immobilized cells at a half liter scale (Figure 2).

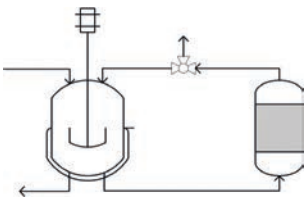

Figure 2: Experimental set-up for the fed-batch fermentation with fixed-bed at lab-scale.

A fermentation time of 69.5 hours is possible. After that the column is blocked with cells in spite of cell immobilization. The column is eluted using ethyl acetate (EtAc) as the most efficient eluent. 0.424 mg FCdiene could be received in total, which relates to a recovery of 8.36 %. It indicates that the fixed bed is not efficient in FCdiene recovery in combination with immobilized cells.

Contact:
lisa.halka@udo.edu
rolf.wichmann @udo.edu

For an *in-situ* liquid-liquid extraction procedure several solvents with different hydrophobicities were tested to extract FCdiene directly from the fermentation broth. The most suitable solvents (EtAc or Bis(2-ethylhexyl)-phthalate (BEHP)) then were applied as the top phase in a two-phase fermentation process in order to determine their influence on the growth of *S. cerevisiae* and the production of FCdiene. This procedure was tested in batch and fed-batch mode. In addition distribution coefficients have been determined to be 2.16 ± 0.23 for EtAc and 1.12 ± 0.08 for BEHP.

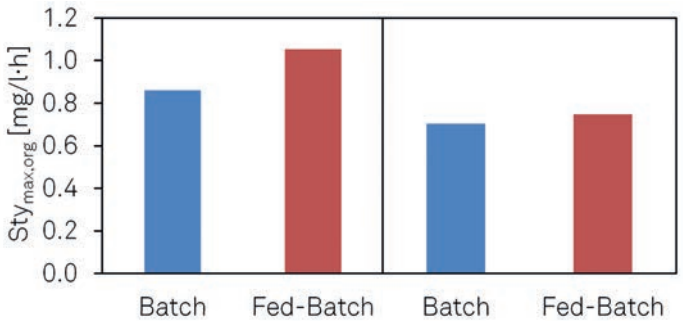

Figure 3: Comparison of space time yields of batch and fed-batch two-phase fermentations with EtAc (left) and BEHP (right).

Figure 3 shows that the space time yield is in both cases a bit higher for the fed-batch mode compared to the batch mode. This shows that higher concentrations can be received in a shorter time. The titer observed in both fermentation modes are in a very similar range (EtAc: batch 61.02 mg L^{-1}, fed-batch 74.70 mg L^{-1}; BEHP: batch 52.81 mg L^{-1}, fed-batch 59.13 mg L^{-1}) compared to fermentations without a second liquid phase (batch 62.75 mg L^{-1}, fed-batch 188.99 mg L^{-1}). Furthermore fed-batch fermentations use a higher amount of substrate than batch fermentations so that the substrate specific product yield ($Y_{P/S}$) is lower for fed-batch fermentations. As an outlook experiments regarding an optimization of the most promising separation method will follow in order to receive a higher amount of pure product.

Publications:
Halka, L., Freder, M., Wichmann, R., "Production of Fusicoccadiene by *Saccharomyces cerevisiae*", Poster Presentation, Himmelfahrtstagung – Scale-up and Scale-down of Bioprocesses, Hamburg, Germany (2015).

Chemical Reaction Engineering (CVT)

Hydrodynamic Analysis of Gas-Liquid-Liquid Slug Flow

Analysis of Flow Patterns and Pressure Drop In a Capillary Reactor

Franziska Horbach, David Hellmann, David W. Agar

The research on liquid-liquid slug flow in microchannels at the chair of chemical reaction engineering has been expanded to gas-liquid-liquid slug flow. The three phase flow offers new opportunities for reactor design and an extended slug flow regime. Experiments with nitrogen, water and different organic phases have been carried out. Based on the experiments, flow pattern and slug sequence can be predicted by capillary number, mass fractions and slug velocity. The measured pressure drop was used to verify a developed pressure drop model for two and three phase slug flows.

Experiments with a continuous organic phase and discrete water and gas phases have been carried out in a one millimeter diameter capillary reactor. Toluene, silicone oil and hexanol were used as organic phases. Flow rates and phase fractions were varied to obtain different flow patterns and pressure gradients. A cross-mixer and a double Y-mixer were used for slug flow generation. The phases were separated in a settler after the microchannel. Due to influence from the measuring volume on the flow pattern, it's disadvantageous to measure pressure drop directly in the microchannel. Therefore pressure drop was measured at the gas feed and exhaust after phase separation. The additional pressure drop was negligible. A digital camera was used to obtain information about flow pattern and slug sequence. All images were analyzed via computer. The performed experiments show interesting results. Depending on volume flow and the used system of substances, gas or liquid slug velocity is higher, which results in different phase sequences. The existence of a third phase stabilizes the slug flow and the transition from slug to bubble flow occurs at higher capillary numbers. This stabilizing effect occurs due to accumulation of bubbles behind a slug (Figure 1a). It is possible that only water slugs develop a continuous phase wall film. In this case they catch up to the slower gas slugs and subsequently lose their wall films (Figure 1b). The transition from gas slugs with wall film to slugs without wall film can be predicted by the capillary number.

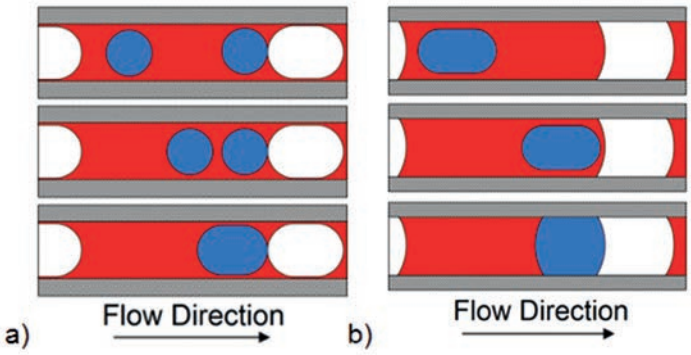

Figure1: a) Slug formation from water bubbles (blue) behind a gas slug (withe). b) Loss of continuous wall film by contact with a filmless gas slug.

The captured images show that mixer geometry has an influence on the resulting flow pattern. A Cross mixer produces a narrower plug length distribution compared to a double Y Mixer. A probable explanation for this result is the existence of two mixing points with independent slug formation frequencies in the double Y mixer. Based on the obtained experimental data, a pressure drop model for two and three phase plug flow was developed. The model can predict pressure drop for the examined fluids with an average error of 16.6 percent (Figure 2). Only the number of slugs in the capillary reactor must still be estimated by experimental data. This work provides a basic knowledge for further research and development on three phase slug flow microreactors.

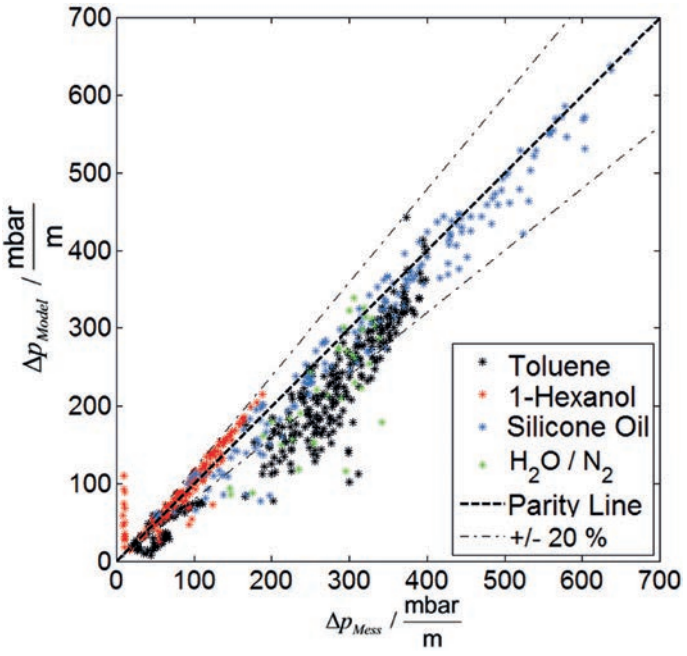

Figure 2: Experimental and calculated pressure drop for different two and three phase flows.

Contact:
david.hellmann@bci.tu-dortmund.de
david.agar@bci.tu-dortmund.de

Process Dynamics and Operations (DYN)

Optimizing Control of a Continuous Polymerization Process in a Tubular Reactor with Multiple Side-Streams

A Control Scheme to Increase the Production Amount While Keeping the Quality Constraints

Reza Hashemi, Sebastian Engell

Intensified continuous processes have a large potential for the production of high quality, high value and customer-specific products at competitive prices in a sustainable fashion. To realize the potential of this technology, tightly controlled, fully automated and optimized production is a must. Starting with the F3 project, the DYN group has investigated the optimizing control of intensified processes, in particular in tubular reactors.

While traditionally following some predefined set points or trajectories is the main goal in the control of chemical processes, from the management point of view, other criteria, such as minimizing the cost or maximizing the thoughput, are important. The concept of optimizing control enables us to define the control problem as an optimization of economically motivated criteria under constraints of the operation conditions or product quality parameters.

We have developed an optimizing controller for a modular tubular reactor which has been designed for the production of different water soluble acrylic acid-based polymers. A schematic view of this reactor is shown in Figure 1.

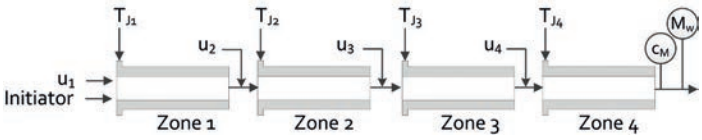

Figure 1. Schematic figure of the modular reactor.

The reactor comprises a total length of 4 meters and a volume of 720 ml. Four side feeds of monomer along the reactor and the jacket temperatures of each zone of reactor, which can be controlled independently, are the manipulated variables to control the product quality and quantity. This reactor set-up is a result of the European Project F3 on intensified modularized continuous production of polymers and speciality chemicals.

The goal of our controller is to maximize the product throughput while the product quality, which is defined by the weight average molecular weight (M_w) and the residual monomer (c_M) of the produced polymer, is kept within given bounds. The polymerization process is described by a set of pdes. The process exhibits steep fronts of state variables along the reactor so that advanced discretization methods must be used and the resulting optimization problems are very large. Simulation results that were obtained with the designed controller for a product changeover scenario are presented in Figures 2 and 3. It can be seen that before the changeover phase (light blue region), the controller increases the first three side feeds gradually and simultaneously reduces the last side feed to zero.

Contact:
reza.hashemi@bci.tu-dortmund.de
sebastian.engell@bci.tu-dortmund.de

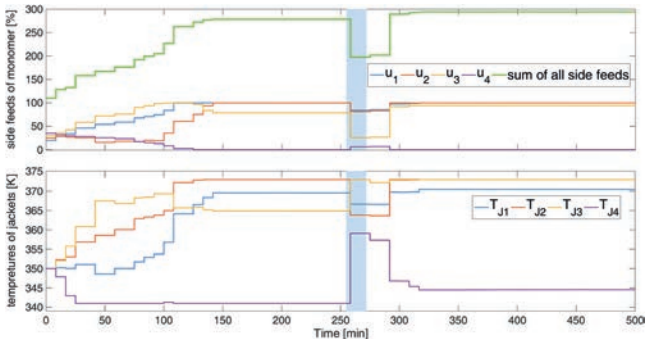

Figure 2. Manipulated variables generated by the optimizing controller.

Also the jacket temperatures of the first three zones are gradually increased while the last zone is set to a lower temperature. The controller increases the product throughput by 2.53 times. In figure 3, it can be seen that the controller is able to satisfy the quality constraints.

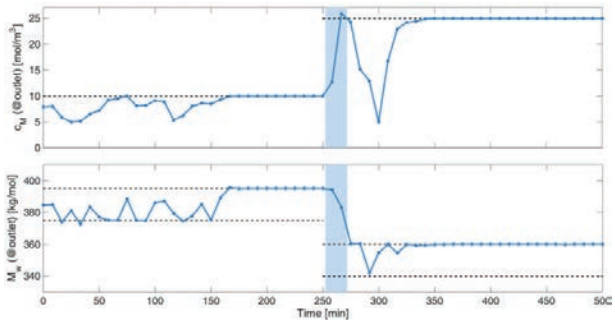

Figure 3. Controlled variables of the reactor system with the optimizing controller.

As the products in the transition phase are considered as off-spec, the designed controller reduces the product throughput in the changeover phase. For this purpose, the controller reduces the side feeds of monomer and manipulates the jacket temperatures to drive the product properties to the new desired values in the shortest possible time. Once the properties of the product are in the new desired range and the transition phase is over, the controller maximizes the throughput again.

Publications:
R. Hashemi, D. Kohlmann, S. Engell, Macromolecular Reaction Engineering, doi: 10.1002/mren.201500034 (2016).
R. Hashemi, R. Schilling, S. Engell, Proceedings of International Symposium on Advanced Control of Chemical Processes, 556-561 (2015).

Fast and Efficient Modelling of Fed-Batch Fermentations for Process Design and Control

A Systematic Modelling Approach Combines the Use of Knowledge of the Metabolism of the Organism and Data-Based Quantitative Analysis to Generate Dynamic Models of Adaptable Complexity

Lukas Hebing[1)], Tobias Neymann[2)], Sebastian Engell[1)]
[1)] DYN, TU-Dortmund, Germany, [2)] Bayer Technology Services, Leverkusen, Germany

In the new modelling procedure, the dynamic influence of the production conditions on the organism is quantified by using a set of Elementary Modes (EM) which appears as macro-reactions with kinetic terms. Reaction rates are estimated from concentration measurements of batch- or fed-batch fermentations and are used for a statistical analysis that reveals the quantitative influence of the process conditions on the metabolic state. The kinetics are chosen on the basis of these correlation and finally the kinetic parameters are fitted to the experimental data.

Fermentation processes are often used for producing high value products, e.g. active ingredients. As changes in the process conditions are allowed in the Quality-by-Design Initiative by the FDA if their effect is understood, operating parameters can be changed to increase the yield or to optimize the product quality. With mathematical models that quantify the influences of the process conditions on the product and on the yield, a characterization of the so-called design space of the process and offline optimization or even online optimizing control are possible. However, due to the lack of time and data and the complexity and the limited quantitative knowledge about the producing organism, sufficiently accurate models are often not available.

The proposed modelling strategy uses background knowledge which is available for most production organisms: the possible cell-internal reactions which form the metabolic network of the cell. So-called Elementary Modes (EM) can be computed from this network. Each EM is a linear combination of reactions inside the cell that are in stationary equilibrium and connects consumption rates of substrates and production rates with a fixed stoichiometry. The EM are used to represent the catalytic activity of the organism as indicated in Figure 1.

A set of EM are identified and selected for inclusion in the process model. A method was developed in which approximated concentration profiles for different selections of EM can be computed by linear programming. These profiles can then be compared with measurement data of the process (Figure 2, left).

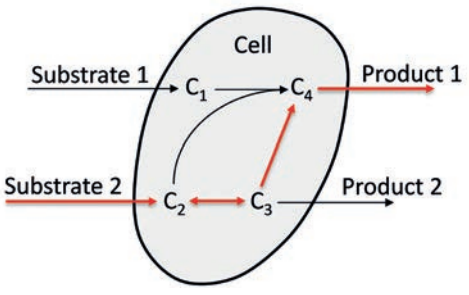

Figure 1: Visualization of an Elementary Mode as a macro-reaction connecting substrates and products of the cell.

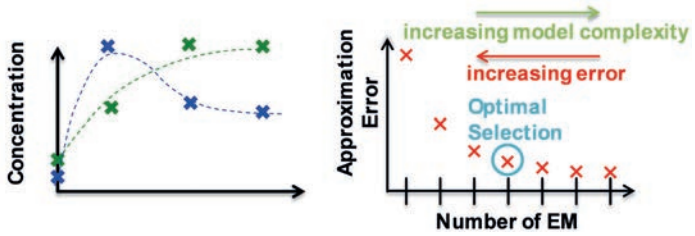

Figure 2: Left: Approximated concentration profile and measurement data of the process. The difference between these two quantities is the approximation error in the right. The Pareto-front shows the trade-off between the number of the EM and the approximation error for different possible sets of EM and approximation error.

The resulting approximation error and the number of selected EM are minimized by a multi-objective genetic algorithm. A Pareto-front for different possible sets of EM is shown in Figure 2 (right). The optimal selection is a set of EM where the measured metabolic behavior can be expressed well enough with a small number of reactions. Thus, the resulting model complexity can be kept as small as possible.

The above mentioned approximation of the concentration profiles also provides trajectories of reaction rates over time. A statistical analysis uses this information to reveal correlations between process conditions as e.g. the pH value or concentrations of substrates with the identified reactions. Kinetic terms are selected based on the results of this analysis. The chosen kinetics can easily be tested separately for each reaction without solving the complete complex nonlinear parameter estimation problem, as it is done usually. This significantly speeds up the selection of the kinetics. As the last step, the kinetic parameters are fitted to the data.

The resulting model describes the dynamics of the process based on basic biochemical insight. If the measurement data is generated within the complete design-space, the model can be used for offline- or online optimization of process trajectories, e.g. of the pH value or of the feeding profile. The fast generation of the model also enables the use of offline optimization techniques during the design phase.

Publications:
L. Hebing, T. Neymann, T. Thüte, A. Jockwer, S. Engell, „Efficient Generation of Models of Fed-Batch Fermentations for Process Design and Control", Proceedings of the DYCOBS/CAB 2016 Conference, Trondheim, Norway (2015).

Contact:
lukas.hebing@bci.tu-dortmund.de
sebastian.engell@bci.tu-dortmund.de

Multi-Criterial Optimization for Decision Support to Improve Energy and Resource Efficiency

Uncover the Inherent Flexibility in Daily Operations of Processing Plants to Improve Energy and Resource Efficiency

Daniel Ackerschott, Sebastian Engell

The high complexity of integrated processing plants complicates the task for managers and operators to find the best operational strategy. It becomes even more difficult when one has to deal with more than one criterion for optimality so that trade-offs between conflicting objectives have to be taken into account. Usually optimisation problems are set-up with a single objective function, and several criteria are combined into one by weighting factors. The result, however, is a single number that does not point out operational alternatives. In contrast, multi-criterial optimisation reveals the room to manoeuvre. Therefore we propose to use multi-criterial optimisation to provide decision support.

In multi-criterial optimization, several objectives are pursued simultaneously. A key concept of multi-criterial optimisation are the Pareto-optimal solutions. These solutions are characterised as points where it is impossible to improve one criterion without degrading at least one other. The Pareto front is the set of Pareto optima and depicts the trade-off between the objectives and reveals important interdependencies. As an example we consider a distillation column that separates a low value substance B from a high value substance A. The latter is obtained as the top product; the low value substance is drawn off at the bottom as a waste stream. Thus, one objective is to maximise the amount of A in the top stream and the conflicting goal is to minimise the steam consumption required for heating the reboiler. By using a large amount of steam it is possible to reduce the losses of A. When the steam consumption is reduced, one has to accept higher losses. Thus, it is up to the operator (or to the plant manager) to choose a compromise between the conflicting goals of a low steam consumption and high product yield.

Within the EU project MORE, the combination of a cooling tower and the Butadiene plant (shown in Figure 1) located at INEOS in Cologne has been investigated in order to evaluate the performance of this approach for decision support. The optimisation goal is the reduction of resource utilisation, while maintaining the production rate and product quality. In the cooling tower model, electricity is the only consumed resource. In the Butadiene plant, a complex distillation process separates a mixture of raw C4 chemicals in order to produce Butadiene as the main product. The two models are connected via the stream of cooling water that is provided by the cooling towers and is used in the Butadiene plant in several condensers. Its temperature strongly influences the overall performance of the destillation columns.

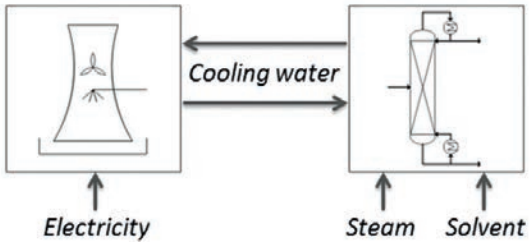

Figure 1: Combination of cooling towers (left) and a Butadiene plant (right) as the case study for resource minimisation.

The Butadiene plant also is a consumer of steam and of a solvent which is necessary to perform the separation task. Due to the interconnections among and within the plants, all three resources (electricity, steam, and solvent) are partly interchangeable. Results of the multi-criterial optimisation can be seen in Figure 2, where computed Pareto optima and an interpolated surface that shows the Pareto front visualise the flexibility of the connected plants.

When one optimum is chosen, further analysis illustrates the most important influencing variables at this optimum in comparison to the current state of the plant. Thereby, the decision-maker is guided to a more resource efficient operation.

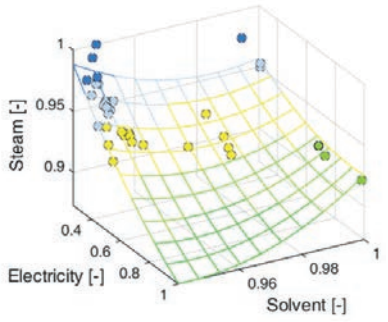

Figure 2: Result of the multi-dimensional optimisation as Pareto points (the surface is a quadratic interpolation).

Contact:
daniel.ackerschott@bci.tu-dortmund.de
sebastian.engell@bci.tu-dortmund.de

Publications:
D. Ackerschott, S. Engell, EURO 2016, accepted.

Dual and Adaptive Control Using Output Feedback Multi-Stage NMPC

Design of a Controller that Handles Estimation Errors in Addition to Plant-Model Mismatch while Improving the Performance by Reducing the Bounds on the Uncertain Parameters

Sankaranarayanan Subramanian, Sergio Lucia, Sebastian Engell

Multi-stage NMPC is a non-conservative strategy to achieve robust constraint satisfaction in the presence of plant-model mismatch. The scheme is extended here to handle the errors of the state estimation in addition to plant-model mismatch. The performance of the controller is further improved by designing the optimizer to choose inputs that implicitly reduce the bounds of the uncertainty in order to improve the objective function (dual control). This results in an improvement of 60% in the objective function for a prototypical CSTR control problem. In addition, we also show the effectiveness of the approach for time varying uncertainties.

Economics-based Nonlinear Model Predictive Control (NMPC) can improve economic objectives for nonlinear systems while satisfying the process constraints over the prediction horizon. If the model is uncertain, there is a need for robust control which is not overly conservative. Multi-stage NMPC is a non-conservative real-time implementable robust scheme which can achieve constraint satisfaction for nonlinear systems under uncertainty (Lucia et al., 2014). The evolution of the uncertainty is modeled by a scenario tree. The important aspect of the approach is that it considers explicitly that measurement information will become available at every new sampling instance and that the decisions that will be taken at every future stage can be adjusted accordingly and thus can act as recourse to counteract the effects of the uncertainties. This improves the performance and reduces the conservativeness compared to the traditional robust NMPC schemes.

In practice, not all state variables are measured but only noisy measurements of some states are available. This additional uncertainty about the current state as well as inexact information about the future states must be taken into account in the control algorithm. The samples of the innovations are modeled as new scenarios in the scenario tree in addition to the parametric uncertainties, and estimation techniques such as the EKF/UKF are used to predict the evolution of the future state estimates. The proposed approach is robust to plant-model mismatches and to estimation errors.

The measurement feedback from the plant can also be used to estimate uncertain parameters. Hence instead of having a global bound on the uncertain parameters, a less conservative local estimate on the bound of the parameters can be obtained online. This information is considered by formulating a dual controller which takes in to account that depending on the available measurements, the bounds on the parameters can be reduced and it chooses a control policy that can implicitly reduce the uncertainty if this helps to improve the control objective because the distance to the constraints can be reduced. The designed dual controller was applied to a CSTR to maximize number of moles produced per hour of the product B ($\dot{n}_b$). The pre-exponential co-efficient of the reaction rate $k_{0,1}$ is uncertain by ±40%. When compared to a standard controller, the dual controller yields an improvement of 60% in the objective for certain realizations of the uncertainty and the results are shown in Figure 1.

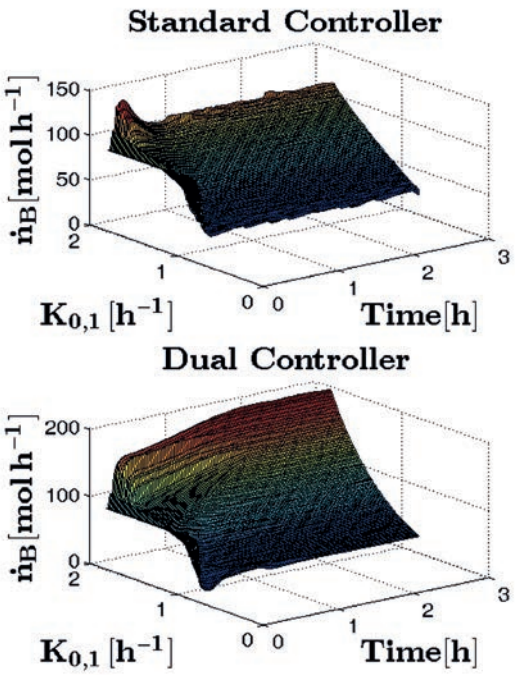

Figure 1: Comparison of Standard multi-stage controller and Dual controller. The improvement in the objective $\dot{n}_b$ by 60% for certain realization of the uncertainty $k_{0,1}$ can be seen.

Publications:
S. Subramanian, S. Lucia, S. Engell, IFAC-PapersOnLine, 48(8), 38-43 (2015).
S. Subramanian, S. Lucia, S. Engell, IFAC-PapersOnLine, 48 (23), 242-247 (2015).
S. Lucia, J. Andersson, H. Brandt, M. Diehl, S. Engell, Journal of Process Control 24(8), 1247-1259 (2014).

Contact:
sankaranarayanan.subramanian@bci.tu-dortmund.de
sebastian.engell@bci.tu-dortmund.de

Solids Process Engineering (FSV)

Aerosol Conditioning for the Preparation of Spray Dried Submicron Particles

A Droplet Separator was Used for Aerosol Conditioning to Produce Small and Uniform Droplets

Ramona Gorny, Gerhard Schaldach, Peter Walzel, Markus Thommes

The preparation of spray dried submicron particles is a significant approach to enhance the bioavailability of poorly water soluble drugs. Since the particle size during the spray drying process is mainly affected by the droplet size, the improvement of the preceding aerosol to produce small and uniform droplets was necessary. The aerosol was conditioned by using a droplet separator before reaching the drying stage. The spray dried particles were in the submicron range and show spherical shape with a narrow size distribution.

The bioavailability of water insoluble drugs is frequently limited by the dissolution rate. According to the Nernst-Brunner equation, the particle size reduction increases the specific surface area and in turn enhances the dissolution rate.
Spray drying is a promising technique for the preparation of submicron particles, since it is a gentle, continuous and single-step process, where particle size, shape and morphology are adjustable by the spray drying conditions. However, the preparation of submicron particles using conventional spray drying is limited. The main problem is the production of small ($d_{50,3}$ < 5 µm) and uniform droplets with conventional atomization techniques. In this work, the aerosol is firstly generated by a pneumatic nozzle containing seven capillaries to disperse the liquid into the gas flow. This primary aerosol was then conditioned by a cyclone separator ($d_{cut\ off}$ = 2.6 µm). The part of the aerosol with a drop size below the cut off diameter reaches the drier.
A 10 wt.% mannitol solution was atomized using compressed air with a constant gas inlet pressure of Δp = 5 bar and a gas mass flowrate in the range of 3.3 – 4.3 kg/h. With a liquid mass flowrate in the range of 1.2 – 6 kg/h, the liquid-to-air mass flow ratio (µ) varies between 0.8 and 1.8. The droplet size distribution was measured by laser diffraction (Spraytec, Malvern Instruments). The measured mean droplet size $d_{50,3}$ of the primary aerosol as well as the conditioned aerosol is shown in figure 1 as a function of the liquid-to-air mass flow ratio.

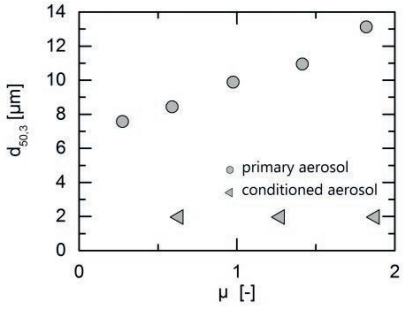

Figure 1: Mean droplet size $d_{50,3}$ of the primary and the conditioned aerosol.

For the primary aerosol the mean droplet size increases with increasing liquid-to-air mass flow ratio. For the conditioned aerosol, the mean droplet size is constant at around $d_{50,3}$ = 1.9 µm over all liquid-to-air ratios with a narrow size distribution (span = 0.2). Fluctuations in the production of the primary aerosol are fairly compensated at the droplet separator.
The conditioned aerosol was subsequently dried in the drying chamber. The particle size distribution was evaluated with a scanning electron microscope (SEM, Hitachi H-S4500 FEG). The SEM image of spray dried mannitol particles (see figure 2) displays mannitol agglomerates with almost spherical particles with a mean particle size of $d_{50,3}$ = 0.77 µm and a narrow size distribution with span values of about 0.7.

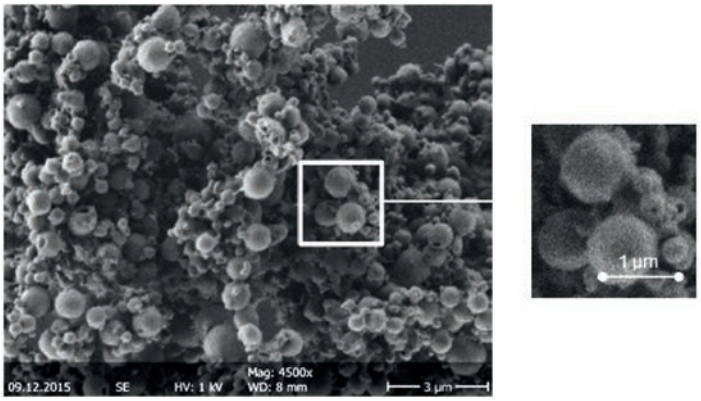

Figure 2: SEM image of spray dried mannitol particles (concentration: 10 wt.% mannitol, particle characteristics: $d_{50,3}$ = 0.77 µm, span = 0.7).

The main advantage is the separation of the usable aerosol and the recycling of the rest without any further classification after the drying step. Moreover, the combination of a pneumatic nebulizer and a droplet separator accomplishes the requirements of a system for industrial applications in case of robustness, simplicity and long-term stability.

Contact:
ramona.gorny@bci.tu-dortmund.de
markus.thommes@bci.tu-dortmund.de

Publications:
R. Gorny, G. Schaldach, P. Walzel, M. Thommes, International Congress on Particle Technology, lecture "Fine Droplets for the Preparation of Spray Dried Submicron Particles", Nuremberg, Germany (2016).

Efficient Precipitation of Submicron Particles Using a Two-Stage Electrostatic Precipitator

Separation of Submicron Particles for Pharmaceutical Applications from a Gas Flow in an Electrostatic Field

Adrian Dobrowolski, Damian Pieloth, Helmut Wiggers, Markus Thommes

Active pharmaceutical ingredients cover a large part of the costs in the production of oral drugs. An increase of the bioavailability leads to a more cost-effective way to produce drug formulations. This goal can be achieved by decreasing the particle size into the submicron range with the help of spray drying for instance. To separate the generated particles electrostatic precipitators can be used.

Poorly soluble pharmaceutical ingredients are a major difficulty in the oral drug application. One technique is to produce particles in the submicron range (100 nm – 1 µm) in order to increase the specific surface area (A). The Nernst-Brunner equation (1) describes the dependency of the mass transfer rate on the specific area and therefore also on the particle size.

$$\frac{dm}{dt} = A \cdot \frac{D}{\delta} \cdot (c_S - c) \qquad (1)$$

D: Diffusivity
δ: Static diffusion layer thickness
c_S*:* Equilibrium concentration
c: Concentration at any time *t*

A transfer of poorly soluble active pharmaceuticals into orally active substances can be achieved by the use of spray dryers. After this process small particles are dispersed in a gas stream. Electrostatic precipitation is a method to collect these small particles effectively with any throughput and moderate operating costs. Another benefit is the collection on an even surface. In fibre filters e.g. a part of the product would be trapped at the fibre itself. Electrostatic precipitators (ESP) can be sterilized also very easily for a pharmaceutical application. First experiments with submicron particles were done using a single-stage ESP at a technical scale, which was developed at the laboratories of solids process engineering in Dortmund.

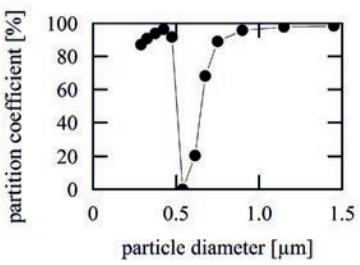

Figure 1: Experimental precipitation results with corundum particles at 0.5 mA/m².

The ESP shows a lack in the deposition of submicron particles (Figure 1). Neither diffusive nor field charging seems to be sufficient to load and therefore deflect the particles in this region. Designing a tailor-made ESP is a possibility to investigate and to solve this specific problem. This work outlines the design of a two-stage tube-type electrostatic precipitator for the collection of submicron particles (Figure 2).

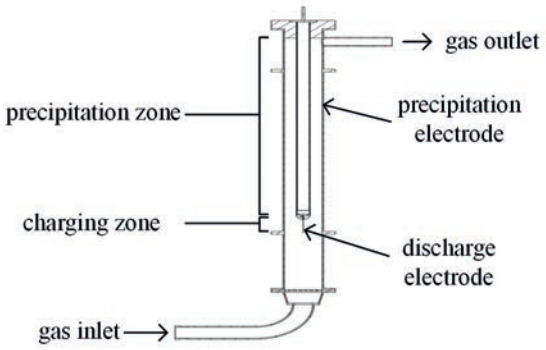

Figure 2: Design Sketch of the two-stage ESP.

Based on the Penney principle the deflection takes place in a laminar flow. The advantage of this method is the avoidance of the reentrainment of separated particles due to turbulences. This simplification leads to an enhanced examination in the precipitation process. In future experiments the study of the collection efficiency will take place. A variation of process parameters like current density, discharge electrode diameter, gas composition and gas velocity shall provide the optimum performance in the collection of submicron particles.

Publications:
A. Dobrowolski, D. Pieloth, H. Wiggers, M. Thommes, XIV International Conference on Electrostatic Precipitation ICESP (2016), Poster “Efficient precipitation of submicron particles for pharmaceutical applications using a two-stage electrostatic precipitator”, submitted.

Contact:
adrian.dobrowolski@bci.tu-dortmund.de
markus.thommes@bci.tu-dortmund.de

Irregularity in the Spray Pattern of Common Spraying Nozzles

Pressure Swirl Nozzles in Industrial Applications as Spray-Drying

Jens Kamplade, Carmen Hannöver, Susan Henning, Maike Schlüter, Markus Thommes, Peter Walzel

Drying of solids as a unit operation is applied in many industrial processes. It is often realized by spray drying, where a liquid feed, which contains the product, is sprayed into an environment with low partial pressure of the solvent. Pressure swirl nozzles are widely in use for this purpose and form a spray like a hollow cone. The construction is simple and can be adapted easily to the requirements. Usually the feed has complex rheology. It may contain particles in form of solid materials or second liquid phase materials. The main characteristics of a spray process are the throughput, the drop size and the width of the drop size distribution as a precursor of the emerging particle size distribution.

Many spray-drying processes are aiming for a high quality product with similar properties of individual particles. To ensure comparable drying characteristic narrow drop size distribution is desired.
The spray characteristic of pressure swirl nozzles (hollow cone nozzles) is well described in literature. During the recent investigation on a special nozzle design for spraying milk products an irregular flow pattern occurred. The spray was not homogeneous and showed denser and sparse parts orientated in flow direction. This behavior has also been observed before. It is described as unwanted because of a negative effect on the drop size. Until now this effect is not quantified and the origin of the strands is not analyzed.
The pressure swirl nozzles applied in this study had two up to six entrance slots for the feed into the swirl chamber. The slots are oriented with an axial and tangential alignment within the nozzle's swirl chamber. In order to determine the source of the strands a test rig was set comprising a line laser. The light sheet passes horizontally through the vertical downward orientated spray.

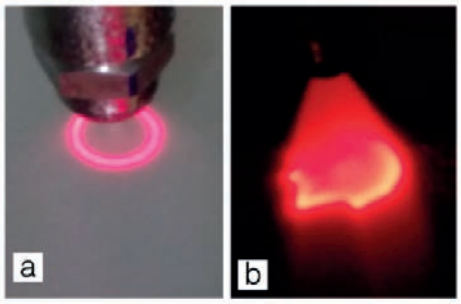

Figure 1: Laser sheet image of a homogeneous (a) and an inhomogeneous spray pattern (b).

In Figure 1 the spray pattern of regular shape (a) and one with strands (b) is shown. In case of a homogeneous spray the spray cone appears with the same brightness along its circumference.

The denser strands reflect more light and the brightness-value of this area is higher in a gray-value image. Based on gray-value distribution the degree of homogeneity can be quantified. The number of strands can also be determined. Several nozzle combinations (orifice, entrance slots) were probed by this technique and the occurrence of strands was evaluated to find the cause of the irregularity. Different process conditions and liquids were investigated for that purpose.
At first it was found that the number of strands is independent of the number of entrance slots. Within the study two sets of nozzles were compared. One was brand-new and the other was used for a short period spraying milk concentrate. The combination of the nozzle sets showed, that the used nozzles are only critical regarding strand formation.

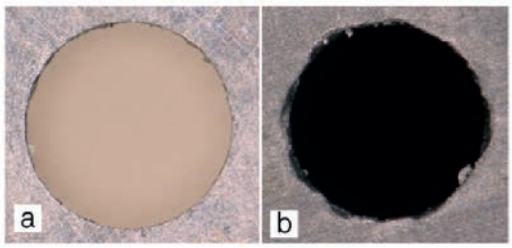

Figure 2: Nozzle's orifice showing regular (a) and inhomogeneous (b) spray pattern.

The comparison of the nozzles in the light microscope shows differences between the brand-new and used orifice (Figure 2). The latter is not round anymore and marked by local indentations. This damage obviously causes the irregular flow pattern and may be traced back to wear.

Finally the spray was divided and the drop size inside dense and sparse parts of the spray has been compared. The drop sizes from a nozzle with a homogeneous spray were also analyzed as a benchmark. As a result the drops inside dense strands are found significantly larger.

Contact:
jens.kamplade@bci.tu-dortmund.de
peter.walzel@bci.tu-dortmund.de

Publications:
J. Kamplade, S. Henning, M. Schlüter und P. Walzel
Jahrestreffen der Fachgemeinschaft Mehrphasenströmung, Lecture „Quantitative Untersuchung zur Strähnenbildung im Sprüh eines Dralldruckzerstäubers mittels Laserschnitttechnik", Lüneburg (2015).

Fluid Separations (FVT)

Superposition of Liquid-Liquid and Solid-Liquid Equilibria of Linear and Branched Molecules

Investigation of the Predictability of Phase Equilibria of Systems Containing Branched Molecules

Thomas Goetsch, Tim Zeiner

In chemical industry the separation of long-chain isomers is a challenging task as distillation is very elaborative because of small separation factors and extraction often does not meet the high purity demands. One promising alternative is the solvent crystallization. The challenge is the appearance of a superposition of a liquid-liquid equilibrium (LLE) and a solid-liquid equilibrium (SLE) during the separation process. This superposition can affect the product properties and has to be understood in order to build up suitable crystallization processes. This work is included in the transregional collaborative research center named "Integrated Chemical Processes in Liquid Multiphase Systems (InPROMPT). InPROMPT is involved in the development of efficient production processes based on chemical reactions in liquid multiphase systems.

Commonly, thermodynamic modelling is used to reduce experimental effort. In the course of modelling one has to fit pure component parameters to experimental data. For branched molecules it is often not possible to gain experimental data because they are barely commercially available in a high purity. Therefore, phase equilibria of systems containing branched molecules can often not be modelled using the common procedure. To overcome this limitation a model-based experimental design was developed in this work (figure 1).

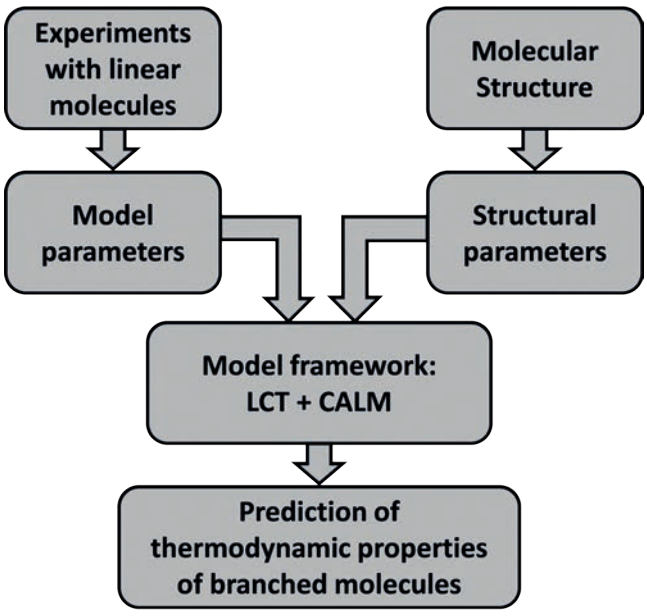

Figure 1: Model-based experimental design for predicting thermodynamic properties of branched molecules.

The idea is to directly take the structure of the molecules into account. Therefore, the lattice cluster theory (LCT) was chosen. The LCT was developed to consider the architecture of molecules without any additional adjustable parameters. It allows for the prediction of thermodynamic properties of branched molecules based on linear molecules thermodynamic properties. Therefore, experiments with linear molecules have to be performed. These experimental data are used to fit the required model parameters. Afterwards, the architectural coefficients of the branched molecules are defined based on their chemical structure. On this way, we are able to predict the thermodynamic properties of branched molecules.

In this work a model system containing hexadecane, 2,2,4,4,6,8,8-heptamethylnonane and ethanol was investigated. The developed model-based experimental design was used to predict binary and ternary phase equilibria of systems containing branched molecules. Figure 2 shows the predicted superposition of liquid-liquid equilibria (LLE) and solid-liquid equilibria (SLE) of the ternary system [1]. Both the predicted LLE as well as the SLE are in good agreement to experimental data. Therefore, it can be concluded that the developed approach is suited for the prediction of phase equilibria of systems containing branched molecules.

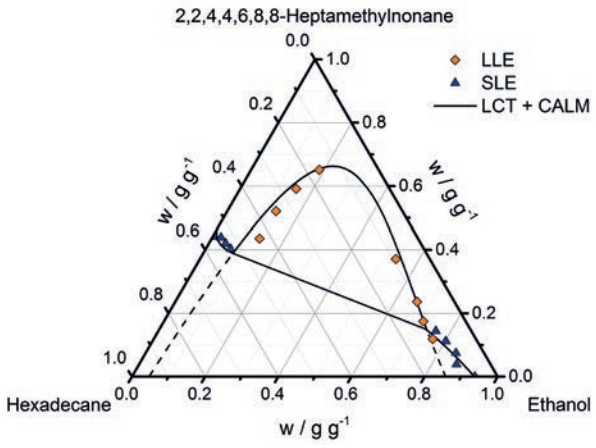

Figure 2: Superposition of LLE and SLE of the ternary system containing hexadecane, 2,2,4,4,6,8,8-heptamethylnonane and ethanol.

Contact:
thomas.goetsch@bci.tu-dortmund.de
tim.zeiner@bci.tu-dortmund.de

Publications:
[1] T. Goetsch, P. Zimmermann, R. van den Bongard, S. Enders, T. Zeiner, lecture "Superposition of Liquid-Liquid and Solid-Liquid Equilibria of Isomers", European Symposium on Applied Thermodynamics 2015, Athens, Greece.

Synthesis of Intensified Processes from a Superstructure of Phenomena Building Blocks

Hanns Kuhlmann, Mirko Skiborowski

Phenomena are the fundamental mechanisms a chemical process or unit operation is based on, e.g. mass transfer, phase contact, phase separation, reaction or energy transfer. By composing processes of phenomena instead of predefined unit operations, the creativity during process synthesis is maximized and process intensification principles can be considered even beyond already existing equipment. The optimization-based method generates promising phenomena-based flowsheet variants which can further be interpreted and translated into equipment by using databases or proposing new equipment that implements the phenomena-based design.

The objective of process synthesis (PS) is the generation of flowsheet variants for a given reaction and/or separation design problem. In the last decades, a considerable number of PS methods have been developed to guide the process engineer through the PS task. However, most of the existing methods are based on the combination of fixed unit operations, mostly neglecting process intensification (PI) during PS. Since the decisions made in this early phase account for up to 80 % of the overall cost, this negligence severely limits the potential benefit of PI options. Therefore, different PS methods focused on the consideration of PI principles have been developed. In order to disconnect from the combination of known unit operations and facilitate further improvements through innovative and new equipment, PS can be performed based on the combination of phenomena. By neglecting equipment-specific constraints, phenomena-based methods maximize the search space for PS exceeding existing equipment. However, since the combinatorial complexity of arbitrary combinations of phenomena is not traceable and would results in a tremendous number of infeasible combinations, the synthesis approach is based on a set of predefined combinations in so-called phenomena building blocks (PBB).

These PBBs are connected to a superstructure (see Figure 1) which is optimized by a combination of a stochastic and a deterministic algorithm in order to generate promising flowsheet variants.

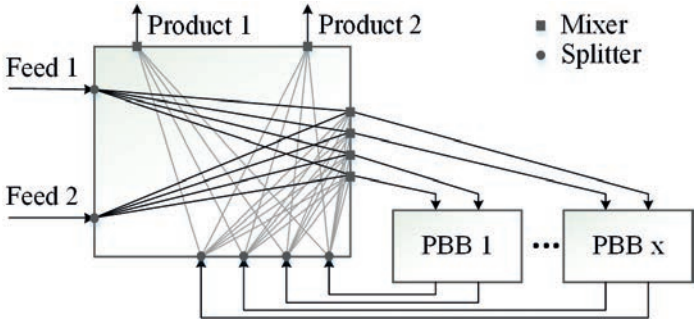

Figure 1: Distribution network of the PBB superstructure.

The elements of this superstructure are PBBs, which are interconnected by a distribution network consisting of streams, mixers and splitters. The mixers are based on mass and energy balances allowing for additional heat transfer in order to adjust temperature and phase state of the outgoing stream. The splitters distribute the streams among the different mixers in the distribution network. The PBBs in the superstructure are defined in a generic way, such that their identity can be changed during optimization.

Applying the approach to the case study of bioethanol dehydration, more than 100 feasible process variants are generated based on vapor-liquid (VL) and vapor permeation (VP) PBBs, for which the best variant (Figure 2) offers more than 20 % savings in operating costs [1].

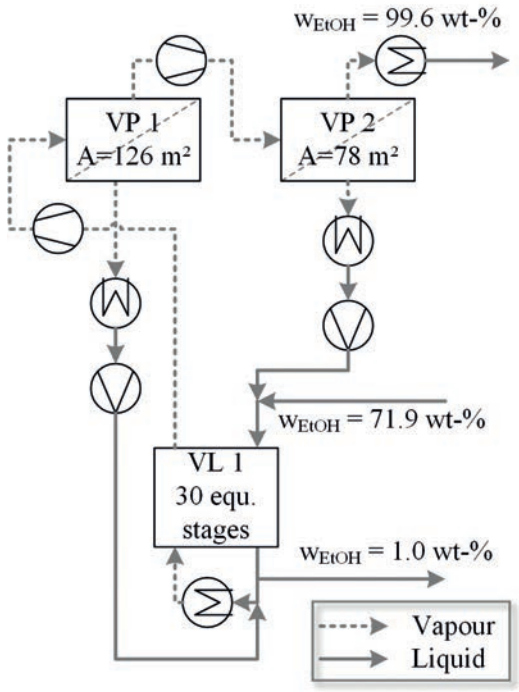

Figure 2: Best result for the dehydration of ethanol.

Publications:
[1] H. Kuhlmann, M. Skiborowski, Poster "Synthesis of Intensified Processes from a Superstructure of Phenomena Building Blocks", 26th European Symposium on Computer Aided Process Engineering 2016, Portorož, Slovenia.

Contact:
hanns.kuhlmann@bci.tu-dortmund.de
mirko.skiborowski@bci.tu-dortmund.de

Fluid Mechanics (SM)

Mass Transfer in Liquid/Liquid Slug Flow

Numerical Modelling of Conjugated Mass Transfer in Micro Reactors

Christian Heckmann, Peter Ehrhard

Mass transfer in multiphase systems finds extensive application in chemical–engineering problems, like chemical reactions, extraction, or adsorption. Last year we introduced a new concept that can handle the hydrodynamics and the mass transfer of conjugated mass transfer systems, considering a high resolution at the free interface. After validation the numerical concept can be applied to technical applications, like multi phase micro reactor systems. The liquid/liquid Slug Flow pattern allows high transport rates and a maximum of process control. A detailed view into the mass transfer of the liquid/liquid Slug Flow pattern is achieved.

Microreactors have been applied for the production of fine chemicals and pharmaceuticals for several years. Owing to the small size of the channels, especially the liquid/liquid slug flow pattern offers large specific areas and high mixing convection due to the segmented flow. A detailed knowledge of the mechanism and characteristics of the mass–transfer process, in conjunction with the geometrical properties of the multiphase system, appears to be crucial for process design. Numerical simulations allow a detailed examination of the local mass–transfer process, since experiments usually remain restricted to integral measurements.

Starting point for the examination of mass transfer is a periodic element of the Slug Flow pattern. We set up a model consisting of two incompressible immiscible and Newtonian liquids, which are acting as solvents for a solute, which is extracted from one phase to the other. Starting point for the hydrodynamics is the imported steady–state interface, taken as output parameter from another numerical model. On both sides of this interface (separate) static computational domains are arranged. The numerical resolution at the free interface can be adapted separate to the rest of each domain to minimize the numerical influence to the transport process.

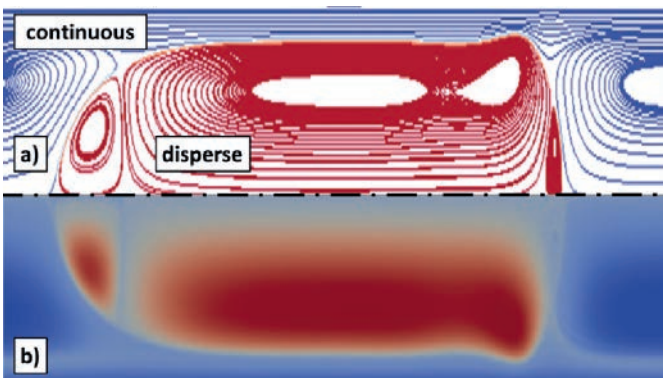

Figure 1: a) stream lines for $Ca_c=Ca_d=10^{-1}$, $Re_c= Re_d=100$, b) concentration distribution for $Pe_c=Pe_d=10^6$, Fo = 0,01.

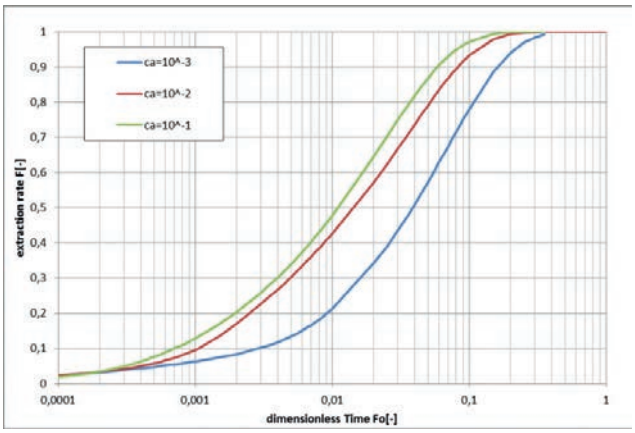

Figure 2: Extraction rate F over dimensionless time Fo for the examined capillary numbers.

Both domains are coupled at the free surface of the multiphase system. The steady-state hydrodynamics form the basis for the mass transfer process. Only dilute concentrations are taken into account, so the back-coupling of the mass transfer to the hydrodynamics of the multiphase system is neglected, hence transport equation of a passive (scalar) concentration is solved at both sides of the interface.

For the present study the influence of the most characterizing dimensionless number for the Slug Flow pattern, capillary number, to the mass transfer process is examined. The extraction direction from disperse to continuous phase is given. Numerical domains with an overall homogenous resolution are set up. The mass transfer process of the different cases is evaluated using the extraction rate and the dimensionless diffusion time, see figure 2. The extraction rate represents the change of the mean solute concentration inside the slug over time. It can be seen in the diagram that the necessary extraction time decreases with an increasing capillary number. Enhanced convection in the systems leads to a faster extraction process.

Contact:
christian.heckmann@bci.tu-dortmund.de
peter.ehrhard@bci.tu-dortmund.de

Publications:
C. Heckmann, P. Ehrhard, Simulation of Mass Transfer in Liquid/Liquid Slug Flow, GAMM, Braunschweig (D), 2016.

Stability of Rivulets

Experimental Investigations on the Stability of Static Rivulets with a Pinned Contact Line

Tim Neumann, Jayotpaul Chaudhuri, Peter Ehrhard

The experimental investigations on the existence of Plateau-Rayleigh instabilities in a static rivulet are carried out. For this purpose an experimental setup was constructed to allow the formation of a static liquid rivulet with a fixed contact line. The setup is externally excited and the induced instabilities in the rivulet are investigated. Due to the difficulties in the direct measurement of contact angle, a theoretical simulation of the surface contour is also carried out. The simulation predicts the contact angle for a given rivulet height and base width.

In the presence of an inclined hydrophobic solid surface a poorly wetting liquid surrounded by gas features a large contact angle and in turn a narrow stream of liquid forms which is termed rivulet. This kind of flow is often encountered in the field of chemical engineering processes, for example in trickle bed reactors and structured packing columns for distillation or evaporation.

To realize a narrow static rivulet, two bars of PTFE (polytetrafluoroethylene) are adjusted parallel, with a gap width of *2b=3mm* in between (cf. figure 2). The length of these bars is *l=180mm*. They are placed in a frame made of PMMA (poly(methyl methacrylate)), which is transparent to allow for an optical access. Deionized water is fed into the gap slowly from below, such that the rivulet forms and successively increases its height until a desired contact angle is achieved. Both contact lines are certainly fixed at the upper corners of the bars. Due to the hydrophobic wetting behavior of PTFE, a large contact angle of up to 130° can be realized.

The surface contour of a rivulet can generally be defined by $\Delta p = -\sigma \nabla \cdot \vec{n}$. The non-linear partial-differential equation describes the pressure difference Δp across a surface between two fluids due to the effect of surface tension σ as a function of the surface curvature $\nabla \cdot \vec{n}$. The numerical solutions of the resulting ODEs leads to the theoretical rivulet cross section contour and the contact angle θ as a function of the rivulet height H. The results are compared with experimentally determined shapes as shown in figure 1 and only small deviations can be seen. This method allows estimating the contact angle θ which is difficult to measure. The mean rivulet height is measured with an optical sensor.

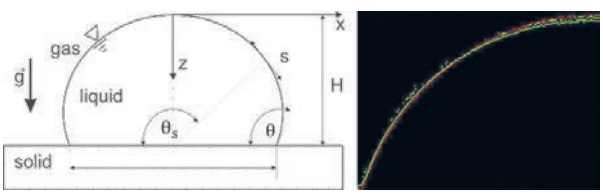

Figure 1: Left-hand side: Draft of the rivulet cross section shape. Right-hand side: Comparison of the rivulet cross section contours under the influence of gravity and with a fixed base width. (-) theoretical results, (-) experimental results,(-) overlapping regions.

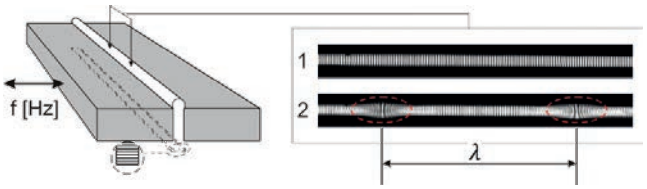

Figure 2: Left-hand side: Experimental setup to form the static rivulet between two PTFE-blocks. The direction of the external excitation is shown. Right-hand side: The view on top of the rivulet shows the distortion of the grid lines. (1) without excitation, (2) with excitation.

In a first set of experiments, the expected instability did not show up at sufficiently–large amplitude of disturbance. A time-periodic mechanical excitation is used to multiply these instabilities. For that purpose the frequency is varied between *10-60 Hz*. The instabilities are only observed at certain frequencies.

Under the PMMA frame a grid is placed. Diffuse light arriving from below is deflected by the rivulet in a similar fashion as by a plane–convex cylindrical lens. If the rivulet is not disturbed along the gap, its upper shape is almost circular in the cross section, and hence the lines of the grid orthogonal to the gap axis remain parallel. However, if the rivulet develops periodic disturbances along its axis, the parallel grid lines will be disturbed by deflections in the direction of the gap axis. As obvious from figure 2, this allows the identification of the maxima of these disturbances along the gap axis and leads to a mean value of the wavelength λ. The wavenumber k is defined as $k = \frac{2\pi b}{\lambda}$.

The results of the experiments are shown in figure 3.

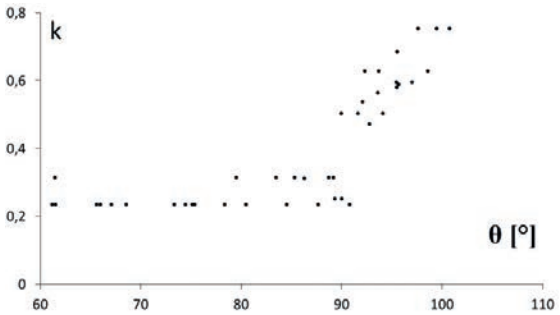

Figure 3: Results of the experiments: wavenumber k against the calculated contact angle θ.

Contact:
tim.neumann@bci.tu-dortmund.de

Technical Biochemistry (TB)

In vivo Validation of *in silico* Predicted Metabolic Engineering Strategies in Yeast

Increasing Microbial Terpenoid Production Based on an *in silico* Stoichiometric Metabolic Network Analysis

Evamaria Gruchattka, Oliver Kayser

Engineering of the central carbon metabolism of Saccharomyces cerevisiae *to redirect metabolic flux towards cytosolic acetyl-CoA has become a central topic in yeast biotechnology. A cell factory with increased flux into acetyl-CoA can be used for heterologous production of terpenoids for pharmaceuticals, biofuels, fragrances, or other acetyl-CoA derived compounds. In a previous study, we identified promising metabolic engineering targets in* S. cerevisiae *using an* in silico *stoichiometric metabolic network analysis. In this study, we validated selected* in silico *strategies* in vivo*.*

One of the most widely used heterologous hosts for microbial terpenoid production, *Saccharomyces cerevisiae*, was analyzed *in silico* in our previous study. Promising metabolic engineering targets were identified to increase terpenoid production. In this study, the sesquiterpenoid patchoulol was produced in a two-phase cultivation process using dodecane as organic layer to capture the volatile terpenoid. The spectrum of sesquiterpenoids was analyzed to estimate the production of total sesquiterpenoids, and the flux in the mevalonate pathway (native terpenoid pathway) was increased by overexpressing a truncated HMG-CoA-Reductase and by the fusion of FPP synthase with patchoulol synthase.

Furthermore, our previous study identified non-fermentable carbon sources such as ethanol as promising approach to increase terpenoid production. Thus, the production of the sesquiterpenoid patchoulol was analyzed during growth on glucose, and on ethanol, which had been produced during glucose-phase.

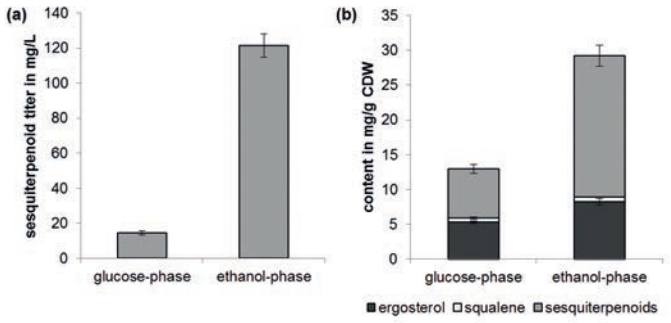

Figure 1: Effect of carbon source on terpenoid production. (a) Sesquiterpenoid titer, and (b) ergosterol, squalene and sesquiterpenoid content during growth on glucose (glucose-phase) and during growth on ethanol (ethanol-phase).

Figure 1 shows the tremendous effect. Sesquiterpenoid titer was increased by a factor of 8.4 (Figure 1a). The yield on cell dry weight (CDW) also increased both for sesquiterpenoids and ergosterol (native sterol, C_{28} terpenoid) as well as squalene (native triterpene, C_{30}), see Figure 1b.

In addition, promising *in silico* predicted metabolic engineering approaches were implemented. Disruption of *α*-ketoglutarate dehydrogenase gene (*KGD1*) was predicted to redirect the metabolic flux via the pyruvate dehydrogenase bypass towards acetyl-CoA (see Figure 2). The metabolic flux was redirected as predicted, however, the flux was interrupted at the level of acetate. High amounts of acetate were produced due to low activity of acetyl-CoA synthetase.

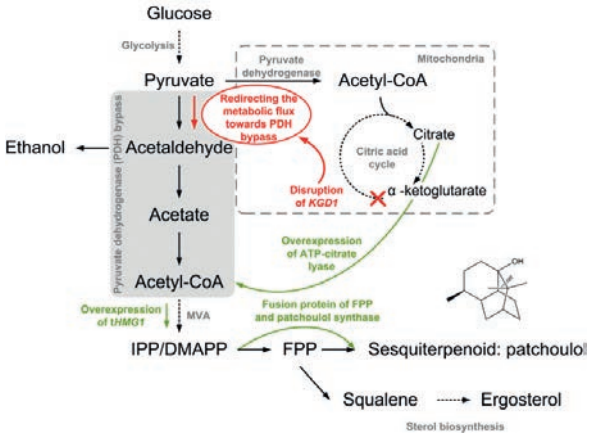

Figure 2: Metabolic engineering approaches in yeast for increased terpenoid production.

As an alternative pathway to synthesize cytosolic acetyl-CoA, ATP-citrate lyase from *Arabidopsis* was expressed as a polycistronic construct, however, *in vivo* performance of the enzyme needs to be optimized to increase terpenoid production. This study demonstrates that *in vivo* activity of both heterologous and native enzymes can interfere with predictions. The inclusion of regulatory circuits and *in vivo* kinetics of enzymatic reactions into *in silico* metabolic network analyses are required to increase the predictive power of these models and thus reduce the time of strain improvement in the future.

Contact:
oliver.kayser@bci.tu-dortmund.de

Publications:
E. Gruchattka, O. Hädicke, S. Klamt, V. Schütz, O. Kayser, Microbial Cell Factories 12(1):84 (2013).
E. Gruchattka, O. Kayser, PLOS ONE 10(12):e0144981 (2015).

Cross-Species Biosynthesis of Maytansine in *Maytenus serrata*

New Insights into Plant-Endophyte Communication for the Biosynthesis of Maytansine

Parijat Kusari, Oliver Kayser

Endophytic bacterial communities harboring different tissues of Maytenus serrata *originating from Cameroon were investigated using targeted genome mining techniques coupled to bioanalytical approaches to elucidate the source of maytansine biosynthesis. It was revealed that the host plant, along with its cryptic endophytic microflora, produces the biosynthetically unique core structural moiety 3-amino-5-hydroxybenzoic acid (AHBA) that serves as the unique starter unit for maytansine biosynthesis. However, the biosynthetic step of halogenase-mediated incorporation of chlorine, which is missing in the host plant, is accomplished by the culturable stem endophytic bacterial community.*

Endophytic microorganisms are ubiquitous in plants in the tissues and apoplastic compartments, where they establish complex communities that can substantially contribute to the overall fitness of the host plants. Given the fact that maytansine was discovered in the 1970s not only in *Putterlickia* species but also in other Celastraceae plants of the genus *Maytenus*, we aimed to investigate the endophytes harbored in *Maytenus serrata* plants. The above- and below-ground plant tissues were extracted and analyzed using HPLC-ESI-HRMS^n which revealed that maytansine was present in the tissues of *M. serrata* sampled only from Cameroon but not from Ghana. The striking results reinforced the notion that biosynthesis of maytansine in *M. serrata* plants is performed by the endophytes and not by the plants themselves. Firstly, we evaluated the different tissues of *Maytenus* plant and the endophytic bacterial community for the presence of genes biosynthesizing the important starter enzyme, AHBA synthase (3 amino-5-hydroxybenzoic acid synthase).

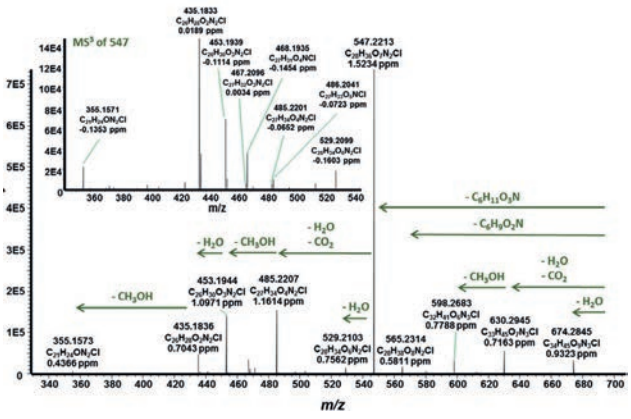

Figure 1: Representative HRMS^2 and HRMS^3 fragmentation of maytansine.

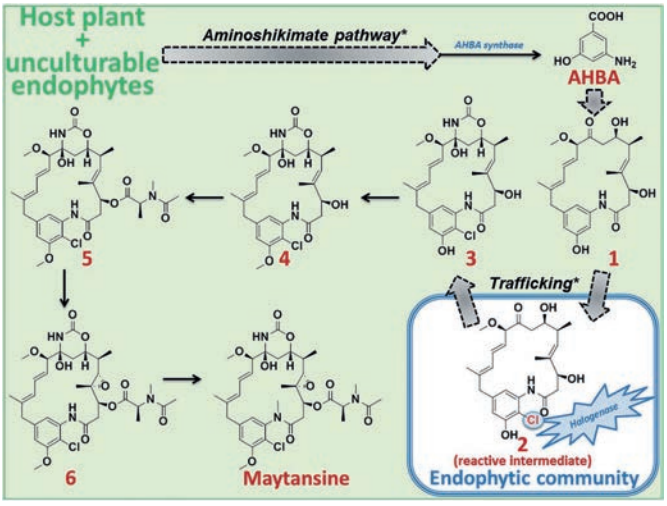

Figure 2: Proposed plant-endophyte cross-species biosynthetic pathway of maytansine in *M. serrata*.

We further aimed to evaluate the plant tissues and the endophytic communities for the presence of halogenase genes in order to elucidate which organism (host plant or endophytic bacterial community) is responsible for incorporation of chlorine towards completing the biosynthesis of maytansine. In our first approach, we evaluated for the presence of halogenase encoded by gene *asm*12, which catalyzes the first step post-polyketide synthase modification responsible for the chlorination step in ansamitocin biosynthesis. In our second approach we further analyzed the presence of any $FADH_2$-dependent halogenase irrespective of *asm*12 gene product in particular. Taken together, our study reveals a unique aspect of plant endophyte communication where only the bark endophytic bacterial community of a selected *M. serrata* plant had coevolved a means to produce maytansine jointly with the host plant, including trafficking of the precursors from and to the host plant.

Publications:
P. Kusari, S. Kusari, D. Eckelmann, S. Zühlke, O. Kayser, M. Spiteller RSC Advances 6, 10011-10016 (2016).

Contact:
parijat.kusari@bci.tu-dortmund.de
oliver.kayser@bci.tu-dortmund.de

Technical Chemistry (TC)

Removal and Recovery of Homogeneous Precious Metal Catalysts via Organic Solvent Nanofiltration

Jens M. Dreimann, Mirko Skiborowski, Andreas J. Vorholt, Andrzej Górak, Arno Behr

In homogeneous catalysis often precious transition metal complexes are used. Ideally the used catalyst in a specific process is recovered in the downstream processing and recycled to the reactor. In contrast to the separation of heterogeneous catalysts, the separation of homogeneous catalysts is a crucial issue: Inefficient catalyst recovery and its loss in undesired process streams may even lead to uneconomic processes. An innovative approach for the recovery of homogeneous catalysts is the application of organic solvent nanofiltration (OSN). It has not been established in industry so far because of some challenging drawbacks.

Homogeneous transition metals are very efficient catalysts, often used in chemical industry. Since these tailor-made catalysts show high activity and high selectivity during the reaction, recycle streams of substrates and waste streams of side products can be reduced significantly. They are unfortunately very expensive, necessitating efficient recycle methods. A promising approach for the separation of product and retaining the catalyst is the application of organic solvent nanofiltration (OSN). Mild separation conditions and low energy demand are additional advantages of OSN over other separation techniques like distillation or crystallization.

In order to design a continuous process consisting of a reactor and a nanofiltration unit several requirements have to be fulfilled:

- Difference in molecular weight of product and catalyst
- High stability of the catalyst during reaction and nanofiltration
- High conversion
- High solubility of catalyst, reactants and products in the applied solvent
- Efficient removal of depleted catalyst species

Hydroformylation is one of the most prominent homogeneously catalyzed reactions. Applying rhodium based catalysts olefins and synthesis gas are converted to aldehydes (Figure 1).

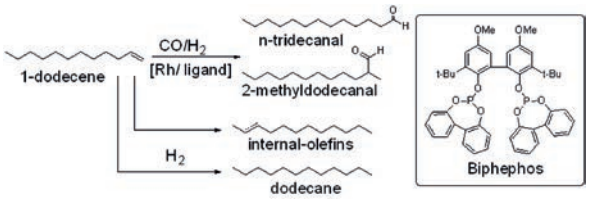

Figure 1: Hydroformylation reaction of 1-dodecene.

We have investigated the separation of catalyst via OSN in hydroformylation, applying different ligands in batch mode. Catalyst rejection was determined and the catalyst performance before and after the nanofiltration step were compared. Figure 2 shows the combination of batch reaction and crossflow nanofiltration.

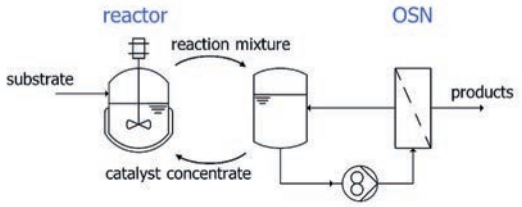

Figure 2: Batch reactor (left), OSN (right).

Three ligands (triphenylphosphine (TPP), Biphephos and Xantphos) were tested in this experimental setup. Substantial rejection of the precious Rh was achieved for all catalyst complexes (94-97%). Comparing the catalyst performance before (left column) and after the nanofiltration step (right column) (Figure 3), the recycle of the Rh/TPP was deemed most promising, since the yield and selectivity for the aldehydes (tridecanal and 2-methyldodecanal) was maintained after the nanofiltration step.

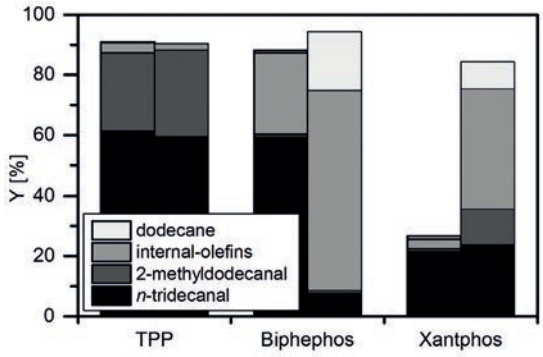

Figure 3: Yields of hydroformylation catalysts applying different ligands before (left) and after (right) catalyst recycling.

In summary, good separation of catalyst and product was demonstrated in batch nanofiltration and recovery of the active catalyst complex for Rh/TPP was achieved. For further investigations these unit operations are now interconnected, so that a process for continuous operation is achieved.

Contact:
jens.dreimann@bci.tu-dortmund.de
arno.behr@bci.tu-dortmund.de

Publications:
J. M. Dreimann, A. Vorholt, M. Skiborowski, A. J. Vorholt, A. Behr, Chemical Engineering Transactions 47, 343-348 (2016).

Telomerization of 1,3-Butadiene with Alcohols Using Pd/NHC-Catalysts

Investigating the Structure-Reactivity-Relationship of Alcohols in a Solventless Reaction

Thiemo A. Faßbach, Robin Kirchmann, Arno Behr, Andreas J. Vorholt

The telomerization is a homogenously catalyzed reaction, incorporating a dimerization of two 1,3-dienes and an addition of an H-acidic nucleophile. It is an industrially used reaction, run by Kuraray and Dow Chemicals. The reaction is mostly catalyzed by palladium/phosphine complexes, but in the last decade palladium complexes with N-heterocyclic carbene ligands have shown to be much more active catalysts with TONs up to 300.000. We were interested in the possibilities and limitations of this catalytic system regarding the alcohol in the telomerization of 1,3-butadiene.

The telomerization of 1,3-butadiene with alcohols is a long-known catalytic reaction and an effective tool to synthesize 2,7-octadienyl ethers using Pd/P-catalysts. Lately Pd/NHC catalysts have been in the focus of several catalytic reactions, including the telomerization of 1,3-dienes with alcohols and other nucleophiles (Figure 1).

Figure 1: Palladium catalyzed telomerization of 1,3 butadiene and methanol to form 2,7-octadienyl-methyl ethers.

In the 1970s Beger and Reichel have shown that the yield of the desired 2,7-octadienyl ethers decrease significantly with the chain-length of the employed alcohol, when the catalytic system palladium/triphenylphosphine is used. Some works suggest that palladium/NHC complexes like **1** (Figure 3) are capable of catalyzing the telomerization of 1,3-butadiene with longer alcohols. We could show that the overall reactivity remains the same for primary, linear alcohols up to a chain-length of eight. Due to the solventless reaction, small amounts of dimers were formed. Even with 1-octanol being the substrate TONs of above 18.000 were measured (Figure 2).

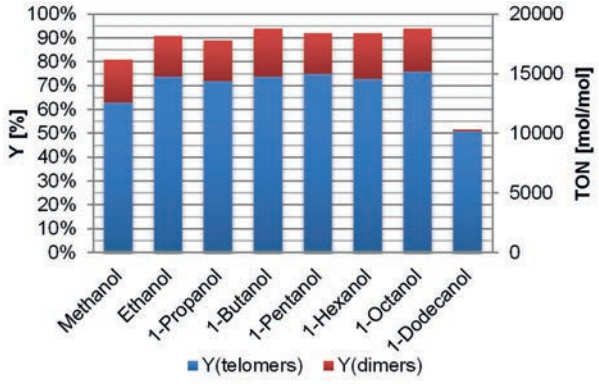

Figure 2: Yields and TONs for different 1-alcohols in the Pd/NHC-catalyzed telomerization of 1,3-butadiene. Reaction conditions: Pd(IMes)(dvds), 0.005 mol% based on 1,3-butadiene, c(NaOH) = 1 mol% based on ROH, T = 100 °C, t = 4 h.

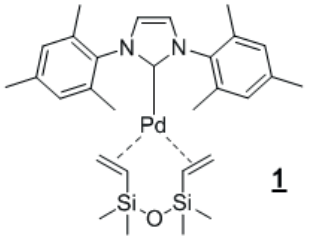

Figure 3: The palladium/NHC complex Pd(IMes)(dvds) used in this work.

Since secondary alcohols are known to be less reactive in the telomerization reaction than primary ones, we wanted to determine the influence that is responsible for this behavior. Using the example of pentanols, we could clearly show a decrease in reactivity from 1-pentanol to 3-pentanol. The reason for this decrease could be the steric hindrance or the electronic properties of secondary alcohols in general. In order to differentiate these two factors, *cyclo*-pentanol has been employed as a secondary alcohol with only little steric demand. The sterically very bulky but primary alcohol on the other hand is *neo*-pentanol (Figure 4).

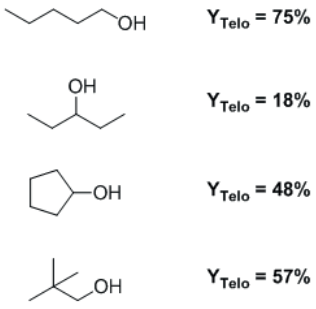

Figure 4: Different pentanols showing unexpected reactivities.

Results show that the sterically very demanding *neo*-pentanol is more reactive than *cyclo*-pentanol. Thus there have to be electronic properties that differ primary from secondary alcohols and are responsible for the loss of reactivity in the latter case.

Publications:
T. A. Faßbach, R. Kirchmann, A. Behr, S. Romanski, D. Leinweber, A. J. Vorholt, Journal of Molecular Catalysis A: Chemical, accepted manuscript (2016).

Contact:
thiemo.fassbach@bci.tu-dortmund.de
arno.behr@bci.tu-dortmund.de

Sustainable Diesters from Methyl 10-Undecenoate – Hydroesterification Catalyst Recycling in Thermomorphic Solvent Systems (TMS)

Development of a Process Concept for the Functionalization of Renewable Resources via TMS Systems

Tom Gaide, Francesco Benski, Michael Terhorst, Alexander Arns, Arno Behr, Andreas J. Vorholt

Herein we present a process concept for the atom economic hydroesterification of renewable methyl 10-undecenoate in thermomorphic multicomponent solvent (TMS) systems. As a suitable recycling technique a thermomorphic multicomponent solvent system consisting of methanol and dodecane is employed. Besides a low loss of the Pd-catalyst, product yields up to 79% and a high regioselectivtiy of 94% to the linear product are obtained.

Due to the shortage of fossil fuels the usage of renewable feedstocks in industrial chemistry gets increasingly important from an economic and ecologic point of view. In the view of their implementation it would be a great advantage if the use of existing production lines could further be used. The hydroesterification of methyl 10-undecenoate (Figure 1), which is readily available from pyrolytic cleavage from methyl ricinoleate, enables an atom efficient access to dimethyl dodecandioate. The corresponding diacid is used in industrial polymer synthesis today.

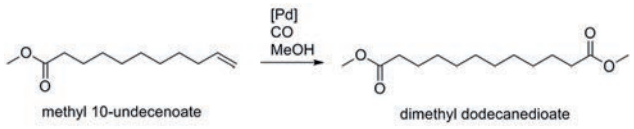

Figure 1: Hydroesterification of methyl 10-undecenoate.

The hydroesterification is a homogeneously, usually Pd-catalyzed reaction. One of the great challenges in homogenous catalysis is the recovery of the valuable catalyst. A promising catalyst recycling approach is the use of thermomorphic multicomponent solvent (TMS) systems. The TMS concept takes advantage of the temperature dependent miscibility gap of a polar and a non-polar solvent. The reaction mixture is homogeneous at reaction temperature, so there are no mass transport limitations during the reaction. Cooling down after reaction leads to formation of a polar, catalyst containing phase and a non-polar product phase (Figure 2).

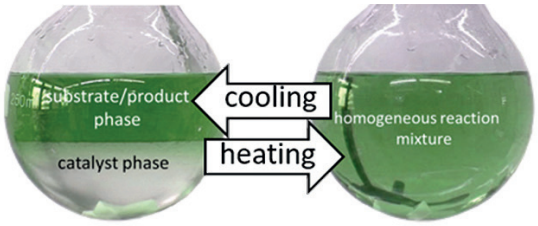

Figure 2: Concept of a TMS system.

We started our investigations in pure methanol in order to find a suitable hydroesterification catalyst which enables a high selectivity towards the desired linear dimethyl dodecandioate. Best results with a selectivity of 94% were obtained with a catalyst consisting of a $Pd_2(dba)_3$-Precursor, the ligand 1,2-DTBPMB and methanesulfonic acid. Afterwards we combined several non-polar solvents as solvent for the product phase in combination with methanol, which is also a substrate in the reaction, as a solvent for the catalyst phase. Best results were achieved with 50/50 mixture of methanol and dodecane. The leaching of the catalyst into the product phase is very low (less than 1% of the Pd). Using this system, yields up to 79% and a selectivity of 94% for desired dimethyl dodecandioate were generated after 23 h at a CO pressure of 30 bar and a Pd-loading of 0.1 mol% (Pd/ligand/methanesulfonic acid = 1/10/35).

Finally, we investigated the recyclability of the catalyst in our TMS System. For this reason, we conducted a reaction for two hours in an autoclave, separated the catalyst phase from the product phase and transferred the catalyst phase back into the reactor to start another reaction. The amount of product in dodecane phase was determined. The results are shown in Figure 3.

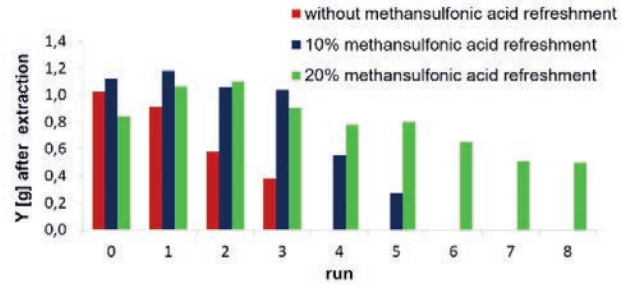

Figure 3: Catalyst recycling; Conditions: t = 2 h T = 90 °C, pCO = 30 bar, $n_{methyl\ 10\text{-}undecenoate}$ = 30 mmol, $V_{solvent}$ = 30 ml, $w_{methanol}/w_{dodecane}$ = 50/50, $Pd_2(dba)_3$, [Pd]=0.1 mol%, acid: methanesulfonic acid, $nPd/n_{methanesulfonic\ acid}$ = 1:35, ligand: 1,2-DTBPMB, n_{Pd}/n_{Ligand} = 1:10, 600 rpm, after reaction: 13.1 ml dodecane, 3 ml methanol, 18 mmol methyl 10-undecenoate.

We were able to show that the refreshment of the methanesulfonic acid is crucial for a successful catalyst recycling. The catalyst was recycled eight times without any loss of selectivity.

Contact:
tom.gaide@bci.tu-dortmund.de
arno.behr@bci.tu-dortmund.de

Publications:
T. Gaide, A. Behr, A. Arns, F. Benski, A. J. Vorholt, Chemical Engineering and Processing: Process Intensification 99, 197-204 (2016).
T. Gaide, A. Behr, M. Terhorst, A. Arns, F. Benski, A. J. Vorholt, Chemie Ingenieur Technik, DOI: 10.1002/cite.201500096.

Scale-Up of Ruthenium-Catalyzed Hydroformylation into Continuously Operated Miniplant

Alexander Kämper, Arno Behr, Peter Kucmierczyk

Hydroformylation (oxo-synthesis) is one of the most important reactions in chemical industry using homogeneous catalysts. The conversion of olefins with syngas into aldehydes and alcohols (oxo-products) leads to a wide range of applications such as solvents, plasticizers and fine chemicals. Because of upcoming metal scarcity and dependent prize trends a possible substitution of common catalysts based on rhodium is of high demand. Therefore, the hydroformylation of 1-octene was performed and optimized with new ruthenium catalysts in laboratory scale followed by the first scale-up into continuous miniplant operation.

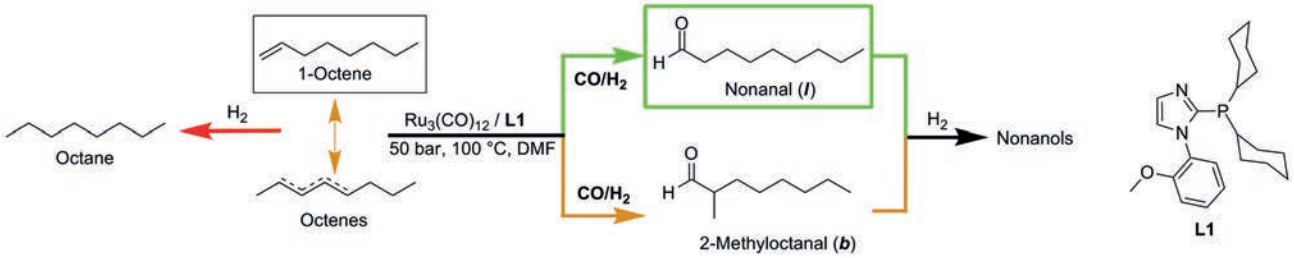

Figure 1: Hydroformylation of 1-octene and side reactions.

In laboratory scale the optimization of 1-octene hydroformylation with ruthenium catalysts (see Figure 1) led to high activities and selectivities, which are partial comparable to rhodium equivalents. After a reaction time of 1 h a maximum conversion (X) of 96% is reached, while the yield (Y) of desired oxo-products (aldehydes + alcohols) is at 79% (see Figure 2). Beside the suppression of side products (e.g. octane) to a minimum of 2%, high regioselectivity (*l*/*b*) of 95% emphasized the catalytic performance of ruthenium-catalysts in the polar solvent DMF (*N*,*N*-dimethylformamide).

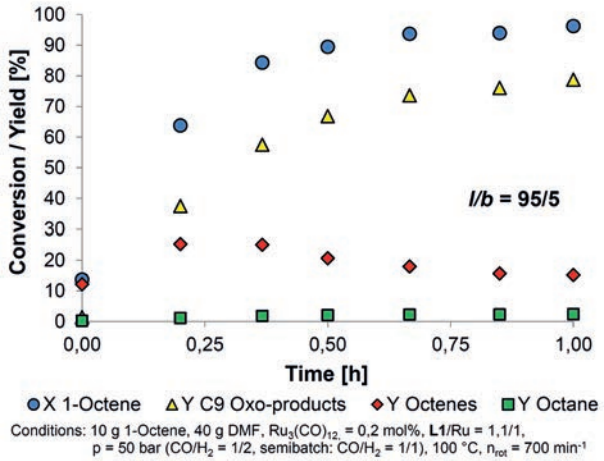

Figure 2: Hydroformylation of 1-octene in laboratory scale.

Using an extraction (with *iso*-octane) as catalyst recycling concept, the catalyst system has been successfully scaled-up into continuous miniplant operation. The refreshment of catalyst during plant operation ensures steady state conditions for more than 30 h including high chemo (76%)- and regioselectivities (94%) (see Figure 3).

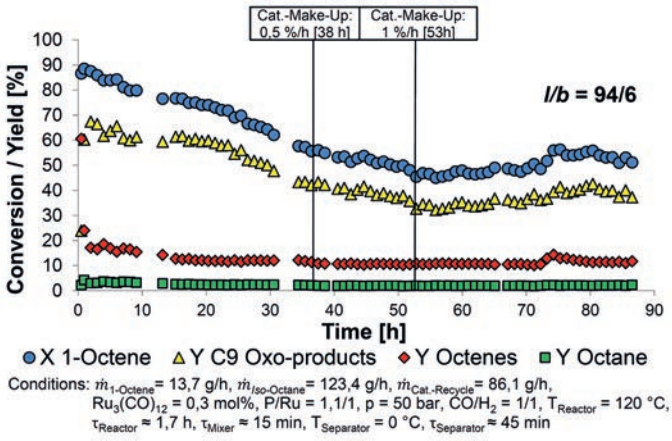

Figure 3: Hydroformylation with ruthenium catalysts in continuous miniplant operation.

Publications:
A. Kämper, A. Behr, P. Kucmierczyk, K. Reiswich, S. J. Warrelmann: Homogeneous Catalyzed Hydroformylation with Alternative Transition Metals in Miniplant Scale. Poster: 48. Jahrestreffen Deutscher Katalytiker, Weimar, 2015.

Contact:
alexander.kaemper@bci.tu-dortmund.de
arno.behr@bci.tu-dortmund.de

Selective Hydrogenation of Carbon Dioxide to *N,N*-Dimethylformamide in Biphasic Solvent Systems

Synthesis of Formamides without Carbon Monoxide

René Kuhlmann, Katharina Haßmann, Anna Prüllage, Arno Behr

Formamides are used as important solvents in the production of polymers. Usually, their syntheses involve carbon monoxide as substrate. In our investigations we show that formamides can be synthesized from carbon dioxide, hydrogen and an amine compound. A model reaction system for the synthesis of N,N*-dimethylformamide shows that a high selective hydrogenation of carbon dioxide to formamides can be achieved since no other byproducts are generated.*

Carbon dioxide is a promising C_1-carbon source for the synthesis chemistry. Due to its abundancy and high concentrations in flue gas, carbon dioxide can be obtained with low costs. As a non-toxic and non-flammable carbon source, it turns out to be an attractive surrogate for carbon monoxide. Recently, many possibilities for the utilization of carbon dioxide to different product classes were described.

A promising option is the catalytic hydrogenation of carbon dioxide to form methanol, formic acid or formamides. The syntheses of these chemicals usually involve carbon monoxide as carbon source. Especially formamides can be applied in organic fine chemistry as intermediates or find utilization as solvents in polymer synthesis. Within the last decades several research groups developed catalytic reaction systems to obtain formamides such as *N,N*-dimethylformamide (Figure 1). These investigations led to highly active reaction systems which often needed supercritical carbon dioxide to obtain the desired product.

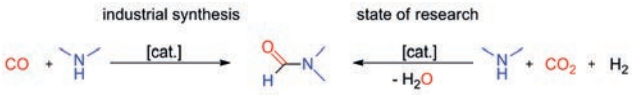

Figure 1: Synthesis of *N,N*-dimethylformamide.

For an industrial application the recovery of the expensive noble metals and ligands is essential. However, in most cases the recycling of the homogeneous catalyst remains untreated.

In our investigations, we developed a homogeneously catalyzed reaction system for the synthesis of formamides with an in situ extraction of the polar products. Therefore we used ruthenium(III)-chloride hydrate as precursor with BISBI as bidentate phosphine ligand as a model catalyst system. The catalyst was immobilized in a nonpolar solvent whereas the product was extracted by water. Long chained branched alcohols like 2-ethyl-1-hexanol seemed to be the suitable solvents for the catalytic complex.

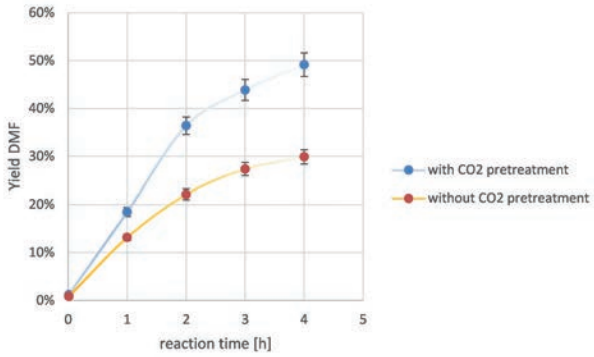

Figure 2: Conversion-time-plot of the homogeneous hydrogenation of CO_2 to DMF. Reaction conditions: 140 °C, 40 bar, c_{RuCl3} = 2.5 mmol/l, c_{BISBI} = 2 mmol/l, $c_{Dimethylamin}$ = 3.9 mol/l $V_{Reaktor}$ = 300 ml,$V_{Fl.}$ = 75 ml.

Even though the water soluble precursor $RuCl_3 \cdot H_2O$ was used, over 97% of the ruthenium was recovered in the nonpolar solvent after the reaction was finished. Interestingly, carbon dioxide could be converted by its absorbance in the aqueous amine phase without adding additional CO_2 into the gas phase resulting in a yield of 49% DMF after 4 h reaction time (Figure 2). Besides formic acid as intermediate, no byproducts could be observed. A continuously operated miniplant (Figure 3) proved that the reaction system is stable for over 100 hours without the addition of fresh catalyst.

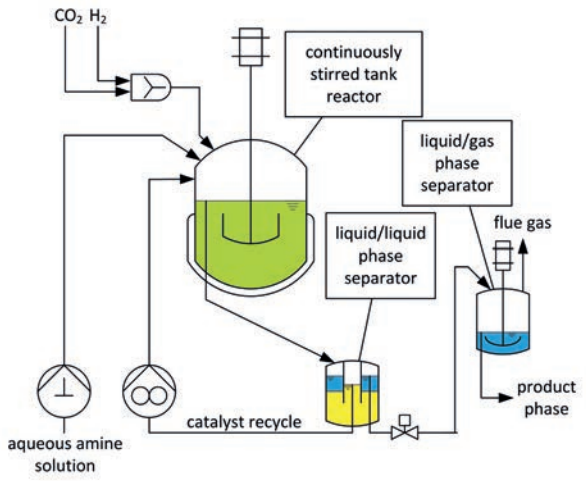

Figure 3: Simplified flow sheet of the continuously operated miniplant.

Contact:
rene.kuhlmann@bci.tu-dortmund.de
arno.behr@bci.tu-dortmund.de

Rhodium-Catalyzed Hydroaminomethylation of Cyclopentadiene

Direct Route from Alkene to Amine

Denys Levikov, Edward Nürenberg, Arno Behr

A one-step rhodium catalyzed direct route from cyclopentadiene (Cpd) to saturated C6-amines is presented via hydroaminomethylation (HAM). The homogeneous catalyst of Rh(II) octanoate dimer without additional phosphorus ligands was established giving a 77% yield of the monoamine species of Cpd with pyrrolidine within 4 h.

The substance class of amines is highly relevant for the chemical and pharmaceutical industry corresponding to 3 million tons of aliphatic amines produced per year worldwide. The application spectrum covers fine-, bulk- as well as large-scale chemicals and therefore is omnipresent in our everyday live [1]. Owing to their importance the development of catalytic synthesis of amines with regard to sustainability is of great interest. Various amines can be synthesized in a simple, efficient and atom-economic way by performing a hydroaminomethylation reaction (HAM).
Cyclopentadiene (Cpd) was chosen as a conjugated cyclic 1,3-diene substrate for the studies on the HAM reaction. Figure 1 shows possible products of the hydroaminomethylation of Cpd and its dimer dicyclopentadiene (Dcpd) with pyrrolidine.

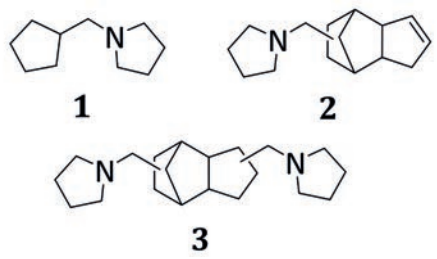

Figure 1: Possible products of the HAM of Cpd and Dcpd with pyrrolidine.

First, the saturated monoamine of Cpd **1** can be obtained through the hydroaminomethylation of cyclopentadiene. Dimerization of Cpd via Diels-Alder-reaction gives dicyclopentadiene, existing in both endo- and exo-isomers, which leads to formation of respective monoamine **2** and the diamine **3**.

The best reaction conditions were established as follows: isopropanol as solvent, a temperature of 130°C, a syngas pressure of 30 bar, alkene:amine ratio of 1:2 and a reaction time of 4 h. Preliminary, different rhodium precursors were screened. Highest yields (77%) of the 1-(cyclopentylmethyl) pyrrolidine **1** were obtained in the presence of the precursor rhodium(II) octanoate dimer.

Investigations about additives showed that ligands or tertiary alkyl amines prevent the reaction almost completely. Furthermore, the influences of the syngas ratio ($CO:H_2$) and the solvent were studied. It was possible to steer the reaction selectively to produce amines of either Cpd or Dcpd. A systematic screening revealed $[Rh[CH_3(CH_2)_6CO_2]_2]_2$ as the best precursor without any additional ligands giving 77% of 1-(cyclopentylmethyl)pyrrolidine **1** within 4 h under mild reaction conditions.

The reaction system is transferable to other cyclic and non-cyclic amine substrates with excellent selectivity up to 100% for the formation of the HAM-products. Hence, Cpd proofed to be an efficient starting chemical for the formation of cyclopentylmethyl amines under mild reaction conditions.

In summary, we have presented the first rhodium-catalyzed hydroaminomethylation of Cpd leading to the formation of the respective saturated C6-amine **1** in high yields in a single step.

[1] M. Baerns, A. Behr, A. Brehm, J. Gmehling, H. Hofmann, U. Onken, A. Renken, K.- O. Hinrichsen, R. Palkovits in: Technische Chemie, 2. Auflage, Wiley-VCH, Weinheim, 2013.

Publications:
A. Behr, D. Levikov, E. Nürenberg, RSC Advances 5, 60667-60673 (2015).

Contact:
arno.behr@bci.tu-dortmund.de

Direct Synthesis of an α,ω-Diester from 2,7-Octadienol as Bulk Feedstock in Three Tandem Catalytic Steps

Karoline A. Ostrowski, Dennis Vogelsang, Thomas Seidensticker, Andreas J. Vorholt

A new tandem catalysis was designed and developed using it as a tool for the direct conversion of the widely available feedstock 2,7-octadienol into an α,ω-diester. This innovative auto tandem catalysis is atom efficient and consists of three consecutive palladium catalysed reactions: ether formation, ether carbonylation and alkoxycarbonylation.

We envisioned a possible diester derived from 2,7-octadienol **(1)** by using three different reactions: an ether formation, an ether carbonylation and an alkoxycarbonylation (Figure 1). If these three mentioned reactions can be merged in one tandem catalysis, a direct access to diester **4** is opened straight from 2,7-octadienol **(1)**.

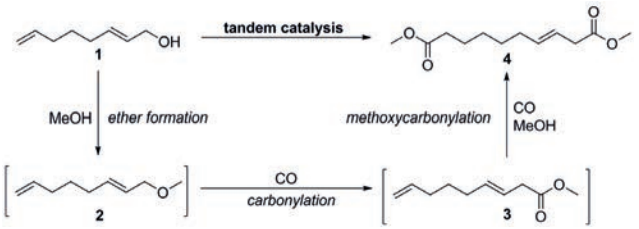

Figure 1: Design of a specific tandem catalysis for the direct conversion of an α,ω-diester from 2,7-octadienol (1).

A tandem catalysis is advantageous over the single step synthesis, since intermediates are not isolated or purified, wherefore downstream processes are reduced, which cost energy, time, solvents, materials, etc. Therefore, tandem catalyses are demanding reaction pathways and still a current and little explored field in chemistry.

In the first test reaction, 2,7-octadienol **(1)** was converted with $Pd(tfa)_2$ as precursor and Xantphos as bidentate ligand activating the catalyst for all three reactions. An excess of methanol was employed, since two equivalents are needed in the overall tandem catalysis and methanesulfonic acid was added as co catalyst. Furthermore, the reaction path was uncovered (Figure 2).

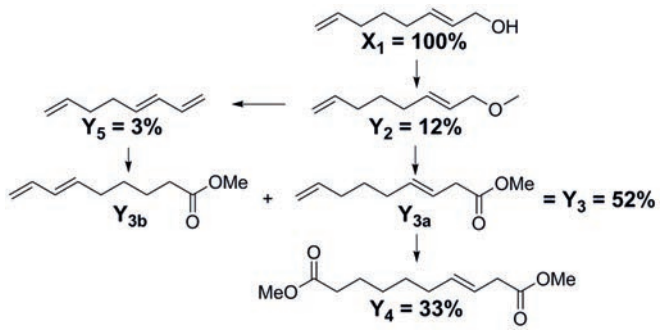

Figure 2: First test reaction. Conditions: 2 mmol **1**, 3 eq MeOH, 1 mol% $Pd(tfa)_2$, 4 mol% Xantphos, 20 mol% MSA, 40 bar CO, 2.5 ml toluene, T = 115°C, t = 18 h, results in %; X = conversion; Y = yield.

A further reaction side path was observed via the intermediate **5**, which can convert into **3a**.

With the aim to enhance the yield of **4**, the significant influence parameters (concentration of methanol and methanesulfonic acid) were determined via design of experiments (DoE), wherein the central composite design CCD was used. Then, in order to get a deeper insight into the tandem sequence, the reaction progress was investigated over time at optimised conditions (Figure 3). The yield of **5** after 8 h and **3** after 16 h are comparable high with ~30%. Based on this fact, NMR experiments were carried out and proven remaining **3b**, which is inactive in the alkoxycarbonylation. The conversion of substrate **1** into intermediate **2** was completed after 1 h.

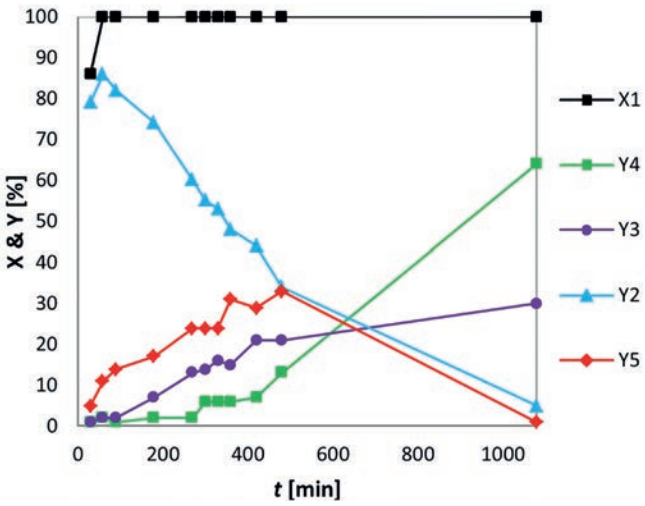

Figure 3: Investigation of the reaction progress by plotting the conversion (X) and yield (Y) over time. Conditions: 2 mmol **1**, 5 eq MeOH, 1 mol% $Pd(tfa)_2$, 4 mol% Xantphos, 25 mol% MSA, 40 bar CO, 2.5 ml toluene, T = 115°C, results in %.

In summary, a new and effective tandem catalysis was developed and optimised, allowing the direct conversion of the readily available 2,7-octadienol into an α,ω-diester with 64% yield. This diester is a potential polymer precursor, describing an already known monomer after hydrogenating the double bond into a saturated C_{10}-Diester.

Contact:
karoline.ostrowski@bci.tu-dortmund.de
dennis.vogelsang@bci.tu-dortmund.de
thomas.seidensticker@bci.tu-dortmund.de
andreas.vorholt@bci.tu dortmund.de

Publications:
K. A. Ostrowski, D. Vogelsang, T. Seidensticker, A. J. Vorholt, Chem. Eur. J. 22, 1840-1846 (2016).

Aminocarbonylation of Aliphatic Alkenes with DMF

Do-It-Yourself CO Production: *N,N*-Dimethylformamide as a CO Surrogate in the Palladium Catalyzed Production of Amides from Aliphatic Alkenes

Thomas Seidensticker, Marc R. L. Furst, Robin Frauenlob, Johanna Vondran, Eckhard Paetzold, Udo Kragl, Andreas J. Vorholt

The palladium-catalyzed aminocarbonylation of aliphatic alkenes is presented for the first time without the need for external CO pressure. N,N-*dimethylformamide (DMF) is used as an* in-situ *source of both the required carbon monoxide and the amine substrate. The applied palladium catalytic system is well-known for a number of carbonylation reactions, including those with CO surrogates and tandem isomerizing carbonylations. Aliphatic alkenes (terminal and internal) are transformed, also in commercial glassware, into the corresponding linear* N,N-*dimethylamides with excellent selectivities.*

Numerous methods exist for the preparation of amides, although their synthesis without the generation of waste and the use of toxic reagents can be challenging. Aminocarbonylation of olefins is an elegant way of producing amides in an atom-economic fashion from readily available starting materials. However, the use of CO as a C_1- building block for the functionalization of alkenes can be difficult due to its inherent toxicity and the need for special equipment. As a result, the substitution of CO in carbonylation reactions by less toxic and easier-to-handle synthetic equivalents is of considerable interest. For amide formation from olefins, formamides, such as *N,N*-dimethylformamide (DMF) represent ideal CO surrogates (Figure 1).

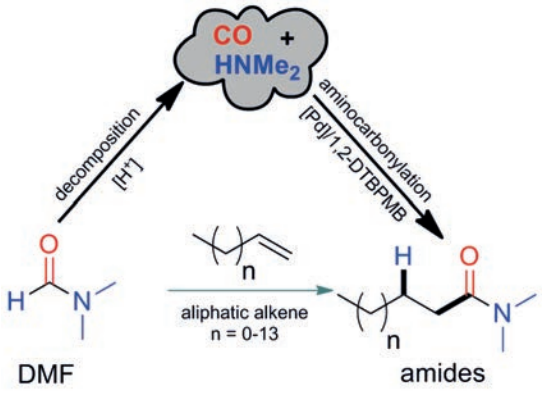

Figure 1: DMF in the aminocarbonylation of aliphatic alkenes.

In this work, DMF is applied in the amino-carbonylation of linear aliphatic alkenes, using a well-known palladium catalytic system comprising of 1,2-DTBPMB as ligand (Figure 2), $Pd(acac)_2$ as precursor, methanesulfonic acid and imidazole as promotor. The reaction pathway was investigated and proved to proceed by an acid-catalyzed DMF decomposition to CO and dimethyl amine with subsequent aminocarbonylation of the alkene.
After optimizing the reaction conditions, various alkenes of different chain length were effectively converted into their respective *N,N*-dimethylamide derivatives (Table 1).

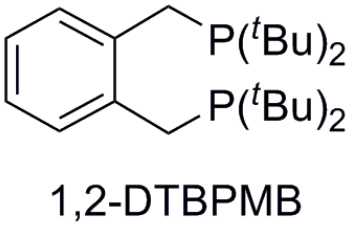

Figure 2: Ligand used in the present study: (1,2 bis((di *tert* butylphosphino)methyl) benzene, 1,2-DTBPMB.

Table 1. Aminocarbonylation of various alkenes with DMF

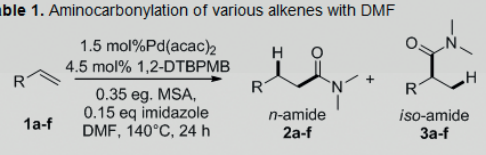

Entry	substrate	S_{2+3}[a] (2:3)	Y_{2+3} [a] (GC)	Y_2 [b] (isolated)
1	propene **1b**, R = methyl	95 (29:1)	94	85
2	1-pentene **1c**, R = *n*-propyl	90 (22:1)	85	82
3	1-hexene **1d**, R = *n*-ethyl	92 (21:1)	80	78
4	1-octene **1a**, R = *n*-hexyl	90 (21:1)	72	69
5	1-decene **1e**, R = *n*-octyl	91 (22:1)	68	61
6	1-dodecene **1f**, R = *n*-decyl	92 (22:1)	67	58

Reaction conditions: 7 mL stainless steel autoclave, **1a–f** (8.8 mmol), $Pd(acac)_2$ (1.5 mol%: 40 mg, 0.133 mmol), 1,2 DTBPMB (4.5 mol%: 105 mg, 0.27 mmol), MSA (0.35 equiv.: 0.2 mL, 3.1 mmol), imidazole (0.15 equiv.: 90 mg, 1.33 mmol), 3 mL DMF, 140°C, 24 h. [a] Yield (Y) and selectivity (S) are given as sum of both amide isomers (**2+3**) reported in % based on GC-FID analysis. [b] isolated yield after chromatographic workup.

With our developed protocol, amide synthesis by aminocarbonylation moves closer to application in standard organic laboratories.

Publications:
T. Seidensticker, M. R. L. Furst, R. Frauenlob, J. Vondran, E. Paetzold, U. Kragl, A. J. Vorholt, ChemCatChem 7, 4085-4090 (2015).

Contact:
andreas.vorholt@bci.tu-dortmund.de

Intensification of Rhodium Catalyzed Aqueous Biphasic Hydroformylation of Mid Chain Olefin 1-Octene in Jet Loop Reactor

Helge Warmeling, Sebastian Gottschlich, Arno Behr, Andreas J. Vorholt

An efficient phase contacting jet loop reactor was applied in the aqueous biphasic hydroformylation of the mid chain olefin 1-octene and high catalytic activity was achieved. Compared to a stirred tank reactor the average reaction rate per catalysts molecule was increased 20-fold. An obvious explanation is the creation of a large interfacial surface and therefore subjacent film volume. The concentration of olefin in the film between the bulk phases is elevated compared to the bulk volume of the catalyst phase which leads to faster conversion rates due to a first order dependence of the kinetic. While several research groups focus on a chemical enhancement of the reaction system a procedural approach has seldom been applied although it offers a great potential for process intensification.

Jet loop reactors are a promising process setup in multiphase reaction engineering and can contribute to process intensification. The reactor type stands out for its interesting micro and macro mixing properties. By partial withdrawal and reinjection through a nozzle in the reactor head a fine dispersion of applied phases can be achieved with high energy efficiency. The jet stream leaving the nozzle is captured in a draft tube and lead to an impact plate where the impulse is redirected and an additional inner circulation is created around the draft tube. The reactor can be used for a variety of phase setups like e.g. liquid-gas, liquid-liquid-gas and solid-liquid-gas reactions. Figure 1 shows the schematic reactor used for the hydroformylation of long chain olefins in a liquid-liquid-gas reaction system.

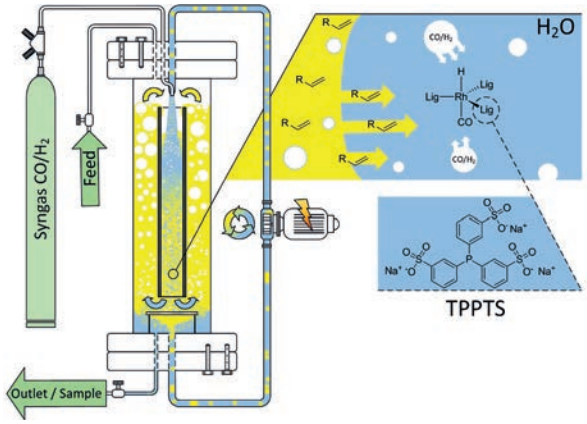

Figure 1: Scheme of the application of a jet loop reactor for the aqueous biphasic long chain hydroformylation.

The hydroformylation is the biggest application of homogenous catalysis in today's chemical industry. An olefin is converted to a +1C elongated aldehyde under syngas (CO/H_2 mixture) pressure catalyzed by different transition metal complexes following equation (1).

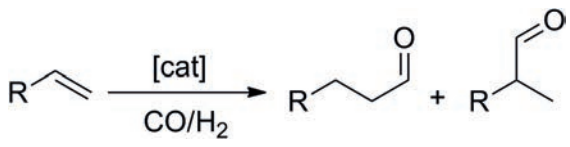

Contact:
Helge.Warmeling@tu–dortmund.de
Andreas.Vorholt@tu–dortmund.de

Most commonly rhodium complexes with different ligands are used due to their high activity. Major drawback of rhodium catalysts is the high and very volatile market price. To achieve economical process performance an efficient catalyst recovery is therefore essential and was introduced in industrial scale in form of the Ruhrchemie/Rhône-Poulenc process. In this process the catalyst is heterogenized in water with a polar water soluble ligand (TPPTS). Unfortunately this elegant technique is only applicable for short chain olefins like ethylene or propylene due to the heavily decreasing solubility with increasing chain length in water. To overcome this limitation the biphasic mid chain hydroformylation of the long chain 1-octene was applied to the jet loop reactor. The turnover frequency for hydroformylation (TOF) was increased from 19 h^{-1} to 388 h^{-1} in average compared to a stirred tank steel autoclave as shown in figure 2. The high reaction rates (max. 1422 h^{-1}) were conceivably achieved through the generation of high amounts of surface near film volume with an elevated substrate concentration.

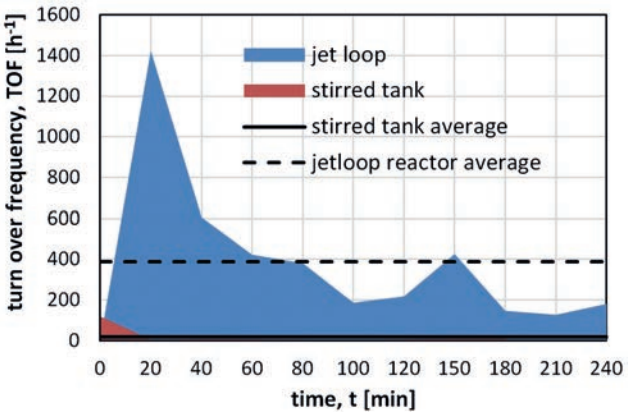

Figure 2: Turnover frequency (mol product per mol catalyst and time) of the aqueous biphasic rhodium catalyzed hydroformylation of 1-octene in a jet loop reactor compared to a stirred tank reactor.

Publications:
H. Warmeling, A. Hüser, C. Breitkreuz, A. J. Vorholt, Posterbeitrag „The Jet Loop Reactor as a Versatile Reactor Concept – Intensifying Biphasic Homogenous Catalysis", DGMK 2015, Dresden.

H. Warmeling, S. Gottschlich, A. J. Vorholt, Posterbeitrag "Process Intensification of Homogenously Catalysed Biphasic Reactions by Application of a Phase Contacting Jet Loop Reactor", 49. Jahrestreffen Deutscher Katalytiker, 2016, Weimar.

Thermodynamics (TH)

Thermodynamics of Enzyme-Catalyzed Esterification

Equilibrium Study of Succinic Acid Esterification with Ethanol Using *Candida Antarctica* Lipase B

Emrah Altuntepe, Gabriele Sadowski, Christoph Held

Esters of dicarboxylic acids are widely used in chemical industry and biotechnology. These esters are typically produced via chemical catalysis. In this work, the enzyme-catalyzed esterification of succinic acid with ethanol is thermodynamically characterized in terms of standard Gibbs energy of reaction and equilibrium constants. It was shown that reaction equilibrium is shifted towards the product site upon increasing initial water and succinic acid concentrations and decreasing reaction temperature. This could be explained by PC-SAFT predicted activity coefficients of reactants and products, which strongly deviate from unity.

Succinic acid is reported as promising component and renewable platform chemical for several derivatives of industrial interest [1]. The esters of succinic acid have very interesting thermo-physical properties and are suggested to be used as intermediates for the production of bio-based polymers. In the specific case of esterification with ethanol, the reaction takes place sequentially with monoethyl succinate as intermediate product and diethyl succinate as final product (Figure 1) [2].

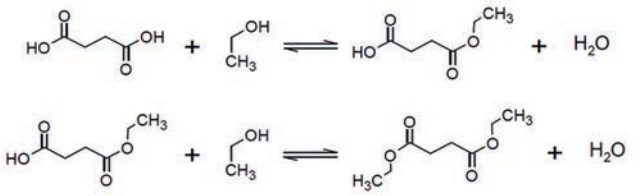

Figure 1: Esterification of succinic acid with ethanol to diethyl succinate via the intermediate monoethyl succinate.

In this work the esterification shown in Figure 1 was carried out via enzyme catalysis by *Candida antarctica* Lipase B immobilized on acrylic resin. Reaction equilibrium was measured yielding the apparent equilibrium constant K_m. It was found that K_m strongly increased with increasing initial succinic acid molality. Besides the succinic acid concentration, the concentration of water is a key parameter in enzyme-catalyzed esterifications, as water is not only a reaction product but it is also relevant to ensure enzyme activity.

The dependence of experimental K_m values on water molality is shown in Figure 2. The higher the water molality at reaction equilibrium, the higher K_m (reaction equilibrium shifted towards the product site).

The reason for the observed concentration dependence of K_m is the non-ideality of the reaction mixture, expressed as ratio of activity coefficients of products to reactants (K_γ). The true equilibrium constant K_a is obtained by $K_a = K_m \cdot K_\gamma$. In this work K_γ was calculated using PC-SAFT based on parameters that were fitted to reaction-independent phase equilibrium data. It can be observed from Figure 2 that PC-SAFT predicted K_γ values decrease with increasing water molality.

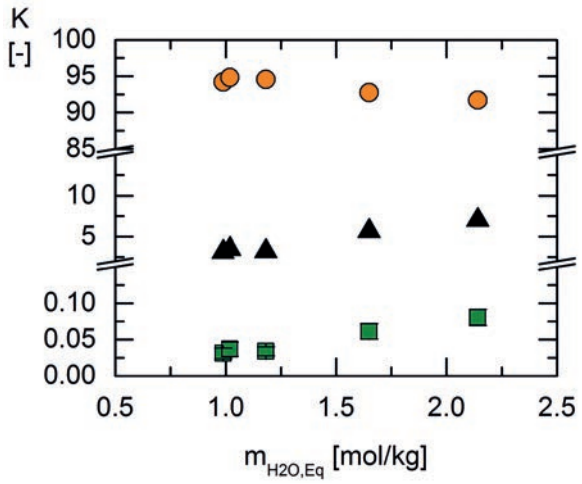

Figure 2: Apparent equilibrium constants K_m (squares) and reactant activity coefficient ratio K_γ (circles) of succinic acid esterification as a function of the water equilibrium molality at 50°C. The product of K_m and K_γ gives K_a (black triangles).

The results further reveal that K_γ values remarkably deviate from unity. That is, K_a significantly differs from K_m. Thus, activity coefficients are crucial for the calculation of thermodynamic equilibrium constants. Finally, K_a was found to be 7±2 for 40°C and 5±2 for 50°C, respectively. The standard Gibbs energy of reaction at 50°C results in a value of $\Delta^R g^0$ = -4.2±0.5 kJ/mol, whereas neglecting activity coefficients yields an even positive value of $\Delta^R g^0$ = +7±1 kJ/mol.

This work shows the importance of thermodynamic studies on esterification reactions, as common simplifications cause high errors for the determination of universal (concentration-independent) properties such as K_a or $\Delta^R g^0$.

Contact:
emrah.altuntepe@bci.tu-dortmund.de
christoph.held@bci.tu-dortmund.de
gabriele.sadowski@bci.tu-dortmund.de

Publications:
[1] R. Landucci, B. Goodman, C. Wyman, Applied Biochemistry and Biotechnology, 45-46 , 677–696 (1994).
[2] A. Orjuela, A. Kolah, C T. Lira, D J. Miller, Ind. Eng. Chem. Res., 50 (15), 9209–9220 (2011).

Purifying Dicarboxylic Acids from Biocatalytic Origin

Development of a Purification Strategy for Cis,Cis-Muconic Acid on the Basis of Reactive Extraction

Jannick Gorden, Tim Zeiner, Gabriele Sadowski, Christoph Brandenbusch

Dicarboxylic acids are an evolving substance class, expected to serve as future platform chemicals within industry. Product concentrations achievable by whole-cell biocatalysis have recently been shown to reach industrial levels, but the development of a downstream processing (DSP) concept still is the bottleneck towards an industrial application. In this work reactive extraction (RE) was positively evaluated as selective and efficient concept for the recovery of dicarboxylic acids from an aqueous solution. Furthermore a DSP concept coupling RE into a biocompatible organic phase (product capture step) and re-extraction (REEX) into an aqueous phase was demonstrated for the workup for cis,cis-muconic acid (CCMA) with high yield.

A DSP for the purification of dicarboxylic acids from biocatalytic origin based on a combination of RE and REEX steps was developed. Figure 1 illustrates the steps involved in the DSP concept as block diagram.

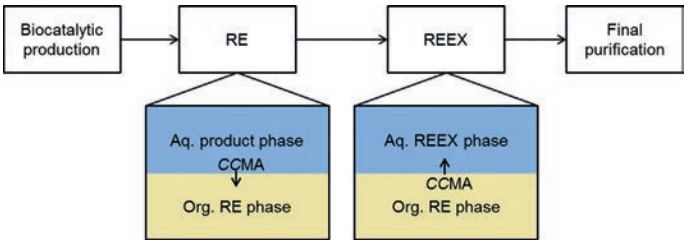

Figure 1: Schematic illustration of the developed DSP for CCMA.

After biocatalytic production, a RE of CCMA into a biocompatible organic phase is performed. RE is thereby performed using the water-insoluble amine tri-n-octylamine (T-C8) as extractant. T-C8 forms a hydrophobic complex with CCMA which is then extracted into a biocompatible organic phase composed of ethyl- oleate and 1-dodecanol ($w_{1\ dodecanol}$ = 0.1).

A T-C8 concentration of 0.15 mol kg^{-1} at 28°C and a phase ratio of 2:1 (m_{org}:m_{aq}) leads to a CCMA extraction yield of X_{RE} = 0.95 ± 0.04. A HPLC analysis after RE revealed that the final T-C8 concentration in the aqueous phase was below the detection limit. This allows for a potential in-situ application of the RE and a simple recycle of the aqueous product phase for further biocatalysis. Further investigations revealed that the RE strongly depends on *pH*. Simultaneous FTIR measurements proved that the complex between the CCMA and the T-C8 is formed via H-bonding, and thus cannot be formed at a *pH* higher than the pK_a of CCMA.

This dependency was used in the REEX as second step of the DSP. For that purpose, measurements were performed using different citrate buffer solutions in a range of 3-7.9 (Figure 2).

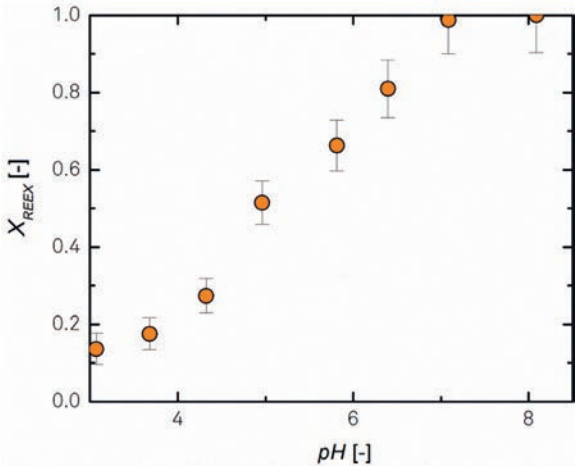

Figure 2: Re-extraction yield of CCMA as function of pH. Re-extraction of CCMA was performed from the organic RE phase (EO, 1-dodecanol weight fraction of 0.1, and T-C8 in a concentration of 0.15 mol kg^{-1}).

The REEX using a citrate buffer with a pH >= 7.09 reached a final re-extraction yield of X_{REEX} = 0.99± 0.08. At this *pH*, CCMA is completely deprotonated and thus leaks the ability to form a complex with the amine T-C8. The existing complex in the organic phase is broken and CCMA is re-extracted into the aqueous re-extraction phase. The CCMA-free organic phase can be recycled for further RE steps without any treatment. A final purification of CCMA from the aqueous re-extraction phase can be achieved via crystallization.

In summary, a new DSP for the dicarboxylic acid CCMA from biocatalytic origin based on the principle of a RE as product-capture step was developed. The results show that a high yield for the overall process can be achieved, allowing for transferring this principle to the purification of other dicarboxylic acids.

Publications:
Gorden, J.; Zeiner, T.; Brandenbusch, C., Fluid Phase Equilibria (2015), 393, 78-84.
Gorden, J.; Zeiner, T.; Sadowski, G.; Brandenbusch C.; Separation and Purification Technologies (2016), 169, 1-8.

Contact:
jannick.gorden@bci.tu-dortmund.de
tim.zeiner@bci.tu-dortmund.de
gabriele.sadowski@bci.tu-dortmund.de
christoph.brandenbusch@bci.tu-dortmund.de

Predicting the pH-Dependent Solubility of Pharmaceutical Cocrystals

Influence of pH-Dependent Dissociation and Salt Formation on the Solubility of Pharmaceutical Cocrystals

Linda Lange, Kristin Lehmkemper, Gabriele Sadowski

To increase the efficiency of cocrystal formation and purification processes, the aqueous solubility of pharmaceutical cocrystals was predicted in this work using PC-SAFT. Modeling results and experimental data of pH-dependent solubilities were compared for the weak base nicotinamide, the weak acid succinic acid, their 2:1 cocrystal, as well as for all occurring salts at 298.15 K. It was found, that the pH-dependent acid-base equilibria of nicotinamide and succinic acid directly influence the solubility of their cocrystal and their salts which could be quantitatively predicted by PC-SAFT.

Pharmaceutical cocrystals (CCs) represent an emerging class of solid drugs that consist of the API and at least one coformer (CF) in a defined stoichiometry, ν_{API} and ν_{CF}. Modeling the concentration range in which stable CCs can form comprises solubility-line calculations of the API, CF, and the CC, whereas the CC formation is modeled as a chemical reaction of its components:

$$CC \overset{K_{s,CC}}{\longleftrightarrow} \nu_{API}\, API + \nu_{CF}\, CF \qquad (1)$$

The CC solubility was determined from the equilibrium concentrations of API and CF of this reaction which were in turn obtained from the CC solubility product $K_{s,CC}$. $K_{s,CC}$ was modeled considering for thermodynamic non-idealities by accounting for the activity coefficients of API and CF. Thus, it does not depend on the solvent or on concentrations nor on pH, but only varies with temperature.

For pharmaceutical applications, CC formation is preferably performed from aqueous solutions. However, API and CF usually have functional groups, which can be ionized in aqueous solutions by pH change. Thus, CC formation is influenced by pH-dependent dissociation and salt formation.

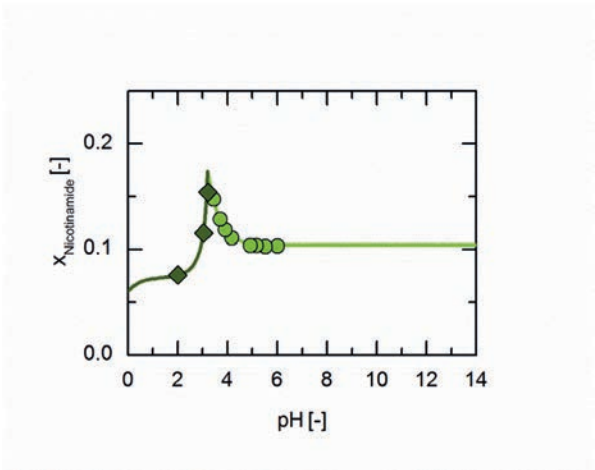

Figure 1: pH-dependent solubilities of nicotinamide (NCT) in aqueous solutions at 298.15 K. Lines correspond to PC-SAFT correlations; symbols represent the experimental data points for NCT (green circles) and its salt NCT hydrochloride (dark green diamonds).

Contact:
linda.lange@bci.tu-dortmund.de
gabriele.sadowski@bci.tu-dortmund.de

In this work, pH-dependent dissociation of basic nicotinamide (NCT) and succinic acid (SA) was considered. As an example, Figure 1 shows the pH-dependent solubilities of NCT and its salt in aqueous solutions containing hydrochloric acid as pH-changing agent. The solubility lines of NCT and its salt could be correlated in very good accordance with the experimental data.

The CC solubility as function of pH was predicted using $K_{s,CC}$, which was determined from only one CC solubility point at pH 3.2.The influence of pH change on CC solubility was calculated by accounting for the dissociation equilibria of NCT and SA. Figure 2 compares the measured and predicted solubility lines of the NCT/SA (2:1) CC for pH 2 and pH 4.

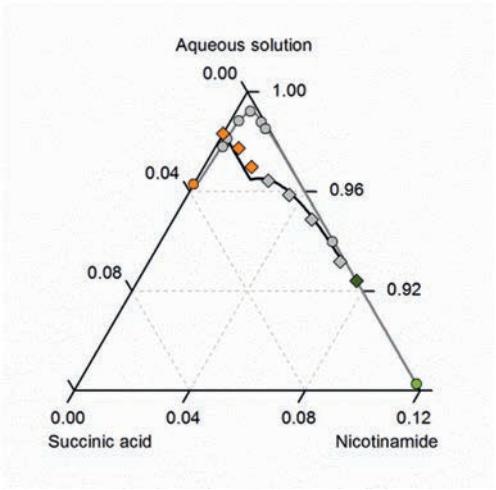

Figure 2: Solubilities for the nicotinamide (NCT)/succinic acid (SA)/water system at pH 2 (diamonds) and pH 4 (circles) at 298.15 K. Aqueous solutions contain water and the pH-modifying agents hydrochloric acid or sodium hydroxide. Solid lines correspond to the PC-SAFT predictions; symbols refer to the experimental data points of SA (orange), the cocrystal (gray), and NTC (green circles) or NTC hydrochloride (dark green diamonds).

Obviously, there is a huge influence of pH on the CC solubility which can be predicted by PC-SAFT in almost quantitative agreement with experimental data.

Publications:
L. Lange, G. Sadowski, Crystal Growth and Design 15 (9), 4406−4416 (2015).
L. Lange, K. Lehmkemper, G. Sadowski, Crystal Growth and Design 16 (5), 2726-2740 (2016).

Solvent Effects on Reaction Kinetics

Quantitative Prediction of Solvent Effects on Esterification Reaction Kinetics

Max Lemberg, Gabriele Sadowski

Due to interactions with the reacting species, solvents can influence reaction kinetics. The classical concentration-based kinetic modeling approach is unable to describe these effects. For the esterification of ethanol and acetic acid in different solvents, a thermodynamic model was applied to account for solvent/reactant interactions. A new activity-based kinetic modeling approach using only one intrinsic kinetic constant for all solvent systems allowed for predicting the solvent effects on reaction kinetics in very good agreement with the experimental data.

The state-of-the-art kinetic description for the esterification of ethanol (EtOH) with acetic acid (HAc) to ethyl acetate (EA) and water is represented by:

$$r = k_1 \cdot c_{EtOH} c_{HAc} - k_2 \cdot c_{EA} c_{H2O} \quad (1)$$

As it is based on the concentration of the reacting species, it cannot account for interactions with solvents. Therefore the kinetic constants k_1 and k_2 depend on the applied solvent and are not transferable to the reaction in other solvents. To facilitate the solvent selection process, a modeling approach with predictive capabilities is desirable. This is achieved by considering the solvent/reactant interactions via the activity coefficients γ_i of the reacting species:

$$r = k_1^* \cdot \gamma_{EtOH}\gamma_{HAc} \cdot c_{EtOH} c_{HAc} - k_2^* \cdot \gamma_{EA}\gamma_{H2O} \cdot c_{EA} c_{H2O} \quad (2)$$

In this novel approach, k_1^* and k_2^* are intrinsic kinetic constants that do not depend on the solvent. They are connected with the thermodynamic reaction-equilibrium constant K_a according to:

$$K_a = \frac{k_1^*}{k_2^*} \quad (3)$$

K_a was determined experimentally in a previous work of our group. The activity coefficients were calculated using the thermodynamic model PC-SAFT.

Figure 1 shows results of the reaction kinetics for the solvent-free reaction for varying mole-ratios of HAc/EtOH.

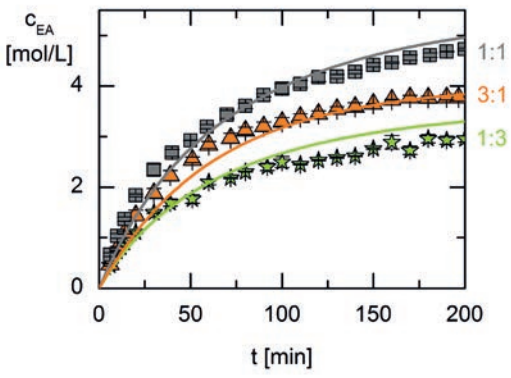

Figure 1: Concentration of EA for the esterification of EtOH with HAc over time at 303.15 K in solvent-free systems at different HAc/EtOH ratios. Symbols are experimental data and lines are modeling/predictions with PC-SAFT.

For the modeling, only one adjustable parameter k_1^* was fitted to the 1:1 system. Hence, the kinetics for the 1:3 and 3:1 system were purely predicted in very good agreement with the experimental data. Figure 2 shows results for the same reaction performed with a equimolar mixture of HAc and EtOH in different solvents ($c_{HAc,0}$ =$c_{EtOH,0}$ =3.5 mol/L in each case).

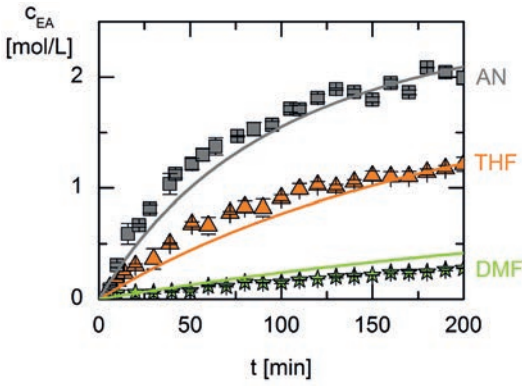

Figure 2: Concentration of EA for the esterification of EtOH with HAc over time at 303.15 K in systems with equimolar HAc/EtOH ratio in various solvents (AN - acetonitrile, THF - tetrahydrofurane, DMF - dimethylformamide). Symbols are experimental data and lines are predictions with PC-SAFT.

As k_1^* was already known from the solvent-free system, all lines in Figure 1 were purely predicted. The predicted promoting effect of AN and suppressing effect of DMF could be validated in very good agreement by the experimental data. In contrast to this, the classical approach would not even be able to predict different kinetics for different solvents but would result in the same kinetics for all solvents or would require different kinetic constants for varying solvents.

However, the applied approach shows that solvent effects on reaction kinetics can be predicted when accounting for the reactant activity coefficients (as long as the catalyst is not affected by the solvent).

Contact:
max.lemberg@bci.tu-dortmund.de
gabriele.sadowski@bci.tu-dortmund.de

ATP Hydrolysis: A Thermodynamically-Consistent Value for Standard Gibbs Energy of Reaction

Determination of standard Gibbs energy of reaction of ATP hydrolysis by measuring and combining reaction equilibria of two biological reactions and relating to standard conditions by activity coefficients

Florian Meurer, Gabriele Sadowski, Christoph Held

Hydrolysis of ATP is one of the most universal and abundant reactions in biological cells. It is therefore of great importance to determine its thermodynamic equilibrium constant. As ATP hydrolysis does never occur spontaneously, access to its equilibrium constant is only possible by combining constants of two independent reactions, one of them containing ATP as reacting agent. One of the drawbacks of values available in literature is that activity coefficients of the reacting agents have not been considered, and thus published equilibrium constants depend on reaction conditions. In this work, activity coefficients were explicitly accounted for to determine a true thermodynamic equilibrium constant allowing for the determination of Gibbs energy of reaction of ATP hydrolysis at biological standard state.

ATP (Adenosine triphosphate) is known as energy currency of the cell as it is one of the main energytransferring compounds in the cell. ATP hydrolysis provides energy for anabolic reactions and even for catabolic reaction pathways in metabolism. Values for the standard Gibbs energy of reaction $\Delta^R g^0$ are required to calculate Gibbs energies $\Delta^R g$, which are applied in systems biology to predict metabolic pathways. However, $\Delta^R g^0$ of ATP hydrolysis is not directly accessible as due to kinetic limitations, ATP hydrolysis does not occur spontaneously. Thus, in this work two reactions were combined according to Figure 1: the Hexokinase reaction (HK) and the Phosphatase reaction (P-ase), which's combination yields the ATP hydrolysis (ATP-H) as net reaction.

$$\Delta^R g^0_{ATP\text{-}H} = \Delta^R g^0_{HK} + \Delta^R g^0_{P\text{-}ase} \qquad \text{(Eq. 1)}$$

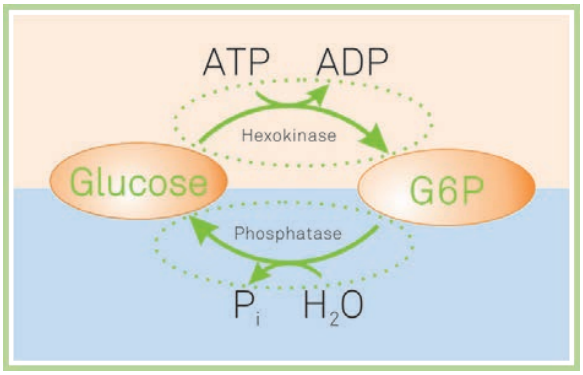

Figure 1: Two-step reaction approach (hexokinase and phosphatase reaction) as an access to $\Delta^R g^0$ ATP of hydrolysis.

In this work, $\Delta^R g^0$ was determined for the HK and the P-ase reactions. Equilibrium concentrations of the reacting agents were measured (→ K_m) and their activity coefficients were modeled using electrolyte PC-SAFT (→ K_γ) yielding the true thermodynamic equilibrium constant K_a and thus $\Delta^R g^0$ according to Eq. 2:

$$\Delta^R g^0 = -RT \ln(K_a) = -RT \ln(K_m \cdot K_\gamma) \qquad \text{(Eq. 2)}$$

K_m-values (and thus also K_γ) for the HK were found to be rather independent of the concentration of the reacting agents, resulting in a value of $\Delta^R g^0 = 18.0 \pm 0.4$ kJ·mol^{-1}. In contrast, measured K_m-values of the P-ase reaction strongly increased with increasing glucose concentration. This could be explained by electrolyte PC-SAFT predicted K_γ-values. The obtained value for K_a yielded a $\Delta^R g^0$-value of -14.4 ± 1.2 kJ·mol^{-1} for the P-ase reaction.

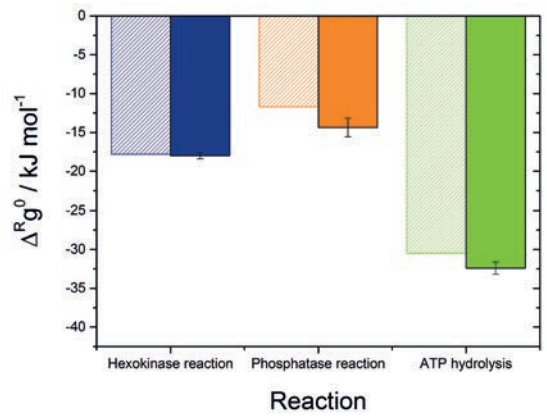

Figure 2: Standard Gibbs energies of the HK, P-ase and ATP-H reactions; full bars: this work, shaded bars: literature data [1], [2].

Figure 2 shows the $\Delta^R g^0$ values for HK and P-ase; using Eq. 1 this yields a value for ATP-H of $\Delta^R g^0_{ATP\text{-}H}$ = -33.4 kJ·mol^{-1}. This value is 3 kJ·mol^{-1} more negative than the value established in biological textbooks, and even 5.5 kJ·mol^{-1} less negative than other literature values (not shown in Figure 2).

This is a dramatic finding given that $\Delta^R g^0$ values of many metabolic reactions (e.g. in glycolysis) are in the range of a few kJ·mol^{-1} only.

Contact:
christoph.held@bci.tu-dortmund.de
gabriele.sadowski@bci.tu-dortmund.de

Publications:
[1] E.A. Robbins, P.D. Boyer, The Journal of biological chemistry 224, 121–135 (1957).
[2] M.R. Atkinson, E. Johnson, R.K. Morton, Biochemical Journal, 79(1) 12–15 (1961).

Impressum

Fakultät Bio- und Chemieingenieurwesen
TU Dortmund

www.bci.tu-dortmund.de

Redaktion: Prof. Jörg C. Tiller